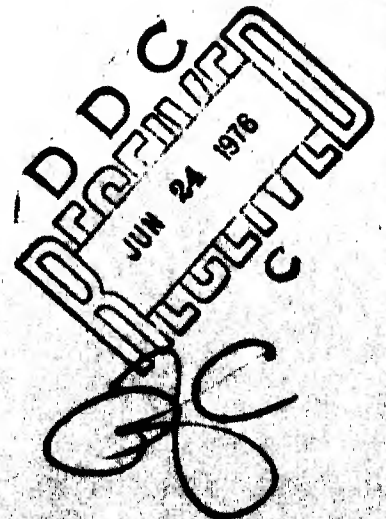AMRL-TR-74-95

ADA025945

FEASIBILITY OF IMPLEMENTING SPECIFIC PERFORMANCE MEASUREMENT TECHNIQUES

QUEST RESEARCH CORPORATION
6845 ELM STREET, SUITE 407
McLEAN, VIRGINIA 22101

MARCH 1976

Approved for public release; distribution unlimited

D D C
JUN 24 1976

NOTICES

TECHNICAL REVIEW AND APPROVAL
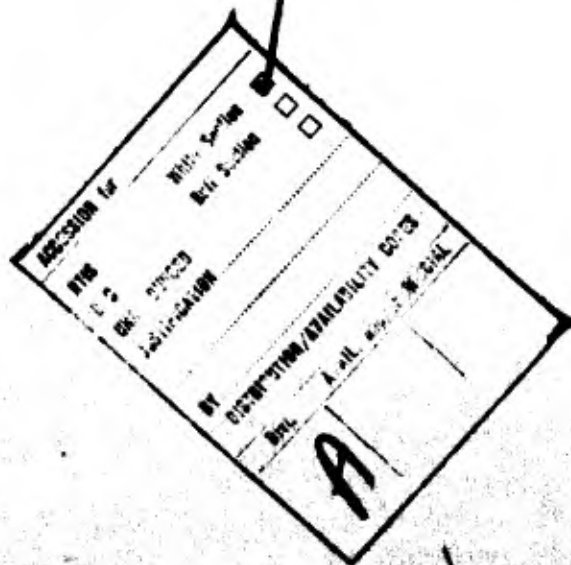
REPORT DOCUMENTATION PAGE		READ INSTRUCTIONS BEFORE COMPLETING FORM
1. REPORT NUMBER AMRL-TR-74-95	2 GOVT ACCESSION NO	3 RECIPIENT'S CATALOG NUMBER
4. TITLE (and Subtitle) Feasibility of Implementing Specific Performance Measurement Techniques.		5. TYPE OF REPORT & PERIOD COVERED Final rept.,
		6. PERFORMING ORG. REPORT NUMBER
7. AUTHOR(s) Diane G. Loental		8. CONTRACT OR GRANT NUMBER(s) F33615-73-C-4121 New
9. PERFORMING ORGANIZATION NAME AND ADDRESS Quest Research Corporation 6845 Elm Street, Suite 407 McLean, Virginia 22101		10. PROGRAM ELEMENT, PROJECT, TASK AREA & WORK UNIT NUMBERS 62202F
11. CONTROLLING OFFICE NAME AND ADDRESS Aerospace Medical Research Laboratory, Aerospace Medical Division, Air Force Systems Command, Wright-Patterson Air Force Base, Ohio 45433		12. REPORT DATE March 1976
		13. NUMBER OF PAGES 111
14. MONITORING AGENCY NAME & ADDRESS(if different from Controlling Office) 110 p.		15. SECURITY CLASS. (of this report) Unclassified
		15a. DECLASSIFICATION DOWNGRADING SCHEDULE

16. DISTRIBUTION STATEMENT (of this Report)

Approved for public release; distribution unlimited

17. DISTRIBUTION STATEMENT (of the abstract entered in Block 20, if different from Report)

18. SUPPLEMENTARY NOTES

19. KEY WORDS (Continue on reverse side if necessary and identify by block number)

1. Pilot Modeling
2. Pilot Control Theory
3. Math Modeling
4. Performance Measurement
5. Flight Simulator
6. Pilot Tracking
7. Markov Theory

20. ABSTRACT (Continue on reverse side if necessary and identify by block number)

The report presents two techniques for performance measurement in a manned weapon system. The particular system studied was the F-106 coplanar attack simulator located at the Systems Effectiveness Branch, Aerospace Medical Research Laboratory, Wright-Patterson Air Force Base, Ohio. The first technique involves a theoretical model of the human operator's flight control policies on the simulator. The second technique is empirical and derives performance measures from the simulator data.

DD FORM 1473 1 JAN 73   EDITION OF 1 NOV 65 IS OBSOLETE

PREFACE

The study was initiated by the Aerospace Medical Research Laboratory, Aerospace Medical Division, Air Force Systems Command, Wright-Patterson Air Force Base, Ohio. The research was conducted by Quest Research Corporation, McLean, Virginia, under Contract F33615-73-C-4121.

TABLE OF CONTENTS

LIST OF FIGURES

LIST OF FIGURES (CONTD)

LIST OF TABLES

I.   INTRODUCTION

This report discusses techniques for developing performance measures and performance criteria for manned systems. Performance data was obtained from the F-106 coplanar attack simulator located at the Systems Effectiveness Branch, Aerospace Medical Research Laboratory, Wright-Patterson Air Force Base, Ohio. The objective of the study was to determine what operator actions produce superior performance as distinguished from actions which produce less than superior performance.

The F-106 attack mission simulation has three phases; spotlight, lock-on and attack. In the spotlight (prelock-on) mode, the pilot controls the aircraft to reduce steering error. In the lock-on phase, he not only controls the aircraft, but must also adjust his antenna azimuth and range gate controls to obtain radar lock-on. Finally, in the attack (post lock-on) mode, he maintains the proper heading and pulls the arming trigger prior to weapons launch. An analysis of the performance demonstrations shows that the pilot controls the steering error in a different way in each of the three phases. Consequently, the operator models suggested here attempt to represent the various pilot steering error controls of each phase.

Operator modeling in this program was limited to the steering error models for each phase. Antenna control and range gate dynamic models were not developed. Analysis of demonstrated performance shows that the operator/pilot employed nonlinear control techniques, such as roll angle saturation and small steering error limit cycles. To accurately represent these control characteristics, we developed a nonlinear pilot modeling technique based on Lyapunov's direct method of stability analysis. This technique can be used to represent both nonlinear convergent control, such as demonstrated by many operators, and unstable control where that characteristic is desired. An important feature of the model is that convergence or stability can be controlled directly while allowing considerable freedom in the selection of control techniques. Another model feature is the representation of limit cycle responses, either by modeling the nonlinear plant and/or operator characteristics providing that limit cycle, or by modeling the

1

limit cycle trajectory itself. Although this modeling technique has not been fully validated, preliminary indications are that it is useful for purposes of performance measurement.

An empirical approach is also formulated whereby flight data from demonstrations of various performance levels are systematically processed to obtain information on system performance. The technique allows us to extract from the data the control policies that result in excellent and less than excellent performance. From these policies, performance measures are formulated. Both operator control models and performance models are developed by the application of Markov theory to the pilot's trajectory patterns in the state space of steering error and steering error rate.

II.   DESCRIPTION OF FLIGHT CONTROL PROBLEM

The F-106 coplanar attack simulator located at the Systems Effectiveness Branch, Aerospace Medical Research Laboratory, Wright-Patterson Air Force Base, Ohio was used to obtain data for this study. This simulator is a representation of the MA-1 fire control system (FCS) which is used by the F-106 interceptor pilot for tracking the target. The actual system is controlled by an on-board analog computer which generates a CRT display that provides information regarding the quickest steering heading to the target, range between the target and the interceptor, bank angle, speed of the interceptor, time to fire and other necessary information. The simulator is almost identical to the actual MA-1 FCS except that the elements of pitch and acceleration are not included because of core limitations. The simulator consists of an IBM 360 model 50 digital computer, I/O equipment, display console and control stick. The operator sits in a chair, moves the control stick, and observes the results on the CRT display. Calculations of problem dynamics, display control and data collection are accomplished by the computer.

The operator's task is to observe the aircraft steering error, roll angle and other data on the display and to direct the aircraft along the required heading. When the aircraft is within radar range of the target, the operator adjusts his radar antenna azimuth and range gate controls to accomplish lock-on. After radar lock-on, the operator continues to direct the aircraft heading by observing the steering error display. When the attack aircraft is within firing range of the target, the operator depresses the arming trigger which allows subsequent automatic firing of the missile. The operator's primary task at all times is to arrive at and maintain the proper heading. Various secondary tasks are also performed such as obtaining lock-on and arming the weapon. (Reference 1 describes the simulator layout in detail.)

The operator has a dual grip control stick which contains all operator controls required for the attack mission. The control stick is moved laterally to control the aircraft's roll angle. Since pitch angle is not included in the simulation, heading is strictly a function of roll angle and the simulation

dynamics, as discussed in Section IV. The left hand grip is
hinged to allow both lateral and fore and aft motion with respect
to the stick. The lateral motion controls the antenna azimuth
and the fore and aft controls the radar range gate. A trigger on
the left hand grip (LT) is used to switch from manual to automatic
radar tracking, i.e., lock-on. Many operators depress the LT
several times as they adjust antenna azimuth and range gate since,
if the adjustments are correct, the LT actuates radar lock-on
immediately. On the right hard grip is a trigger (RT) which is
used to arm and automatically fire the missile. It is depressed
at any time after lock-on is achieved.

Description of Display

The simulator display is a CRT surrounded by a radar
scope face plate such as is found on the MA-1 Fire Control
System. The simulator generates displays for prelock-on and post
lock-on as indicated in Table 1. A sketch of the display appears
in Figure 1.

The Range Indicator Lights show the numerical value
of the range scale being used. Range can assume values of
4, 16, 40, 80 and 200 nautical miles. The range value displayed
is chosen automatically on the basis of the minimum scale needed
to contain the target position in range; for example, a target at
38 miles requires a range scale of 40. The Fighter Wings appear
as a horizontal line intersecting the center of the display. The
Artificial Horizon appears as a line through the center of the
display such that the angle between it and the Fighter Wings line
represents the roll attitude of the aircraft. The Reference Circle
is a 3/16 inch diameter circle around the center of the display.
The Steering Dot appears on the Artificial Horizon line at a
distance from the Reference Circle representing the amount of
steering error for which the pilot must correct. The Target Marker
Circle, 3/4 inch in diameter, is positioned where radar video of
the target is expected. The Target Video appears as a 1/4 inch
line inside the Target Marker Circle. The Range Gate Indicator is
a U-shaped marker controlled by moving the left hand grip. To
attempt lock-on, the pilot moves the Range Gate Indicator inside
the Target Marker Circle until it encircles the Target Video line.
The B-Sweep line extends vertically from the top to the bottom
of the CRT. It is moved horizontally by the pilot using the

4

TABLE 1. DISPLAYS GENERATED FOR EACH PHASE

Spotlight and Lock-on Phases	Attack Phase
Range Indicator Lights	Range Indicator Lights
Fighter Wings	Fighter Wings
Reference Circle	Reference Circle
Artificial Horizon	Artificial Horizon
Steering Dot	Steering Dot
Target Video	Target Video
Target Marker Circle	B-Sweep Line
Range Gate Indicator	Time-to-Go-to-Fire Circle
B-Sweep Line	Big X
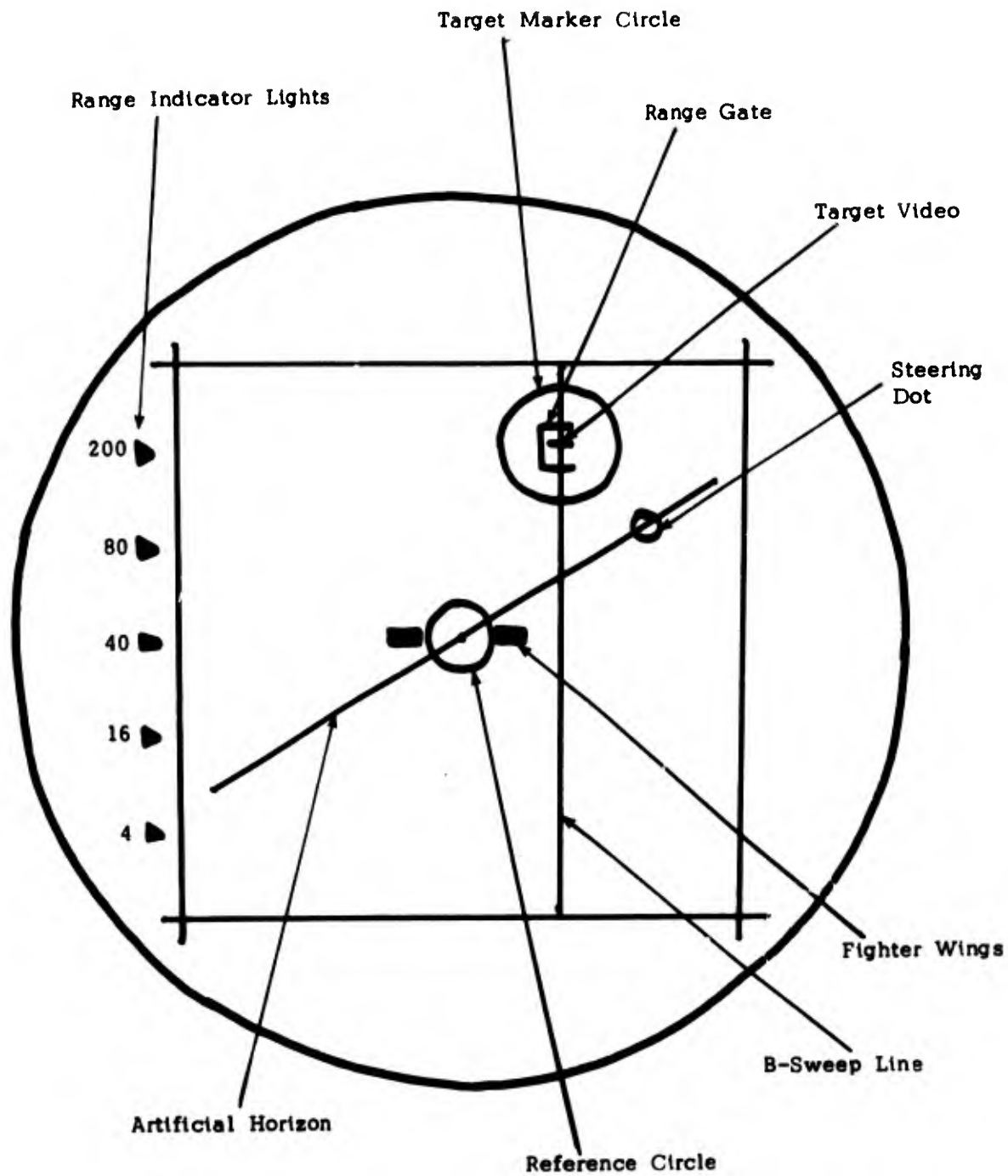
FIGURE 1. SIMULATOR DISPLAY

6

antenna azimuth control on the left hand grip. It indicates the bearing of the radar antenna and must be aligned with the Target Marker Circle to obtain lock-on.

Once lock-on is obtained, a Time-to-Go-to-Fire Circle appears on the display. Initially 3 inches in diameter, it begins to shrink at 20 seconds prior to firing. The Time-to-Go-to-Fire Circle provides the operator with a sense of criticality as the time to firing approaches. When a hit occurs, a large "X" appears on the display.

III.   DESCRIPTION OF EXPERIMENTAL DATA

The experimental data for this study comprise 188 missions performed on the F-106 simulator by nine operators of varying experience levels. General trends noted in the data are discussed first, then the actual data is presented.

General Trends in the Data

The three phases of the flight control problem, i.e., spotlight, lock-on and attack appear to require several different steering control policies. During the spotlight phase, the pilot must, in general, correct for a large steering error; consequently, he rolls to and maintains a large roll angle until the steering error is reduced substantially. Because the maximum roll possible on the simulator is $\pm 75^\circ$, the operator often uses this hard limit to produce a "saturation" type of steering control. To reduce the steering error further, the operator reduces the aircraft's roll angle to lower the turning rate. This is a monotonic or "linear" type of control policy, since the steering error is maintained as a direct function of roll angle as both are decreased simultaneously toward zero. Finally, when the steering error is small, a "limit cycle" appears to exist. Limit cycles are caused by changes in the control policy and/or controlled object as a function of the error amplitude. Possible causes of the limit cycle patterns are:

1. The operator's inability to discern the steering error or the rate of change of steering error on the display,

2. His opinion of the importance (or lack of importance) in reducing the error further, and

3. His inability to move the control stick in small increments.

In the lock-on phase, the operator must manipulate his range gate and antenna azimuth controls while maintaining a small steering error. Concentrating on these secondary tasks results, in general, in an increase in the size of the "limit cycle". (Note that we are only guessing that a limit cycle exists. Its existence has not been proven mathematically.)

8

During the attack phase, the size of the steering error limit cycle decreases, since only the primary task remains. It is of interest to note that the amplitude increases again when the Time-to-Go-to-Fire Circle begins to shrink, an action which seems to startle the pilot.

There are several problems involving the simulator hardware. One that is apparent from the data is a time lag of several seconds between a change in roll angle and the corresponding change in steering error. A second problem is the existence of a random drift of between 5 and 10 degrees in the stick's center position. Both of these problems were present when the experimental data were collected.

Detailed Description of the Data

Nine operators were selected from three experience categories. One category consisted of operators highly practiced on the simulator and knowledgeable in the simulator display. A second category included operators who were moderately experienced with the simulator; and the third consisted of operators with little exposure to the simulator. The individuals in these categories were selected to obtain a range of performances. Individual category data were not used for any scoring purpose and, in fact, considerable modification of operator ranking based on demonstrated performance was possible after the data runs were analyzed.

Three types of problems were presented to each operator. The initial target position was 100 and 50 nautical miles east and north respectively from an arbitrary reference point in each problem. The target's heading was maintained at 270° during the simulated mission, and the attacker's initial heading was 90°. Table 2 shows the initial conditions for each of the three problems.

Problem A was used as a learning problem for each operator. It was presented first and only once to the operators experienced with the simulator. The less experienced operators were given additional Problem A runs to become familiar with the simulator. Problem A is considered to be the easiest because of the relatively large (50 mile) initial range which provides a

9

TABLE 2.   SIMULATOR FLIGHT PROBLEMS

PROBLEM CODE	INITIAL POSITION OF ATTACK AIRCRAFT		INITIAL RANGE (NM)	INITIAL TIME TO GO (SEC)	TIME TO LOCK-ON RANGE (SEC)
	X_0 (NM)	Y_0 (NM)			
A	60	20	50	115	50.2
B	80	65	25	45	0.0
C	75	50	25	50	0.0

Initial Target Position X_0 = 100 NM

Y_0 =   50 NM

10

time-to-fire (missile launch) of 115 seconds and a time-to-lock-on of 50 seconds. Figure 2 is a plot of the attacker and target trajectories in the horizontal plane.

Problem B is more difficult than Problem A since the aircraft is initially located within radar lock-on range. Figure 3 is a plot for Problem B of the attacker and target trajectories in the horizontal plane. The attacker must turn immediately to reduce his steering errors and simultaneously attempt radar lock-on. Following lock-on, he has a short time to reduce the steering error and arm his weapon.

Problem C is the third type problem presented to each operator. Figure 4 provides a plot of the attacker and target paths in the horizontal plane. This situation is a head-on attack with small initial steering errors but a very short range and rapid closure. Thus, the operator must achieve lock-on rapidly. A premium is placed on being able to achieve radar lock-on without greatly disturbing the steering error.

The results of the experimental data are presented in Table 3. Group 1 operators (1, 2 and 3) had considerable experience with the simulator; Group 2 operators (4, 5 and 6) were moderately experienced; and Group 3 operators (7, 8 and 9) had the least experience with the simulator. The trials are presented in the order that each operator performed them. The data is expressed in terms of steering error and steering error rate at the time-of-fire (missile launch). The performance level was assigned on the basis of the deviation from the origin in the error-error rate plane.

It is desirable to include steering error rate as well as steering error in evaluating operators and individual runs because the two variables give a more complete description of the control policy than just steering error alone. However, it is difficult to compare errors with error rates; for instance, how do we evaluate a small error with a large error rate against a large error with a small error rate? One approach to this problem is to examine the data in two-space and see if an empirical measure presents itself. Steering error and error rate data for each run

FIGURE 2. REFERENCE (HIGH PERFORMANCE) TRAJECTORY
FOR SIMULATION PROBLEM A
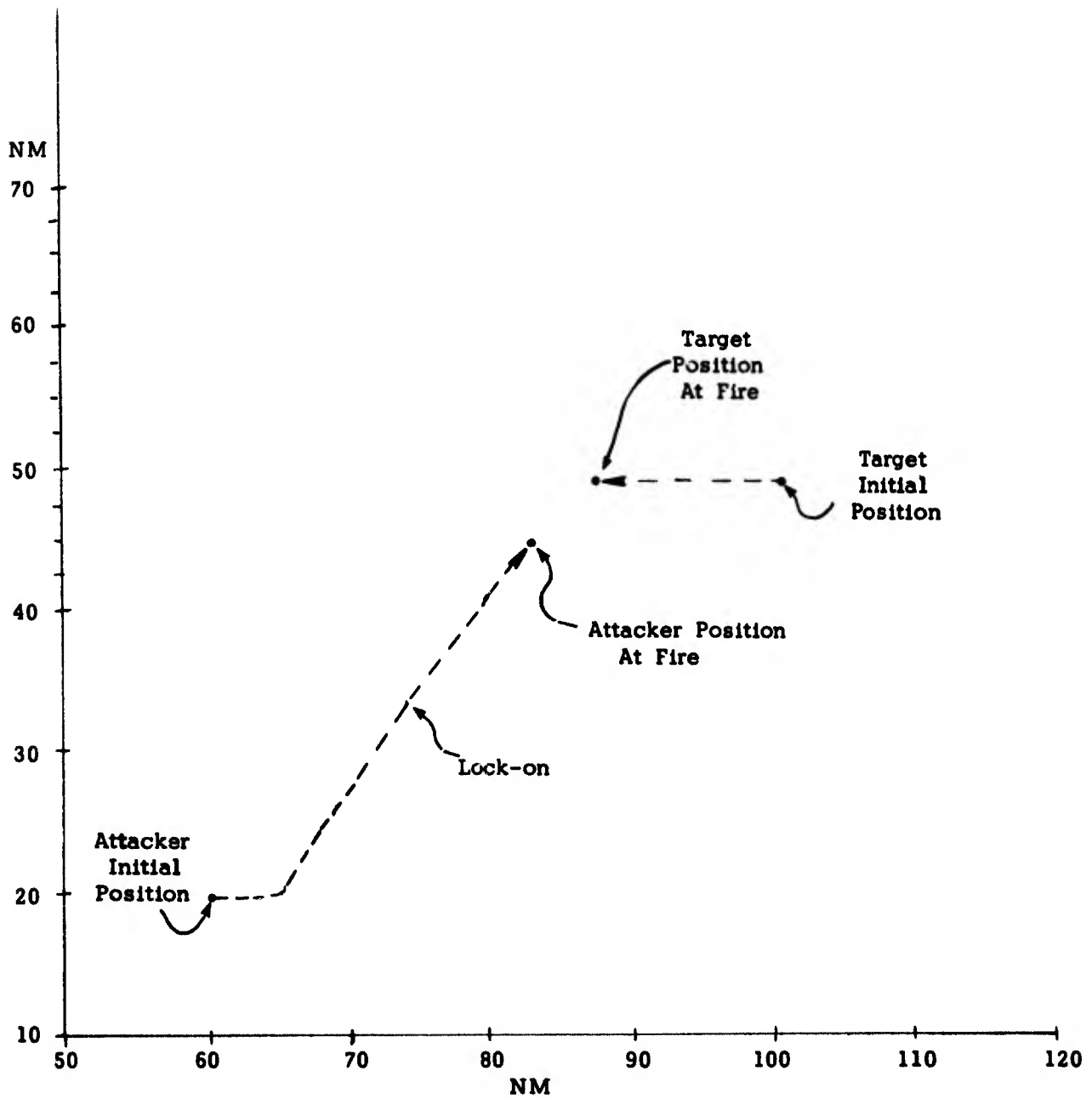
FIGURE 3. REFERENCE (HIGH PERFORMANCE) TRAJECTORY
FOR SIMULATION PROBLEM B

13
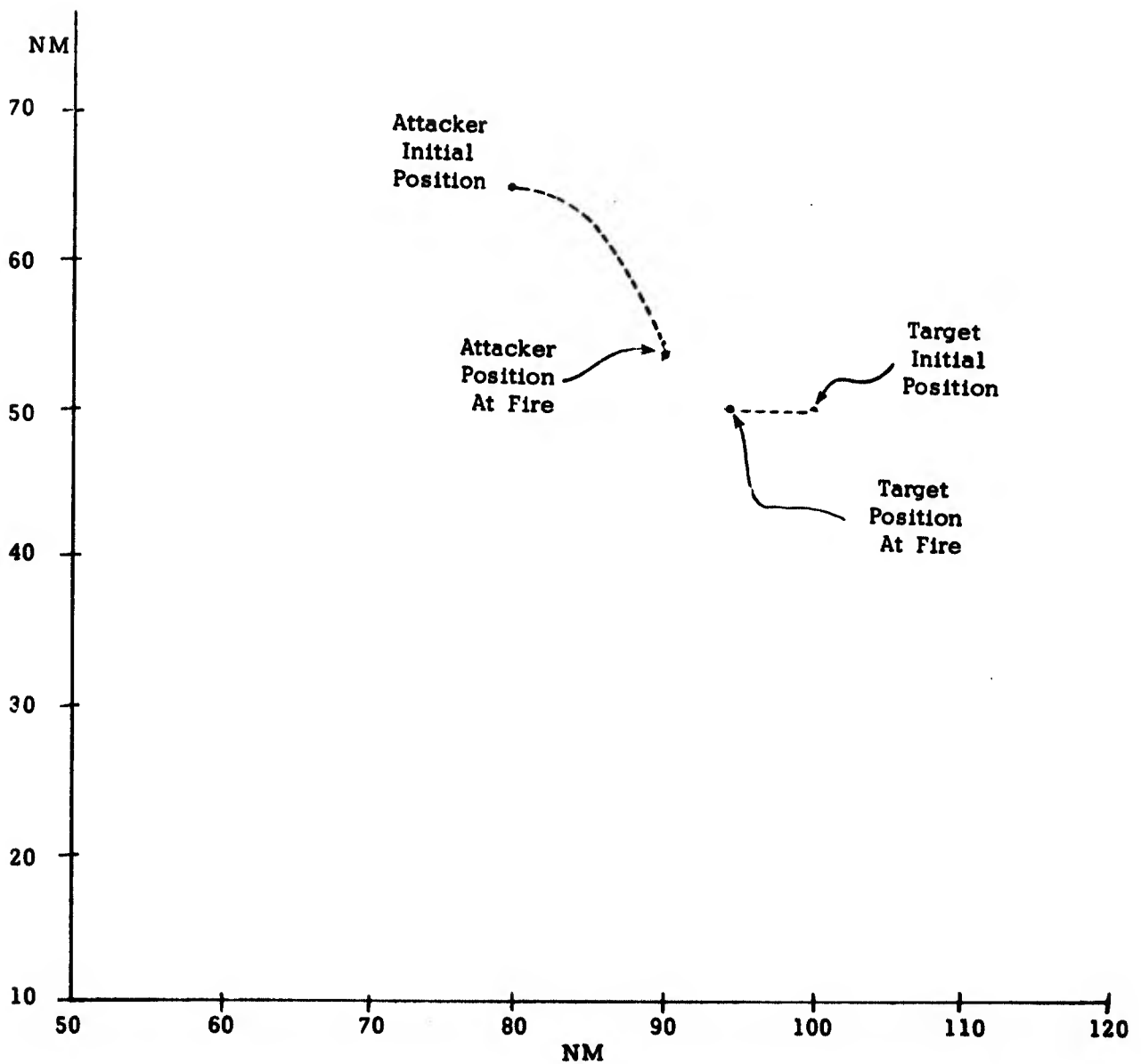
FIGURE 4. REFERENCE (HIGH PERFORMANCE) TRAJECTORY FOR SIMULATION PROBLEM C
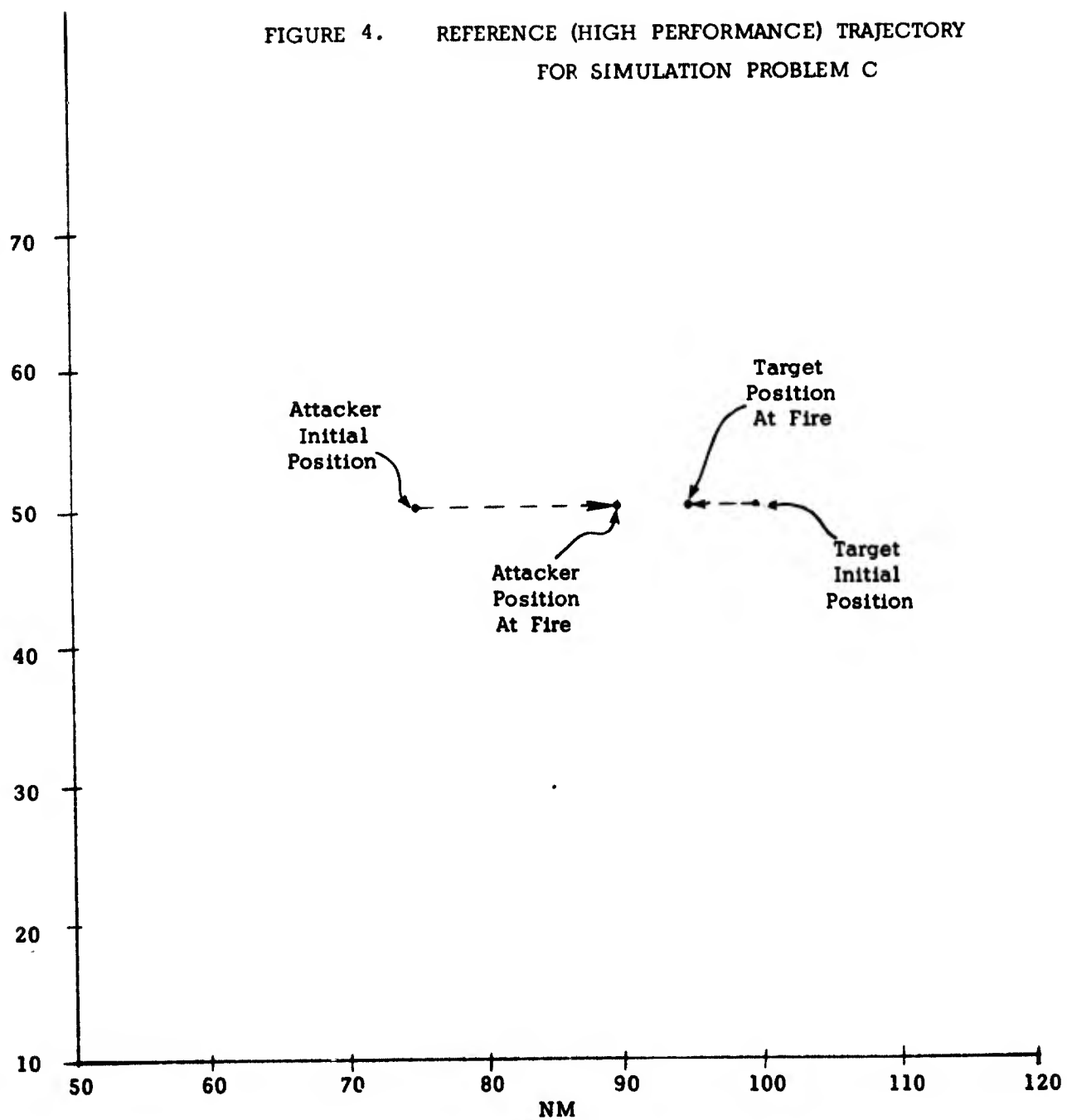
TABLE 3. OPERATOR PERFORMANCE DATA

Operator	Problem Type	Steering Error (degrees)	Steering Error Rate (deg/sec)	Performance Rating	Computer Data Code
1	A	-5.2	0.5	1	111
1	B	1.8	0.5	1	1121
1	B	1.3	0.2	1	1122
1	B	1.0	0.1	1	1123
1	C	1.0	0.1	1	1131
1	C	1.2	0.3	1	1132
1	C	1.0	0.1	1	1133
2	A	2.4	0.5	1	123
2	B	1.8	0.2	1	1221
2	B	-0.6	0.1	1	1222
2	B	1.3	0.1	1	1223
2	C	-2.7	0.3	1	1231
2	C	2.0	0.3	1	1232
2	C	0.7	0.3	1	1233
3	A	27.6	10.3	4	131
3	A	-28.4	11.5	4	132
3	A	5.3	4.0	3	133
3	B	-9.7	4.5	4	1321
3	B	-12.9	9.4	4	1322
3	B	10.4	3.0	3	1323
3	C	15.7	3.0	3	1331
3	C	8.6	2.7	3	1332
3	C	-7.6	0.3	1	1333
4	A	-0.4	1.7	2	211
4	B	0.0	0.1	1	2121
4	B	1.4	1.7	2	2122
4	B	2.1	0.2	1	2123
4	C	-3.9	1.5	2	2131
4	C	-0.3	1.4	2	2132
4	C	0.1	0.7	1	2133
5	A	-4.8	2.3	3	221
5	A	7.5	4.6	4	222
5	A	-7.7	1.5	2	223
5	B	5.8	1.4	2	2221

15

TABLE 3.   OPERATOR PERFORMANCE DATA (CONTD)

Operator	Problem Type	Steering Error (degrees)	Steering Error Rate (deg/sec)	Performance Rating	Computer Data Code
5	B	3.C	0.4	1	2222
5	B	2.4	0.6	1	2223
5	C	-77.4	5.6	4	2231
5	C	-1.2	0.9	2	2232
5	C	2.5	0.3	1	2233
6	A	-58.6	2.4	4	231
6	A	-45.2	8.4	4	232
6	A	16.6	3.5	3	233
6	A	-5.9	7.9	4	234
6	A	-1.0	2.6	3	235
6	B	-0.4	5.7	4	2321
6	B	48.3	2.4	4	2322
6	B	9.5	6.1	4	2323
6	C	-27.4	8.9	4	2331
6	C	6.5	8.0	4	2332
6	C	14.6	5.0	4	2333
7	A	4.4	10.2	4	311
7	A	-51.5	3.0	4	312
7	A	-23.8	7.7	4	313
7	A	-1.8	0.9	2	314
7	A	-20.7	4.6	4	315
7	B	16.7	4.9	4	3121
7	B	8.6	7.6	4	3122
7	B	-12.7	5.7	4	3123
7	C	90.0	0.0	4	3131
7	C	-18.7	8.7	4	3132
7	C	1.6	8.0	4	3133
8	A	-90.0	0.0	4	321
8	A	-90.0	0.0	4	322
8	A	7.2	0.1	1	323
8	A	-17.5	3.1	3	324
8	A	-23.0	2.0	3	325
8	A	-5.1	1.1	2	326
8	A	-26.0	2.0	3	327
8	A	-26.2	6.8	4	328
8	A	-2.0	0.9	2	329

16

TABLE 3. OPERATOR PERFORMANCE DATA (CONTD)

Operator	Problem Type	Steering Error (degrees)	Steering Error Rate (deg/sec)	Performance Rating	Computer Data Code
8	B	90.0	0.0	4	3221
8	B	4.4	1.3	2	3222
8	B	-90.0	0.0	4	3223
8	C	-17.3	1.0	2	3231
8	C	-21.3	8.2	4	3232
8	C	-30.2	8.3	4	3233
9	A	2.5	4.0	3	331
9	A	-2.8	1.2	2	332
9	A	12.2	12.8	4	333
9	A	-9.3	5.0	4	334
9	A	12.8	6.1	4	335
9	B	-37.3	8.7	4	3321
9	B	0.6	3.1	3	3322
9	B	26.6	6.6	4	3323
9	C	21.1	8.7	4	3331
9	C	-26.0	6.4	4	3332
9	C	3.9	6.0	4	3333

are plotted in Figure 5. The absolute value of the steering error
(ψ_e) data taken directly from Table 3 is plotted on the abscissa.
Likewise, the absolute value of the aircraft steering error rate
($\dot{\psi}_e$) is plotted on the ordinate. Using this plot, we can now
formulate a quantitative performance measure for each run.

In Figure 5, four performance regions have been
identified arbitrarily based on grouping of runs in the ψ - $\dot{\psi}$ state
space and are indicated by dotted lines. A mathematical measure
which weights and adds ψ and $\dot{\psi}$ according to their relative
importance to performance would be more appropriate here, instead
of an arbitrary selection of regions. Table 4 shows the boundaries
for each of the four regions. Table 5 shows the portion of each
operator's runs that falls in each performance category and the
resulting operator ordering. The "Operator Performance Rating"
assigned in Table 5 is based on the region in which at least 50%
of the runs fall. For instance, operator 3 is assigned a rating
of "3" since 56% of his runs are within the tolerances for
Region 3. In Table 3, performance is assigned based on the
results of the individual run. The performance regions 1, 2, 3
and 4 can be considered to be excellent, good, fair and poor,
respectively.

Trajectories for Problem A

Table 6 presents Run 111, an excellent flight by
operator 1, in tabular form. PSI and PSIDOT are the steering
error and error rate, respectively, expressed in degrees. Figure 6
shows the trajectory for the spotlight phase; Figure 7 shows the
lock-on and attack phases, and Figure 8 shows the roll angle
control policy as a function of time. The technique used by
operator 1 is to roll the aircraft rapidly to the maximum roll angle
of -75° (285°). When the steering error has decreased to about
-10°, he begins to roll back to a nearly wings level attitude. In
the lock-on and attack phases, he oscillates around the origin,
but manages to maintain small values of steering error and error
rate. The discontinuities shown in Figure 7 are probably caused
by the simulator hardware. This run demonstrates excellent
control: the operator reduces the steering error rapidly during the
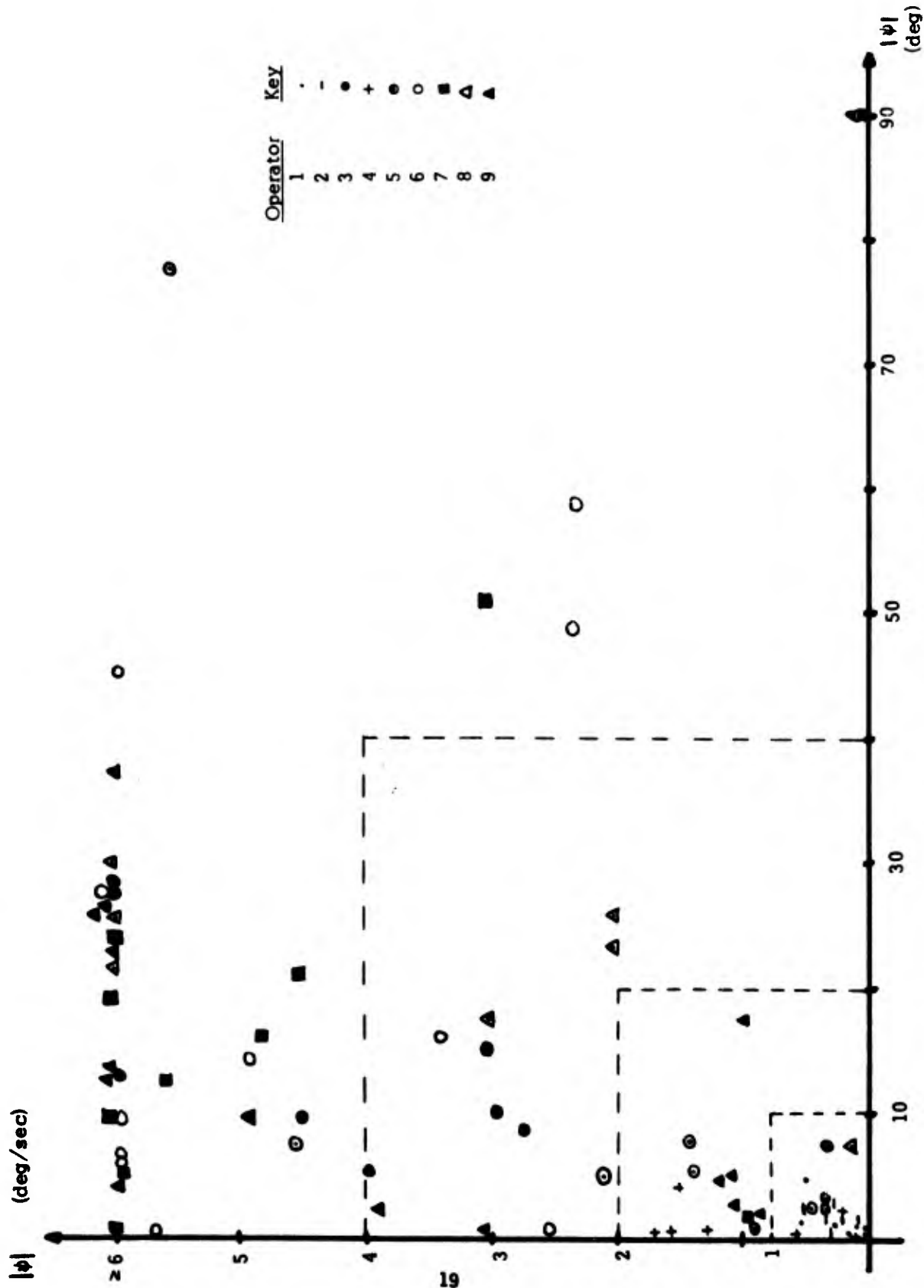
FIGURE 5. OPERATOR SCORE DATA

TABLE 4.　BOUNDARIES OF PERFORMANCE REGIONS

Region	ψ (degrees)	$\dot{\psi}$ (degrees/sec)
1	$\psi \le 10$	$\dot{\psi} \le 0.8$
2	$10 < \psi \le 20$	$0.8 < \dot{\psi} \le 2.0$
3	$20 < \psi \le 40$	$2.0 < \dot{\psi} \le 4.0$
4	$\psi > 40$	$\dot{\psi} > 4.0$

TABLE 5.　OPERATOR ORDERING

Operator	Fraction of Runs in Performance Region				Operator Performance Rating
	1	2	3	4	
1	1.00				1
2	1.00				1
3	.12		.44	.44	3
4	.43	.57			2
5	.33	.33	.12	.22	2
6			.18	.82	4
7		.09		.91	4
8	.06	.27	.20	.47	3
9		.09	.18	.73	4

　　　　　Excellent　Good　　Fair　　Poor

Ordering of Operators from Best to Worst:

　　(1, 2, 4, 5, 3, 8, 9, 6, 7)

20

TABLE 6. DATA FOR RUN 111

RUN CODE 111

TIME	TIME TC GO	FSI	RCLL	PSIDOT
1.03	113.43	-90.00	21.5E	0.0
1.50	113.35	-90.00	31.45	0.0
1.97	112.99	-90.00	41.04	0.0
2.44	112.55	-90.00	40.68	0.0
2.90	112.20	-90.00	24.15	C.C
3.37	111.80	-90.00	6.53	0.0
3.84	111.41	-90.0C	349.7C	0.0
4.31	111.01	-90.0C	332.42	0.0
4.78	11C.62	-90.0C	315.16	0.0
5.25	110.58	-90.0C	297.67	C.C
5.72	110.18	-90.00	285.0C	0.0
6.19	1C9.78	-90.0C	285.CC	C.C
6.66	109.38	-90.00	285.0C	0.0
7.12	1C8.96	-90.0C	285.0C	0.0
7.59	108.55	-90.0C	285.CC	C.0
8.06	108.13	-90.0C	285.00	0.0
8.53	1C8.04	-90.0C	285.CC	0.0
9.00	107.61	-90.00	285.0C	0.0
9.47	107.17	-9C.0C	285.0C	0.0
9.94	106.73	-90.0C	285.CC	C.0
10.41	106.28	-90.00	285.00	0.0
10.88	105.83	-5C.0C	285.CC	0.0
11.34	106.05	-90.00	285.0C	2.79
11.81	105.59	-90.0C	285.00	5.60
12.28	105.13	-84.78	285.CC	7.84
12.75	104.66	-79.52	285.0C	10.64
13.22	1C4.19	-75.26	285.CC	10.68
13.69	103.72	-6'.99	285.00	10.68
14.16	103.25	-6..71	285.CC	11.21
14.63	102.77	-59.45	285.CC	1C.74
15.10	1C2.30	-54.19	285.00	10.70
15.56	1C1.82	-49.51	285.CC	10.73
16.07	101.31	-44.27	285.0C	10.76
16.57	100.79	-38.64	285.0C	11.22
17.07	100.28	-33.CC	285.CC	11.27
17.57	99.77	-27.36	285.00	11.22
18.07	99.26	-21.73	285.CC	10.75
18.58	98.75	-16.09	285.CC	10.75
19.08	98.59	-11.39	285.0C	10.21
19.58	99.08	-5.76	286.33	8.81
20.08	97.57	-1.21	296.37	7.32
20.55	97.1C	1.26	3C8.55	5.02
21.02	96.63	2.82	320.55	3.05
21.49	96.17	3.83	331.49	1.98
21.95	95.7C	4.5C	339.70	1.31
22.42	95.23	4.96	344.77	0.84
22.89	94.77	5.27	352.15	0.54
23.36	94.30	5.41	356.53	0.38
23.83	93.83	5.51	353.C6	0.26
24.29	93.37	5.67	354.41	0.18
24.76	92.90	5.76	359.63	0.11
25.23	92.44	5.75	1.47	0.02
25.70	91.97	5.72	1.31	0.47
26.16	91.50	5.7C	1.16	C.46
26.83	90.72	6.64	1.13	0.47
27.10	90.25	6.61	1.12	C.46

TABLE 6. DATA FOR RUN 111 (CONTD)

27.57	89.79	6.59	1.12	-0.05
28.04	89.32	6.56	1.11	-0.05
28.50	88.86	6.54	1.13	-0.05
28.97	88.40	6.52	1.19	-0.05
29.44	87.93	6.49	1.24	-0.05
29.90	87.47	6.47	1.29	-0.05
30.37	87.00	6.44	1.35	-0.05
30.84	86.54	6.42	1.41	-0.05
31.31	86.07	6.39	1.47	-0.05
31.78	85.61	6.37	1.51	-0.05
32.24	85.15	6.35	1.55	-0.05
32.71	84.68	6.32	1.60	-0.05
33.18	84.22	6.30	1.66	-0.05
33.64	83.75	6.27	1.70	-0.05
34.11	83.25	6.25	1.77	-0.05
34.58	82.82	6.23	1.82	-0.05
35.05	82.36	6.20	1.87	-0.05
35.51	81.90	6.18	1.91	-0.05
35.98	81.43	6.15	1.95	-0.06
36.45	80.97	6.13	2.01	-0.08
36.92	80.51	6.08	2.05	-0.09
37.38	80.04	6.03	2.11	-0.11
37.85	79.58	5.98	2.17	-0.11
38.32	79.11	5.93	2.23	-0.11
38.79	78.65	5.88	2.28	-0.11
39.26	78.18	5.83	2.33	-0.11
39.72	77.72	5.78	2.38	-0.11
40.19	77.25	5.73	2.44	-0.11
40.66	76.79	5.68	2.49	-0.10
41.13	76.32	5.63	2.54	-0.10
41.60	75.86	5.59	2.60	-0.10
42.06	75.40	5.54	2.66	-0.10
42.53	74.93	5.49	2.70	-0.11
43.00	74.47	5.44	2.76	-0.11
43.46	74.01	5.39	2.80	-0.11
43.93	73.54	5.34	2.86	-0.11
44.40	73.07	5.29	2.91	-0.11
44.87	72.61	5.24	2.97	-0.12
45.34	72.14	5.18	3.03	-0.14
45.80	71.67	5.11	3.06	-0.15
46.27	71.21	5.03	3.10	-0.16
46.74	70.74	4.96	3.14	-0.16
47.20	70.28	4.89	3.21	-0.16
47.67	69.81	4.81	3.26	-0.16
48.14	69.34	4.74	3.32	-0.16
48.61	68.88	4.67	3.36	-0.16
49.08	68.41	4.59	3.43	-0.16
49.54	67.95	4.52	3.48	-0.16
50.01	67.48	4.45	3.53	-0.16
50.48	67.02	4.37	3.59	-0.16
50.94	66.55	4.30	3.64	-0.16
51.41	66.08	4.22	3.71	-0.16
51.88	65.62	4.15	3.84	-0.16
52.35	65.15	4.08	3.98	-0.18
52.82	64.68	3.99	4.14	-0.19
53.28	64.22	3.89	4.30	-0.21
53.75	63.75	3.79	4.24	-0.21
54.22	63.29	3.69	4.07	-0.20
54.68	62.82	3.60	3.92	-0.19
55.15	62.36	3.52	3.88	-0.19
55.62	61.89	3.43	4.54	-0.21

22

TABLE 6.   DATA FOR RUN 111 (CONTD)

56.12	61.39	3.33	5.14	-0.23
56.63	60.89	3.19	5.66	-0.26
57.13	60.39	3.06	6.11	-0.30
57.63	59.89	2.90	6.54	-0.31
58.15	59.36	2.73	6.86	-0.33
58.69	58.83	2.55	7.16	-0.34
59.22	58.30	2.36	7.03	-0.31
59.76	57.76	2.18	5.06	-0.25
60.29	57.23	2.07	3.32	-0.17
60.83	56.69	2.01	1.75	-0.05
61.36	56.16	1.99	0.27	-0.03
61.90	55.62	1.99	358.82	0.03
62.44	55.09	2.01	357.98	0.06
62.97	54.55	2.07	357.82	0.07
63.51	54.02	2.12	358.57	0.06
64.04	53.48	2.14	359.66	0.02
64.58	52.94	2.14	0.74	-0.02
65.11	52.41	2.12	1.84	-0.07
65.65	51.87	2.07	2.89	-0.12
66.18	51.34	2.00	3.73	-0.16
66.72	50.81	1.89	4.55	-0.21
67.25	50.27	1.77	5.36	-0.25
67.78	49.74	1.63	6.13	-0.29
68.31	49.21	1.46	6.90	-0.31
68.85	48.68	1.28	6.76	-0.32
69.36	48.16	1.12	6.44	-0.30
69.83	47.69	0.97	5.54	-0.23
70.30	47.22	0.87	2.98	-0.15
70.77	46.75	0.83	0.25	-0.04
71.25	46.28	0.83	357.51	0.03
71.72	45.80	0.90	357.68	0.03
72.19	45.33	0.92	1.12	-0.01
72.67	44.86	0.89	3.22	-0.10
73.14	44.38	0.81	4.42	-0.16
73.61	43.91	0.71	4.39	-0.19
74.08	43.44	0.62	3.83	-0.18
74.56	42.97	0.54	3.67	-0.17
75.03	42.50	0.47	3.52	-0.16
75.50	42.02	0.39	3.32	-0.15
75.97	41.55	0.32	3.07	-0.14
76.44	41.08	0.26	2.80	-0.12
76.92	40.61	0.21	2.51	-0.62
77.39	40.14	0.16	2.25	-0.60
77.86	39.81	-0.85	2.00	-0.59
78.32	39.34	-0.87	1.74	-0.58
78.79	38.87	-0.90	1.47	-0.05
79.25	38.41	-0.92	1.20	-0.04
79.71	37.94	-0.94	0.94	-0.03
80.18	37.48	-0.95	0.68	-0.02
80.64	37.01	-0.95	0.50	-0.01
81.11	36.54	-0.95	0.51	0.0
81.57	36.08	-0.95	0.53	0.0
82.04	35.61	-0.95	0.60	0.0
82.50	35.14	-0.95	0.66	-0.01
82.97	34.68	-0.95	0.73	-0.01
83.43	34.21	-0.96	0.80	-0.01
83.90	33.74	-0.96	0.88	-0.01
84.37	33.28	-0.96	0.95	-0.01
84.83	32.81	-0.96	1.01	-0.03
85.30	32.34	-0.98	1.10	-0.03
85.76	31.87	-1.01	0.98	-0.03

TABLE 6. DATA FOR RUN 111 (CONTD)

86.23	31.41	-1.01	0.73	-0.02
86.69	30.94	-1.01	0.46	0.0
87.16	30.47	-1.01	0.22	0.0
87.63	30.00	-1.01	359.97	0.0
88.09	29.54	-1.01	359.70	0.0
88.56	29.07	-1.01	359.44	0.0
89.03	28.60	-1.01	359.19	0.02
89.49	28.13	-1.01	358.93	0.03
89.96	27.66	-0.98	358.67	0.04
90.42	27.20	-0.96	358.52	0.05
90.89	26.73	-0.93	358.57	0.05
91.35	26.26	-0.91	358.63	0.05
91.82	25.80	-0.89	358.69	0.05
92.28	25.33	-0.86	358.75	0.05
92.75	24.86	-0.84	358.74	0.05
93.22	24.40	-0.81	358.67	0.05
93.68	23.93	-0.79	358.60	-0.48
94.15	23.46	-0.77	358.51	-0.48
94.62	22.99	-1.73	358.42	-0.48
95.08	22.52	-1.71	358.31	-0.48
95.55	22.05	-1.68	358.26	0.05
96.02	21.59	-1.66	358.21	0.06
96.48	21.12	-1.64	357.97	0.08
96.95	20.65	-1.59	357.62	0.09
97.41	20.18	-1.54	357.26	0.12
97.88	19.72	-1.49	356.91	0.13
98.35	19.25	-1.41	356.55	0.15
98.81	18.78	-1.34	356.42	0.18
99.28	18.31	-1.26	355.42	0.23
99.74	17.85	-1.15	353.70	0.27
100.21	17.38	-0.99	352.06	0.27
100.68	16.91	-0.84	355.57	0.22
101.15	16.44	-0.76	358.16	0.13
101.61	15.97	-0.74	359.39	0.05
102.08	15.50	-0.74	0.45	-0.02
102.55	15.04	-0.75	1.49	-0.56
103.01	14.57	-0.75	2.42	-0.60
103.48	14.10	-1.79	2.94	-0.63
103.94	13.63	-1.86	3.40	-0.62
104.41	13.17	-1.92	2.09	-0.06
104.87	12.70	-1.95	359.87	-0.01
105.34	12.23	-1.94	357.95	0.07
105.80	11.77	-1.88	356.24	0.15
106.27	11.30	-1.79	354.79	0.21
106.74	10.83	-1.67	354.61	0.23
107.20	10.36	-1.55	355.09	0.22
107.67	9.89	-1.45	356.12	0.19
108.14	9.42	-1.37	357.02	-0.35
108.61	8.95	-1.32	357.20	-0.37
109.07	8.49	-2.20	357.46	-0.39
109.54	8.02	-2.15	357.36	-0.38
110.01	7.55	-2.10	356.99	0.13
110.47	7.08	-2.03	356.64	0.14
110.94	6.62	-1.96	356.45	0.16
111.41	6.15	-1.88	356.30	0.16
111.87	5.68	-1.81	356.10	-1.19
112.34	5.21	-1.73	355.86	-1.19
112.81	4.77	-4.18	356.25	-1.20
113.28	4.29	-4.11	357.45	-1.23
113.76	3.81	-4.07	358.43	0.07
114.23	3.34	-4.05	359.42	0.03

TABLE 6.   DATA FOR RUN 111 (CONTD)

|				
114.70	2.86	-4.05	0.34	-0.51
115.18	2.38	-4.05	1.17	-0.54
115.65	1.90	-5.04	1.98	-0.57
116.12	1.43	-5.08	2.80	-0.62
116.60	0.95	-5.14	3.63	-0.62
117.07	0.47	-5.22	4.08	-0.68
117.54	0.0	-6.22	4.39	-0.75
117.89	-0.35	-6.29	4.62	-0.81
118.23	-0.70	-6.37	4.87	-0.23
118.58	-1.05	-6.45	5.10	-0.92
118.92	-1.40	-6.54	5.27	-0.93
119.27	-1.75	-7.56	5.39	-0.94
119.61	-2.10	-7.65	5.43	-0.93
119.95	-2.45	-7.74	5.48	-0.92
120.30	-2.80	-7.83	5.52	-0.91
120.64	-3.15	-8.82	5.56	-0.91
120.99	-3.49	-8.91	5.60	-1.57
121.33	-3.84	-9.00	5.65	0.0
121.68	-4.19	-9.99	5.70	0.0

25
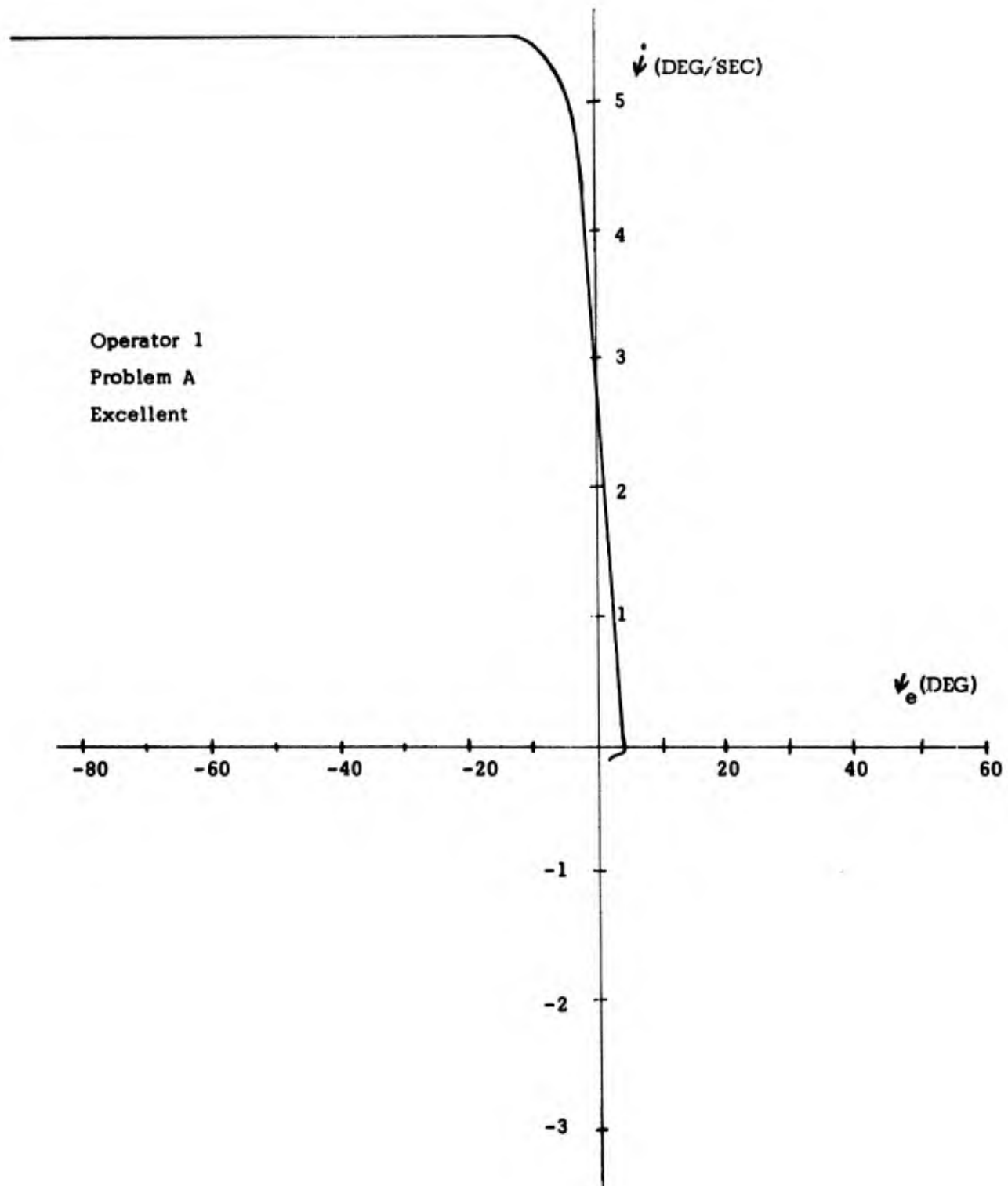
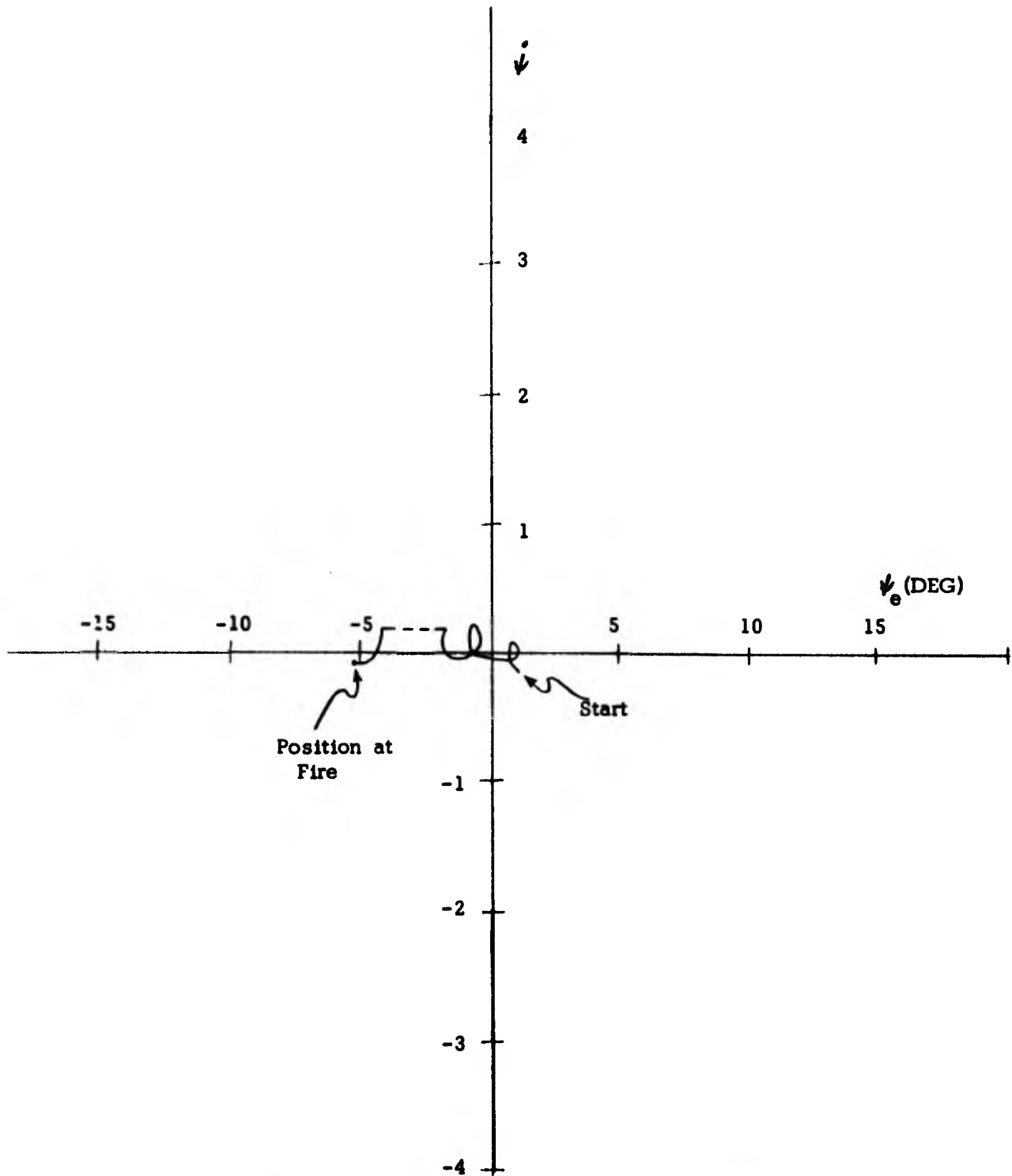FIGURE 6.   TRAJECTORY FOR RUN 111 (SPOTLIGHT PHASE)

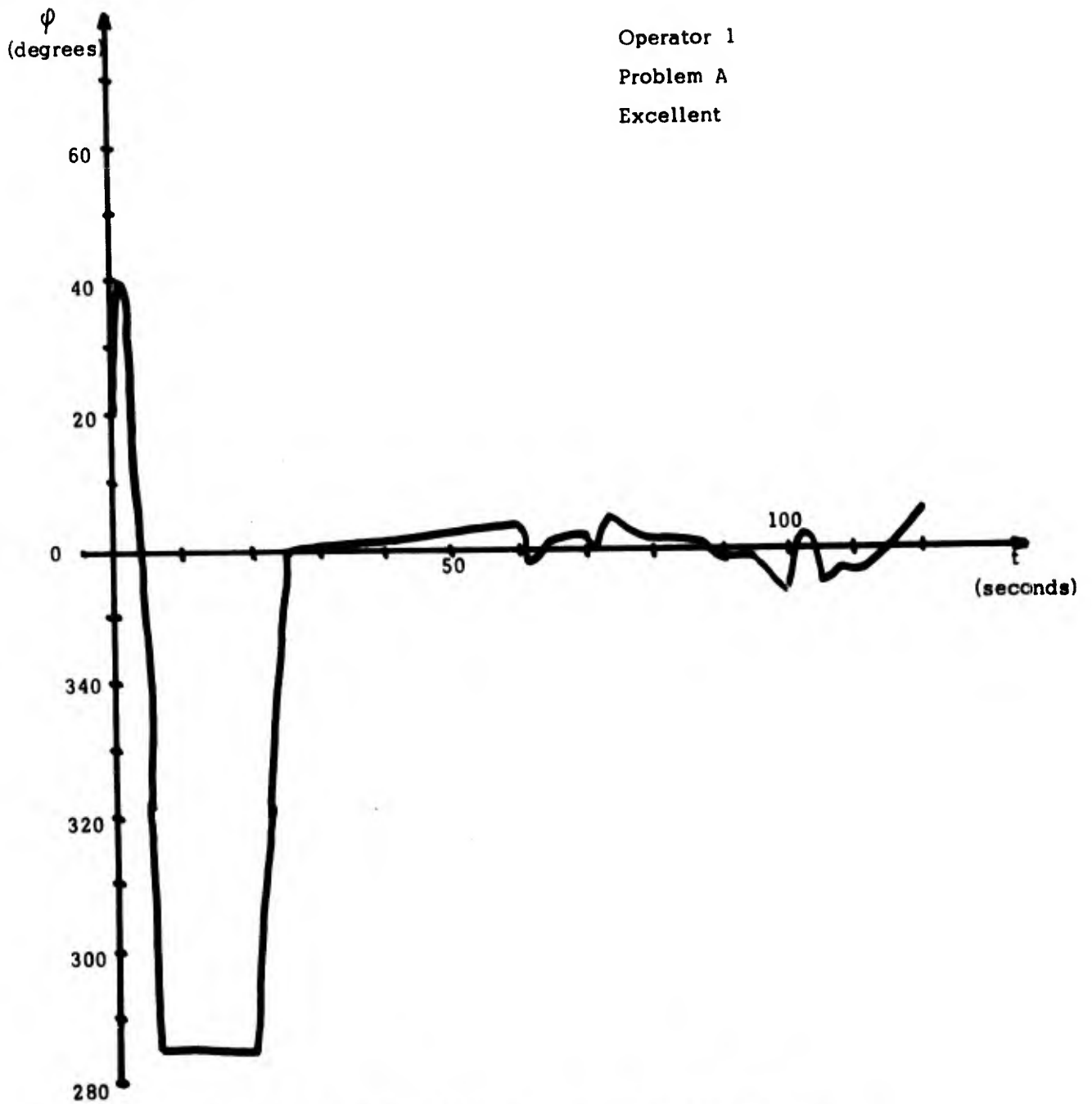FIGURE 7.   TRAJECTORY FOR RUN 111 (LOCK-ON AND ATTACK PHASES)

27

FIGURE 8. ROLL ANGLE VERSUS TIME FOR RUN 111

28

spotlight phase; he introduced little error while attempting lock-
on, and he maintained a small error and error rate during the
attack.

In contrast, Run 131 is presented (Figures 9 and 10
and Table 7) as an example of a poor run by Operator 3. His
control of the stick, as indicated by the resultant roll angle
trajectory in Figure 10 is uneven and oscillatory, rolling to -75$^{\text{o}}$,
then to +75$^{\text{o}}$, where he obtains lock-on, then back to -75$^{\text{o}}$, where
the missile is launched. He is not able to predict the effect of
stick movement on the resultant roll and steering error.

Trajectories for Problem B

Figure 11 presents the trajectory of Run 1121, an
excellent performance by Operator 1 on his first attempt at
Problem B. He rolls rapidly to the roll saturation limit of 75$^{\text{o}}$
but rolls out late at approximately 2$^{\text{o}}$ steering error producing a
7$^{\text{o}}$ overshoot. In spite of this overshoot, he recovers nicely and
produces an oscillatory response with a decreasing steering error.
Since, in Problem B, the target is initially within radar lock-on
range, the pilot's control technique is to roll to the 75$^{\text{o}}$ roll
angle hard limit and adjust the antenna azimuth and range gate
to obtain lock-on while the aircraft is against that hard limit.
This technique is useful in the simulator but unrealistic since
the actual aircraft has no hard limit.

Run 1323, shown in Figure 12, illustrates Operator
3's third attempt on Problem B and is rated fair. He also uses
the "roll-to-saturation" technique but rolls out with a large
steering error to attempt lock-on. This may be the result of an
independent motion of the stick or a plan to reduce steering error
rate during lock-on. In either case, he achieves lock-on
and subsequently rolls the aircraft back to 75$^{\text{o}}$ (apparently to
increase the rate of error reduction). Finally he rolls out at
approximately 18$^{\text{o}}$ steering error and achieves a large oscillatory
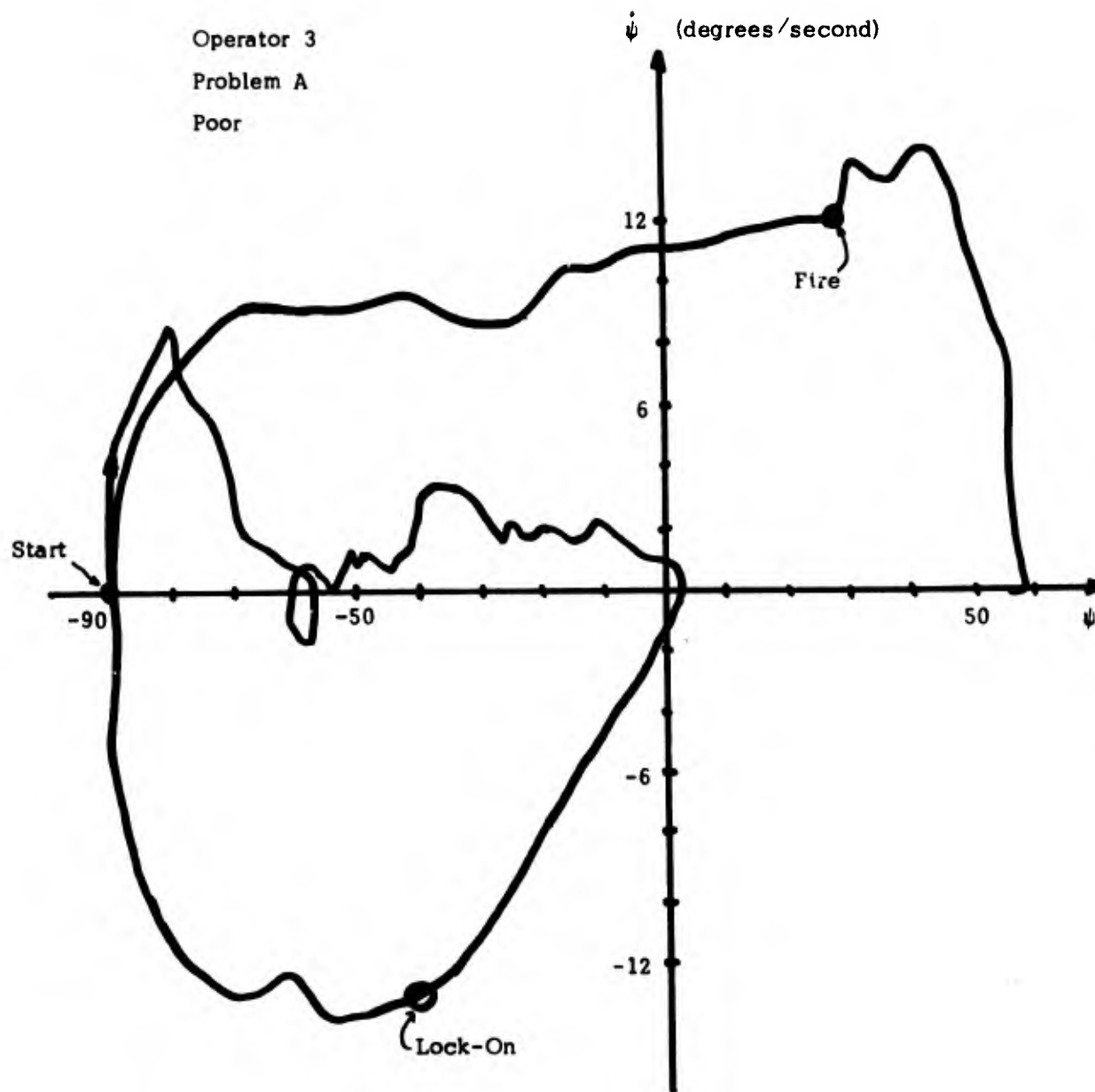cycle.

FIGURE 9.   TRAJECTORY FOR RUN 131

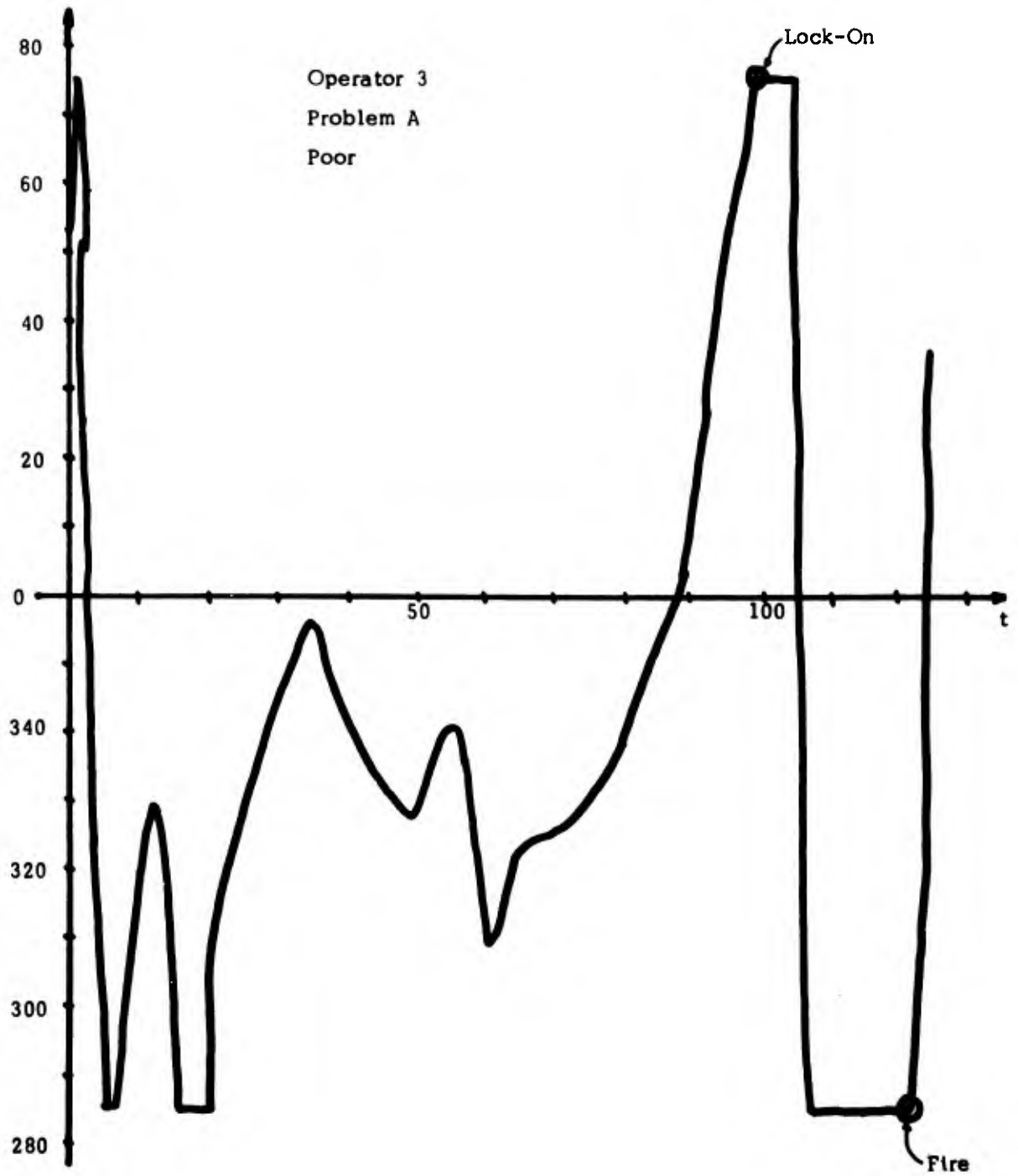FIGURE 10.   ROLL ANGLE VERSUS TIME FOR RUN 131

31

TABLE 7.   DATA FOR RUN 131

RUN CCDE   131

TIME	TIME TO GO	PSI	RCLL	PSIDOT
1.00	113.46	-90.00	53.9E	0.0
1.47	113.42	-90.CC	75.CC	0.0
1.94	113.C2	-90.0C	75.CC	U.0
2.41	112.64	-5C.CC	72.54	C.0
2.87	112.26	-90.00	50.47	0.0
3.34	111.88	-90.00	15.7E	U.0
3.81	111.51	-90.CC	24C.56	0.0
4.28	111.14	-90.00	307.48	0.0
4.75	111.11	-5C.CC	285.CC	0.U
5.22	110.73	-90.00	285.CC	0.0
5.69	110.35	-90.00	285.CC	0.0
6.16	109.95	-5C.0C	285.CC	C.C
6.63	109.56	-90.00	285.35	0.0
7.10	109.16	-5C.0C	287.54	0.0
7.57	108.75	-90.00	3C1.32	U.0
8.03	1C8.34	-90.00	309.26	0.0
8.50	108.27	-90.0C	316.79	0.0
8.97	107.85	-90.0C	321.C1	C.0
9.44	107.43	-90.00	321.88	0.0
9.91	107.01	-90.0C	322.22	0.0
10.38	1C6.5S	-90.CC	322.79	0.0
10.85	106.86	-90.0C	323.5S	0.0
11.31	1C6.43	-90.0C	324.61	0.C
11.78	106.01	-90.00	325.69	0.0
12.25	105.58	-90.0C	32S.35	0.0
12.72	1C5.16	-5C.CC	329.58	0.0
13.19	104.73	-90.00	315.56	0.0
13.66	104.31	-5C.0C	3C1.5C	C.0
14.13	1C4.25	-90.00	255.3S	0.0
14.60	103.82	-90.0C	287.51	U.0
15.07	103.3S	-90.00	285.0C	0.0
15.54	102.95	-90.0C	285.0C	0.0
16.01	102.51	-90.00	285.CC	0.0
16.47	102.07	-90.00	285.00	0.0
16.94	101.62	-9C.0C	285.CC	0.11
17.41	101.17	-90.GC	285.00	2.91
17.88	100.71	-89.8C	285.00	4.35
18.35	10C.25	-84.53	285.CC	6.93
18.82	5S.79	-81.82	285.82	8.57
19.29	100.00	-76.9E	251.6C	6.41
19.76	5S.53	-73.7E	3C0.33	5.84
20.22	99.06	-72.54	308.72	3.95
2C.6S	98.58	-7C.9C	315.04	2.87
21.16	98.11	-69.5S	319.34	2.34
21.63	97.63	-68.3S	32C.55	2.05
22.10	57.16	-68.14	321.75	1.92
22.57	96.68	-67.C4	322.96	1.81
23.C4	96.21	-65.9E	324.15	1.71
23.51	95.73	-64.9E	325.38	1.60
23.98	95.25	-64.95	32E.6C	1.5C
24.44	5S.12	-64.04	327.83	1.41
24.91	94.64	-63.17	329.05	1.33
25.38	94.16	-62.34	330.2S	1.24
25.85	93.68	-62.45	331.46	1.16
26.32	93.21	-61.70	332.6S	1.09
26.79	92.73			

32

TABLE 7.   DATA FOR RUN 131 (CONTD)

27.29	92.22	-6C.95	334.C1	1.01
27.79	91.71	-60.23	335.3C	0.93
28.30	91.19	-6C.46	336.60	0.86
28.80	90.68	-59.82	237.51	0.77
29.30	90.17	-59.23	339.21	0.69
29.80	89.66	-58.68	340.52	0.62
30.30	89.47	-59.07	341.83	0.54
30.80	88.96	-58.59	343.1C	0.04
31.31	88.44	-58.15	343.85	0.44
31.81	87.93	-58.59	344.6C	0.37
32.31	87.42	-58.19	245.92	C.29
32.81	86.90	-57.84	348.48	0.17
33.32	86.39	-57.57	350.8C	0.05
33.82	85.88	-58.25	252.54	-0.07
34.32	85.37	-58.09	355.C9	-1.73
34.82	84.85	-57.58	252.48	-1.2C
35.33	84.64	-61.04	347.16	-1.06
35.83	84.13	-60.67	243.77	-0.90
36.33	83.62	-6C.23	343.64	C.35
36.83	83.1C	-59.79	343.43	0.44
37.33	82.59	-6C.25	243.12	C.45
37.84	82.08	-59.79	242.76	0.03
38.34	81.56	-59.32	342.34	0.51
38.84	81.05	-59.73	341.87	C.53
39.34	80.54	-59.23	241.38	0.12
39.85	80.02	-58.72	240.81	0.6C
40.36	79.81	-59.08	339.79	0.65
40.86	79.29	-58.52	238.39	C.7C
41.38	78.77	-57.90	237.64	0.76
41.88	78.25	-57.29	336.81	0.83
42.38	77.74	-57.54	235.59	C.87
42.88	77.22	-56.85	335.14	0.49
43.39	76.71	-56.15	334.2C	1.00
43.89	76.20	-56.31	233.20	1.05
44.39	75.68	-55.54	332.16	1.11
44.87	75.19	-54.77	231.11	C.3C
45.34	74.71	-53.99	330.53	0.35
45.84	74.73	-55.72	230.47	0.38
46.34	74.22	-54.86	330.24	-0.01
46.85	73.70	-54.C1	329.54	1.28
47.35	73.18	-54.02	329.66	1.30
47.85	72.66	-53.14	329.38	1.32
48.35	72.15	-52.25	329.1C	1.31
48.86	71.63	-51.35	328.81	1.33
49.36	71.11	-51.39	328.52	1.35
49.86	70.60	-50.46	228.22	C.9C
50.36	70.08	-49.54	327.92	1.40
50.86	69.84	-49.54	327.63	1.41
51.37	69.32	-48.58	227.37	1.42
51.87	68.80	-47.62	327.83	1.36
52.37	68.28	-46.65	230.11	1.25
52.87	67.77	-46.81	332.98	1.11
53.38	67.25	-46.06	335.24	0.95
53.88	66.73	-45.39	337.39	0.8C
54.38	66.21	-44.79	339.54	0.67
54.88	65.70	-45.21	341.57	0.61
55.38	65.18	-44.72	340.27	0.64
55.89	64.66	-44.16	237.28	0.72
56.39	64.15	-43.51	334.82	0.88
56.89	63.63	-43.77	332.46	1.04
57.39	63.11	-42.96	330.1C	1.21

TABLE 7.   DATA FOR RUN 131 (CONTD)

57.89	62.59	-42.07	327.62	0.65
58.40	62.08	-41.07	324.03	0.91
58.90	61.80	-42.47	320.22	1.20
59.40	61.29	-41.14	316.57	1.57
59.91	60.77	-39.64	312.97	3.23
60.41	60.25	-37.91	309.38	3.16
60.91	59.73	-35.97	305.84	3.47
61.42	59.21	-34.75	304.66	3.48
61.92	58.69	-32.67	309.88	3.22
62.42	58.18	-30.92	314.51	3.29
62.93	57.66	-29.46	319.10	2.24
63.43	57.14	-28.22	323.68	1.91
63.93	56.63	-28.16	324.64	1.76
64.44	56.11	-27.07	323.41	1.73
64.94	55.60	-25.93	322.29	2.29
65.44	55.08	-24.74	321.26	2.33
65.95	54.57	-23.54	322.65	1.85
66.45	54.05	-22.38	322.79	1.82
66.96	53.77	-22.20	322.92	1.78
67.46	53.25	-21.07	323.94	1.73
67.96	52.74	-19.97	324.62	2.19
68.48	52.21	-18.87	324.99	2.16
69.01	51.67	-17.71	324.76	2.14
69.55	51.12	-16.56	324.45	1.67
70.09	50.57	-15.41	324.16	1.68
70.62	50.03	-15.29	323.86	1.71
71.16	49.48	-14.10	323.54	1.73
71.69	48.94	-12.90	323.21	2.25
72.21	48.41	-11.74	322.81	2.24
72.72	47.89	-10.57	323.64	2.19
73.22	47.39	-9.48	325.08	2.14
73.75	46.85	-8.39	325.65	2.05
74.25	46.35	-7.37	326.72	1.97
74.79	45.81	-6.33	328.16	1.89
75.32	45.27	-5.34	329.32	1.79
75.84	44.75	-4.44	330.76	1.70
76.38	44.21	-3.56	332.32	1.59
76.89	43.69	-2.77	333.63	1.00
77.39	43.19	-2.05	334.93	0.90
77.89	42.68	-2.40	336.14	0.82
78.40	42.18	-1.75	337.20	0.75
78.90	41.68	-1.13	338.30	1.18
79.43	41.15	-0.53	339.76	1.10
79.96	40.61	0.05	341.34	1.02
80.50	40.08	0.57	342.91	0.94
81.00	39.57	1.02	344.35	0.84
81.50	39.07	1.42	345.74	0.77
82.01	38.57	1.78	347.08	0.69
82.51	38.07	2.11	348.44	0.61
83.01	37.57	2.40	349.80	0.54
83.52	37.07	2.65	351.11	0.46
84.02	36.57	2.86	352.40	0.39
84.52	36.06	3.04	353.70	0.32
85.03	35.56	3.18	354.81	0.26
85.53	35.06	3.30	355.92	0.20
86.03	34.56	3.39	357.03	0.14
86.54	34.06	3.44	358.14	0.08
87.04	33.56	3.47	359.26	0.03
87.54	33.06	3.47	0.37	-0.01
88.05	32.56	3.46	1.48	-0.07
88.55	32.06	3.42	3.24	-0.17

TABLE 7.   DATA FOR RUN 131 (CONTD)

89.05	31.56	3.32	6.68	-0.32
89.55	31.06	3.12	10.54	-0.50
90.05	30.56	2.82	14.24	-0.70
90.55	30.06	2.41	17.25	-0.88
91.04	29.58	1.93	20.10	-1.06
91.54	29.08	1.36	22.92	-1.24
92.04	28.58	0.72	26.19	-1.42
92.54	28.08	-0.06	29.06	-1.63
93.04	27.57	-0.92	32.11	-1.87
93.55	27.07	-1.91	35.76	-2.11
94.06	26.56	-3.05	39.40	-2.42
94.56	26.05	-4.33	43.02	-2.79
95.10	25.52	-5.90	47.21	-3.19
95.63	24.98	-7.72	51.33	-4.14
96.16	24.45	-9.75	55.26	-4.73
96.68	24.01	-13.10	59.19	-5.42
97.21	23.47	-15.89	63.20	-6.36
97.75	22.93	-19.22	67.20	-7.07
98.28	22.38	-23.23	71.20	-9.07
98.82	21.83	-28.22	75.00	-10.34
99.35	21.28	-35.31	75.00	-12.57
99.89	20.73	-41.34	75.00	-13.12
100.36	20.42	-49.37	75.00	-13.17
100.84	19.93	-54.72	75.00	-13.89
101.31	19.43	-61.13	75.00	-12.41
101.78	18.95	-67.60	75.00	-13.05
102.26	18.46	-72.55	75.00	-13.01
102.73	18.05	-79.39	75.00	-11.79
103.21	17.57	-85.84	75.00	-9.02
103.68	17.09	-90.00	75.00	-5.61
104.15	16.69	-90.00	75.00	-2.21
104.62	16.22	-90.00	69.94	0.0
105.09	15.77	-90.00	26.32	0.0
105.56	15.38	-90.00	339.75	0.0
106.03	14.98	-90.00	293.64	0.0
106.51	14.52	-90.00	285.00	0.0
106.98	14.05	-90.00	285.00	0.0
107.46	13.70	-90.00	285.00	0.0
107.93	13.29	-90.00	285.00	0.0
108.41	12.81	-90.00	285.00	1.18
108.88	12.39	-90.00	285.00	3.34
109.36	11.91	-87.75	285.00	4.64
109.83	11.42	-83.65	285.00	6.74
110.30	10.99	-81.23	285.00	7.72
110.78	10.50	-77.20	285.00	7.63
111.25	10.07	-73.15	285.00	9.15
111.73	9.57	-69.16	285.00	9.13
112.20	9.08	-63.84	285.00	9.09
112.68	8.63	-55.86	285.00	9.09
113.15	8.13	-55.87	285.00	9.09
113.63	7.64	-51.89	285.00	9.14
114.10	7.15	-46.56	285.00	9.81
114.57	6.69	-42.58	285.00	9.78
115.05	6.15	-37.24	285.00	9.77
115.53	5.70	-33.31	285.00	6.88
116.00	5.21	-27.99	285.00	8.92
116.48	4.77	-25.61	285.00	8.98
116.95	4.28	-20.29	285.00	-0.16
117.42	3.79	-16.34	285.00	10.54
11.79	3.30	-11.01	85.00	10.49
118.37	2.82	-5.68	85.00	11.21

35

TABLE 7.   DATA FOR RUN 131 (CONTD)

118.85	2.34	-0.36	85.CC	0.20
119.32	1.87	4.96	85.00	11.21
119.79	1.40	10.29	285.0C	11.26
120.27	0.94	15.61	285.00	11.94
120.74	0.48	2C.92	285.CC	12.00
121.22	0.03	27.64	285.0C	12.08
121.60	-0.34	32.01	285.00	14.00
121.95	-0.67	35.9C	285.CC	13.39
122.3C	-0.98	42.76	285.0C	14.35
122.64	-1.29	46.65	285.0C	13.26
122.99	-1.60	51.96	288.93	9.99
123.34	-1.90	54.33	312.15	8.22
123.68	-2.2C	56.54	34C.32	4.17
124.03	-2.5C	58.08	8.48	0.0
124.38	-2.80	57.75	36.54	0.0
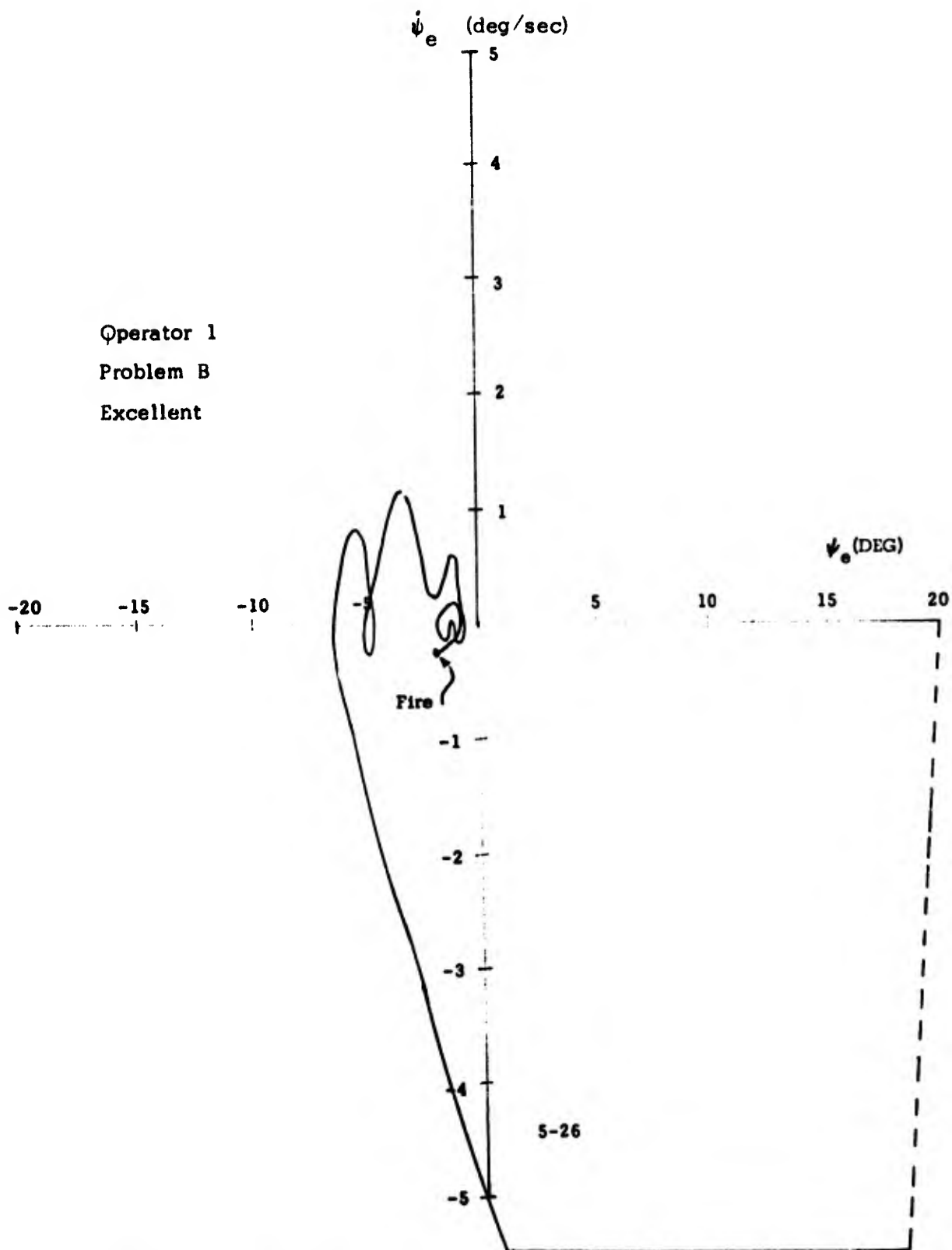
FIGURE 11. TRAJECTORY FOR RUN 1121 (ATTACK PHASE)

37
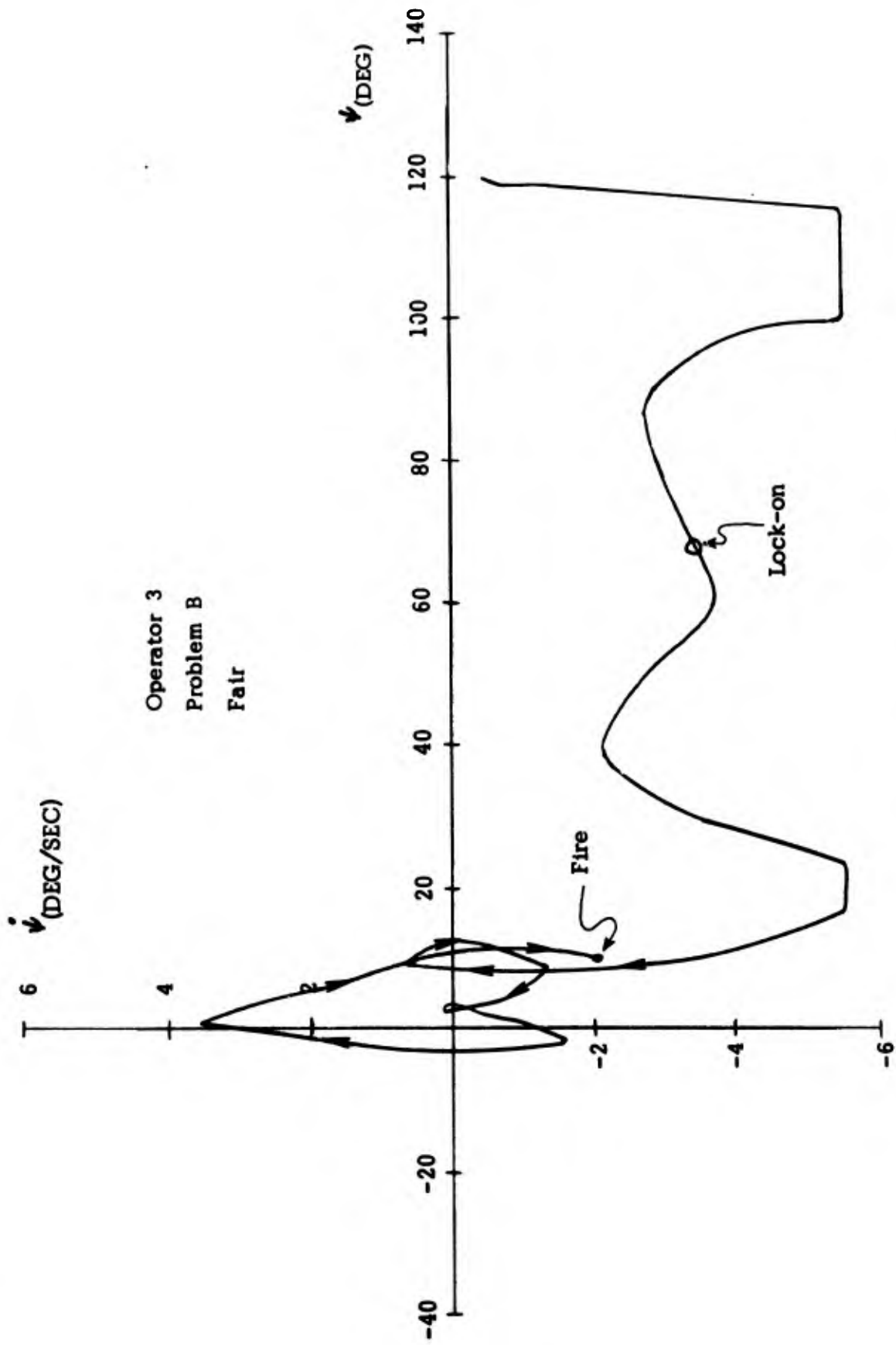
FIGURE 12. TRAJECTORY FOR RUN 1323 (ATTACK PHASE)

Figure 13 presents the trajectory for Run 3222, in which Operator 8 received a good rating. He also uses the roll-to-saturation technique and obtains lock-on during that portion of the flight. He rolls out early (at approximately 22° steering error), which produces an undershoot. However, he recovers well and systematically reduces the steering error.

Trajectories for Problem C

This is a head-on attack situation on a very short range. The operator is presented initially with zero steering error but with very high closing rates. Figure 14 shows the trajectory for Run 1131 on which Operator 1 achieves an excellent rating on his first attempt at problem C. Since the target is initially within radar lock-on range, the operator attempts lock-on almost immediately and thus the spotlight phase exists for only a few seconds. He is able to achieve lock-on while introducing a steering error of only 4° and requiring only 3.5 seconds.

Operator 3 received a fair rating on Run 1332, as is shown in Figure 15. He starts with a near zero error and introduces a 21° steering error while attempting lock-on. In addition, he consumes a considerable amount of time in achieving radar lock-on. As a result, time is short when he attempts to reduce the error in the attack phase. In spite of the lack of time, he recovers nicely and would have had a small error except for an incorrect roll a few seconds before missile launch which increased the size of the steering error.

Run 3232, performed by Operator 8, received a poor rating, as is shown in Figure 16. As with the other operators, he starts with a small initial error, but as he attempts lock-on, he introduces an increasing oscillation until roll saturation of $\pm75^C$ is obtained and steering errors ranging from $+50^O$ to -40° are produced. This is an example of a divergent control policy.

At this point it is necessary to discuss the time lag mentioned earlier. Referring to Tables 6 and 7, it is seen that a change in the roll angle (ROLL) does not produce the corresponding change in heading (PSI) for about 10 seconds. The appropriate amount of lag should be one or two seconds. This
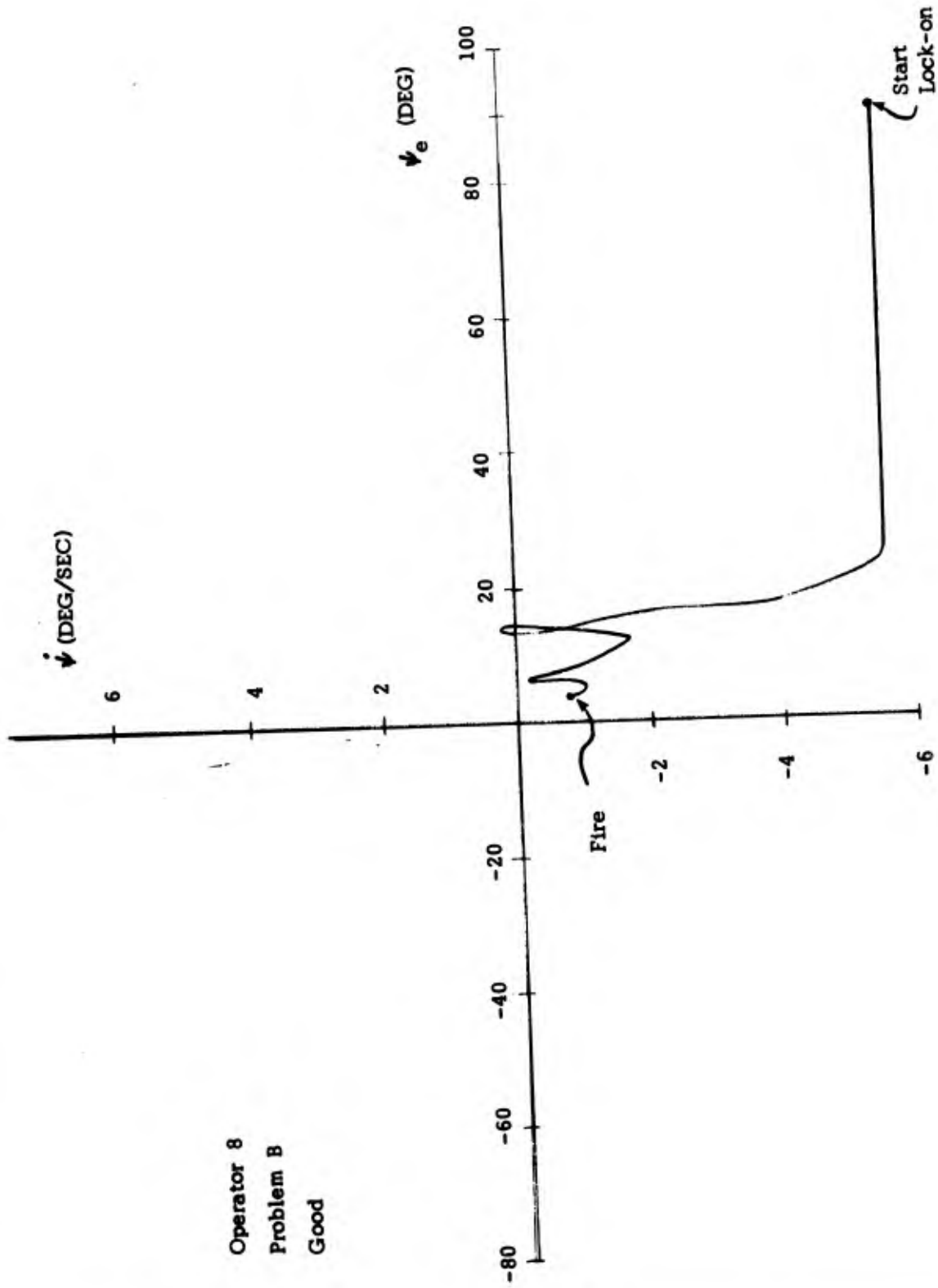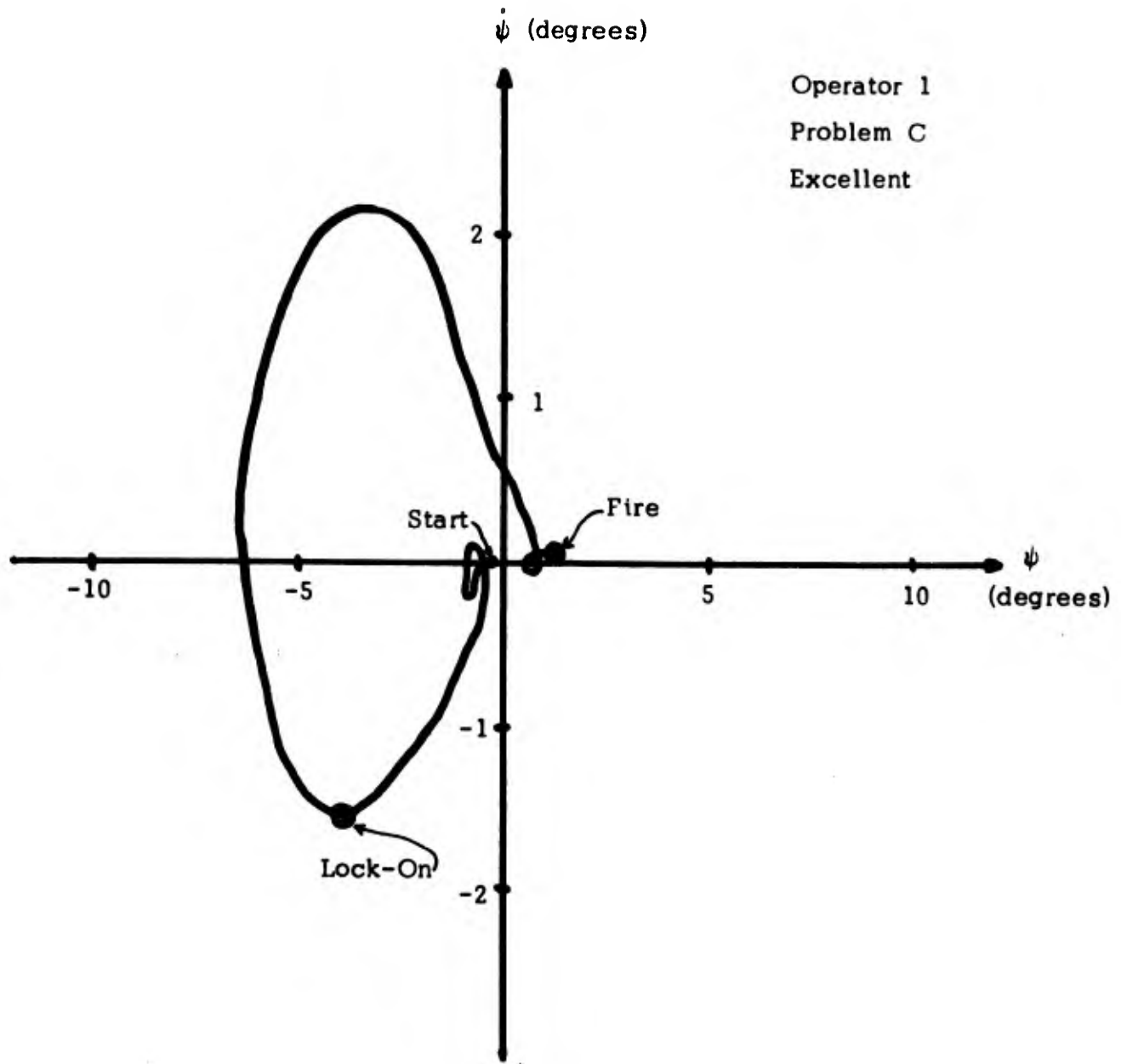
FIGURE 13. TRAJECTORY FOR RUN 3222

Operator 8
Problem B
Good

$\dot{\psi}$ (DEG/SEC)

ψ_e (DEG)

Start
Lock-on

Fire

40

FIGURE 14.   TRAJECTORY FOR RUN 1131

41

$\dot{\psi}$ DEG/SEC

6

4

2

Fire

Start

Lock-on

-20

-40

-60

-80

ψ_e (DEG)

100

80

60

40

20

-2

-4

-6

FIGURE 15. TRAJECTORY FOR RUN 1332

Operator 3
Problem C
Fair

42

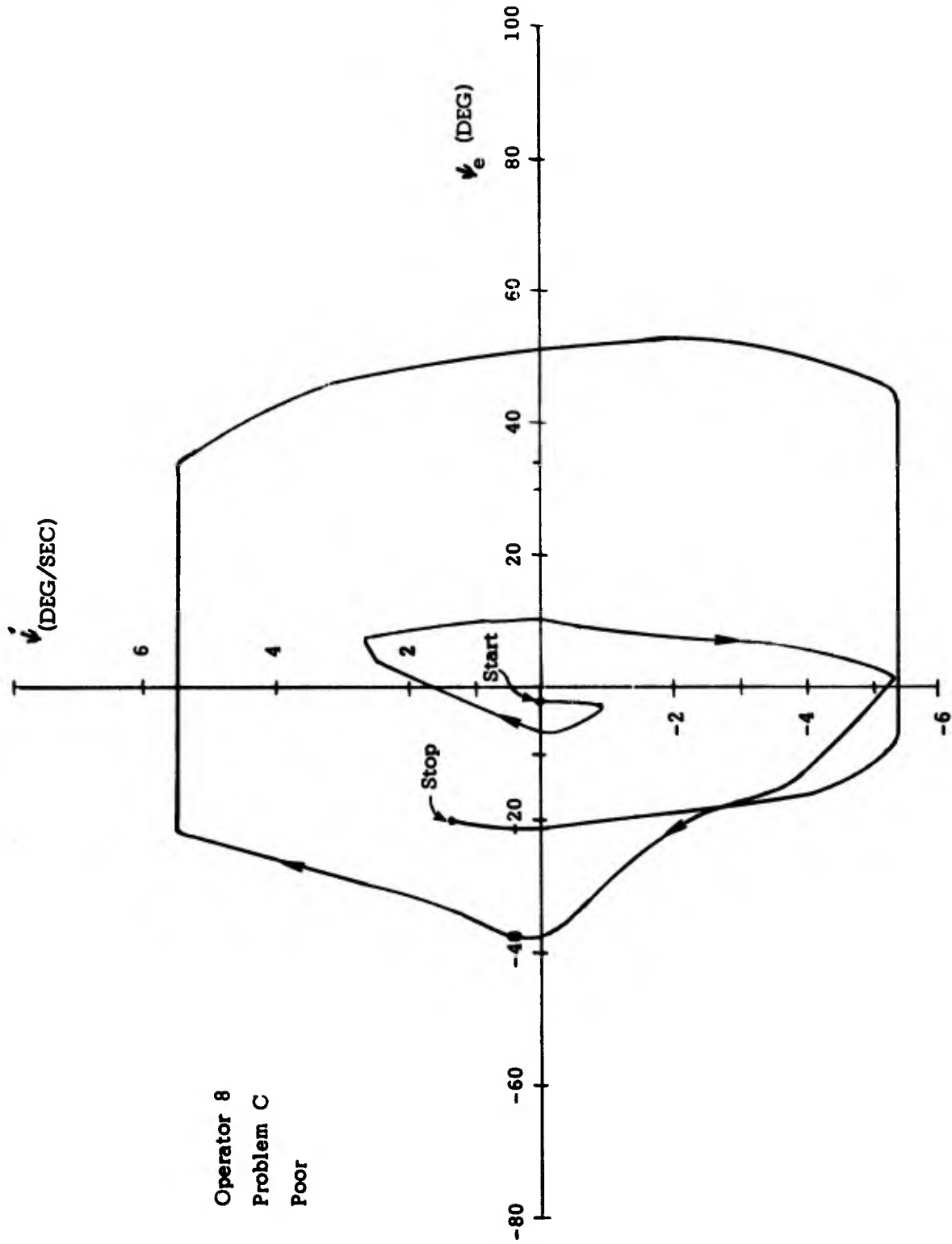FIGURE 16. TRAJECTORY FOR RUN 3232

Operator 8
Problem C
Poor

43

lag results in several problems. Steering error rate (PSIDOT) in this simulator should be a function of the roll angle:

$$\dot{\psi} = g \tan \varphi / v$$

where: g = gravity
            v = velocity of A/C
            φ = roll angle
            $\dot{\psi}$ = steering error rate

This relationship does not hold, however, because of the time lag. The values of $\dot{\psi}$ shown in Tables 3, 4 and 5 and Figure 5, were computed from the derivative of PSI and, hence, reflect the steering error rate displayed to the operator. All of the $\psi - \dot{\psi}$ trajectories were computed using the tangent function, because the inconsistencies between the function and the data were not discovered until the work was completed. This leads to a more severe problem. The operator moves his stick and waits for the corresponding display change. It doesn't occur within the time he expects (for an experienced pilot), so he makes a second change in the stick position, at which time he observes the results of his first stick motion but attributes it to his second stick motion. The seriousness of this problem has not been analyzed, but it causes us to be suspicious of the conclusions on pilot response and performance presented in the remainder of this report. However, we are interested in the performance measurement techniques, and they are applicable regardless of the accuracy of the data.

IV.   MODELING PILOT RESPONSE

Two approaches to performance measurement are presented in this report.   In one approach, we form pilot models by comparing the experimental data to a set of candidate pilot models.   The model that provides the closest fit to the experimental data in a certain region of the problem state space is selected as the representative model for that region.   Thus, several models, where each model represents a different type of control, may be used in sequence to represent a given operator's control policy on a single trial run.   After a number of runs are completed, the pattern of representative model sequences is identified and a generalized operator model is constructed.   Such a generalized model is an approximation of the operator's actual control policy. This section discusses the pilot response approach to performance assessment.   The second approach is an empirical one in which performance criteria are derived from the experimental data.   It is discussed in Section V.

This particular operator-simulator problem involves changing to and maintaining a desired heading (the primary task) and obtaining radar lock-on (the secondary task).

Candidate Operator Models

Aircraft heading control appears to be accomplished in several ways, some of which are:

1.   Rapid reduction of heading error (perhaps used to correct large heading errors), involving a saturation control policy,

2.   Slow reduction without overshoots of heading error (perhaps used to correct small errors), as in a linear control policy,

3.   Slow drift of heading error (perhaps a maintenance mode where wings are kept level to ensure near zero heading errors while other tasks are accomplished), such as a limit cycle, and

4.   Uncontrolled heading.

The pilot models that are derived in this study are based on these four control policies. As mentioned previously, the existence of saturation and limit cycle controls has not been proved and is only assumed in this report in order that we may use control theory approaches. Candidate pilot models are constructed for each of the four steering control policies listed above. The derivation is quite lengthy and is presented in Reference 2.

The Problem State Space

The approach we have chosen in analyzing the operator's control policies throughout the flight is to divide the problem state space into discrete cells and mutually exclusive problem situations. The flight control problem consists of three phases: spotlight, lock-on and attack, each of which requires different control techniques. Since each phase can occur with a time-to-go of greater than or less than 20 seconds (a function of the simulator), there are actually 6 possible problem phases or problem situations. The "20-seconds-to-go" was included because it causes additional stress on the operator and influences his control policy in a substantial portion of the runs. Next, each problem situation (PS) is quantized into 60 cells in the $\psi - \dot{\psi}$ plane of steering error and steering error rate.

For purposes of computation, a Boolean notation is used to identify the six problem situations. Using these and two parameters to identify the specific state space cell, we have five state variables:

|		
1.	ψ	Steering Error
2.	$\dot{\psi}$	Steering Error Rate
3.	MLT	Attempted Lock-On
4.	LO	Lock-On
5.	MT	Time-to-Go

These five variables describe every possible flight situation. Depressing the left trigger signals the end of the spotlight phase and the beginning of the lock-on phase. The attempted lock-on (MLT) condition is formed by using the left trigger and not obtaining lock-on. Figure 17 shows the six possible states that can occur using the latter three state variables (MLT, LO, MT). Once lock-on occurs (LO = 1), additional usage of the left trigger is not considered an attempted lock-on. This provides a total of 360 distinct Boolean cells. The problem state space is now represented as six $\psi - \dot{\psi}$ planes and is shown in Figure 18.

Model Selection

Portions of the trajectories representing linear control, saturation control, limit cycles, and divergent control are combined to form several possible pilot models. The structures of these models are based on an evaluation of selected trajectories in each of the performance categories. To determine which model best represents the data obtained from the F-106 simulator, a comparison of the trajectories described by simulator data and those produced by each model must be made for each cell in the problem state space. The comparison is made on a cell-by-cell basis to identify the differences in flight performance in the six problem situations.

Four models were constructed from the component tools described in Reference 2. These models provide representative trajectories for the four performance levels based on the simulator runs. Figures 19 through 22 illustrate the response trajectories characterizing each model. The Model 1 trajectory shown in Figure 19 is initially at 90° steering error and 2° roll angle. A rapid bank to roll saturation (75°) produces a 5.5° per second turning rate and requires only a 7° change in steering error. The roll saturation is maintained until approximately 10° steering error. The aircraft roll angle is then reduced producing an error overshoot of approximately 7°. Finally, a small limit cycle bounded by $\pm 2^\circ$ error and $\pm 0.6^\circ$ per second error rate is achieved. Model 1 is intended to closely represent the control policy of a superior operator.
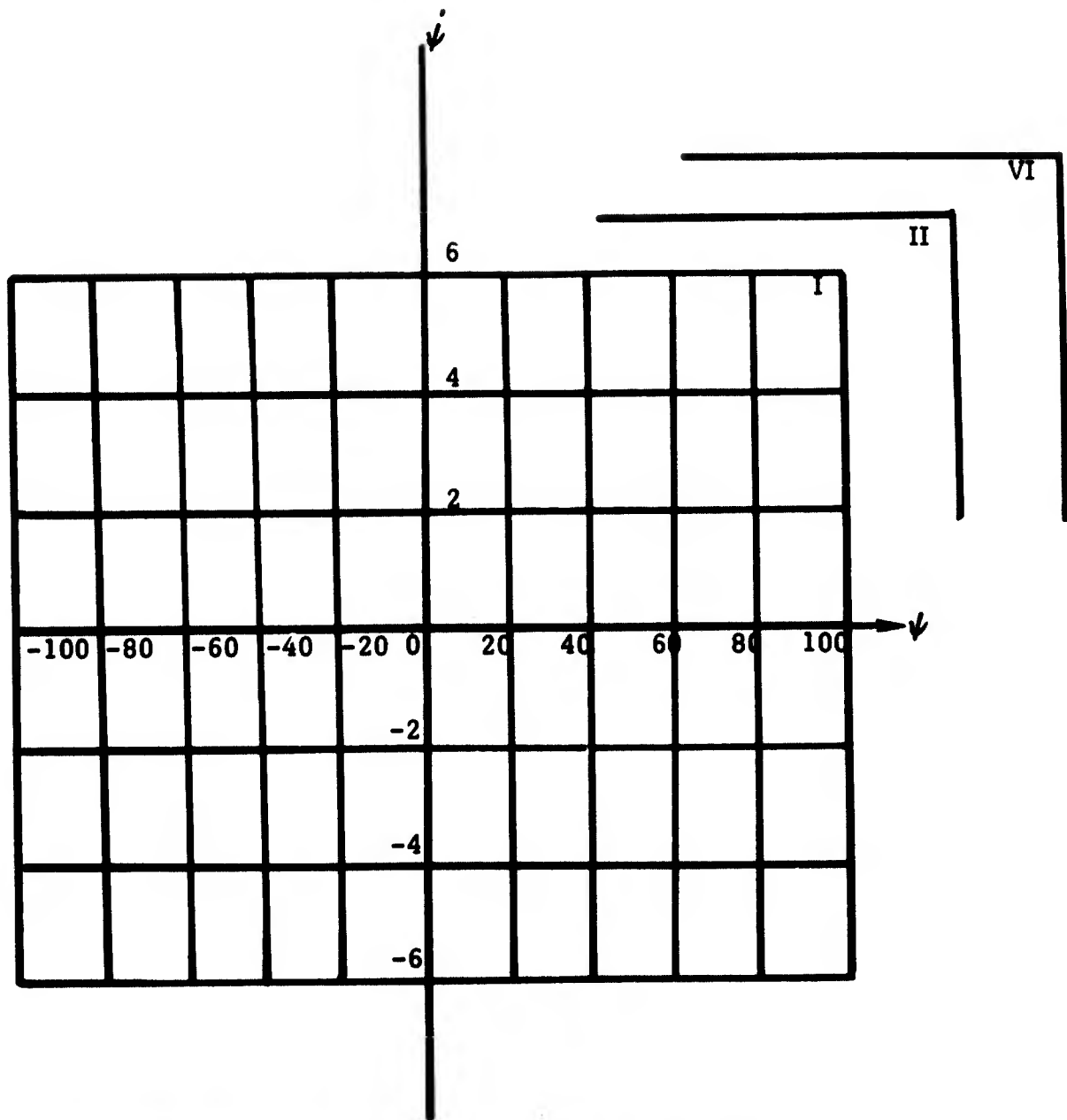
State	MT	LO	MLT	LT
0	0	0	0	0
1	1	0	0	0
2	0	0	1	1
3	1	0	1	1
4	0	1	0	0 or 1
5	1	1	0	0 or 1
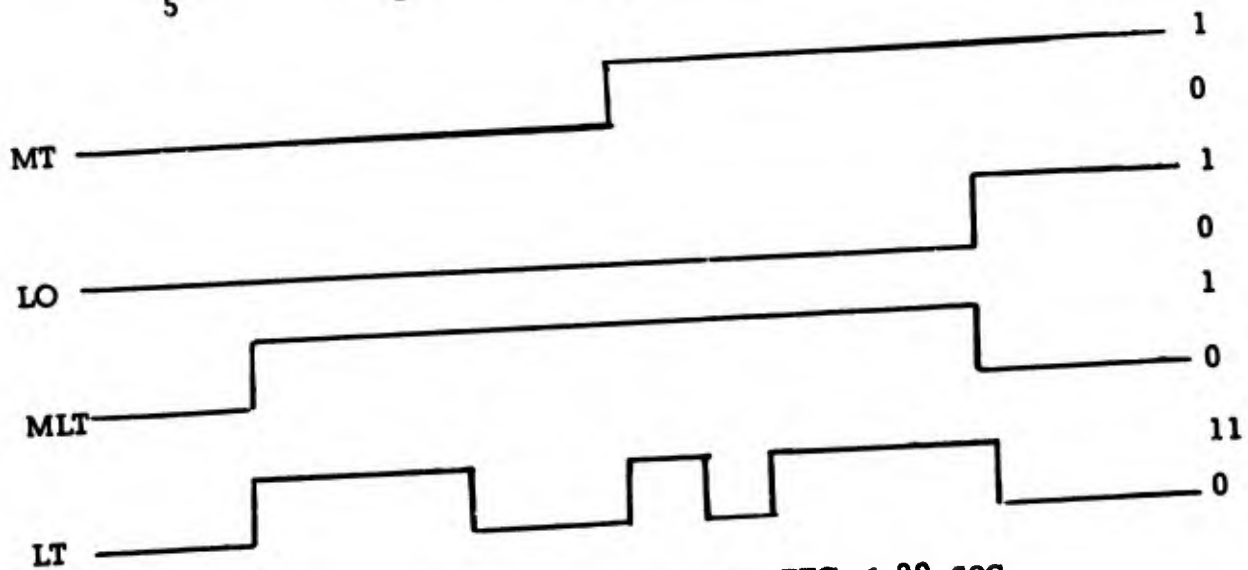
MT -- time to go -- true when TTG ≤ 20 sec
LO -- lock-on
MLT -- attempted lock-on
LT -- left trigger

Note: MT can occur at time before, during, or after lock-on

FIGURE 17. SIX PROBLEM SITUATIONS

48

60 Regions in Each State *6 States = 360 Cells in
Function Space
$\dot{\psi}$ = Steering Error (Degrees)
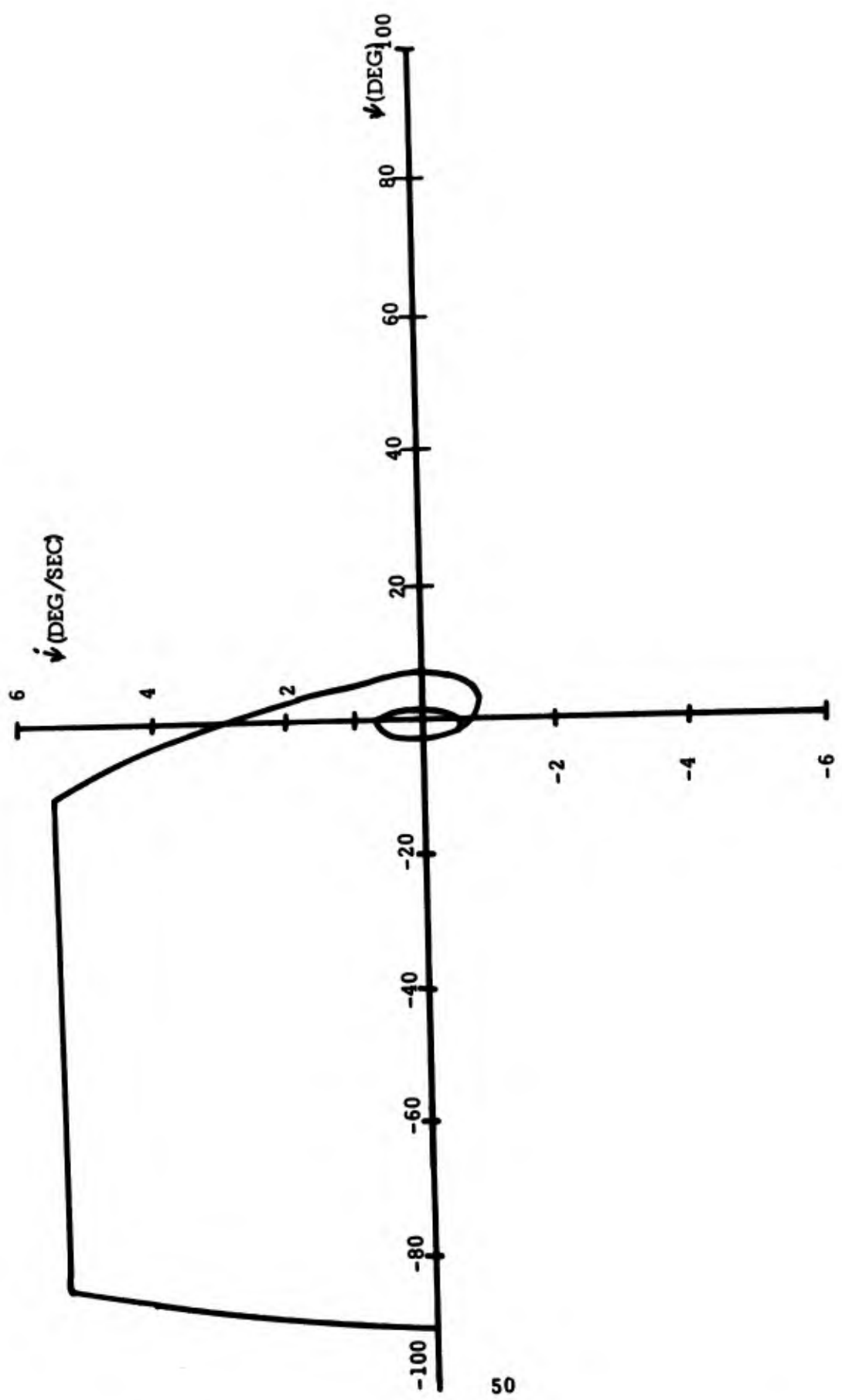$\dot{\psi}$ = Steering Error Rate (Degrees/Sec)
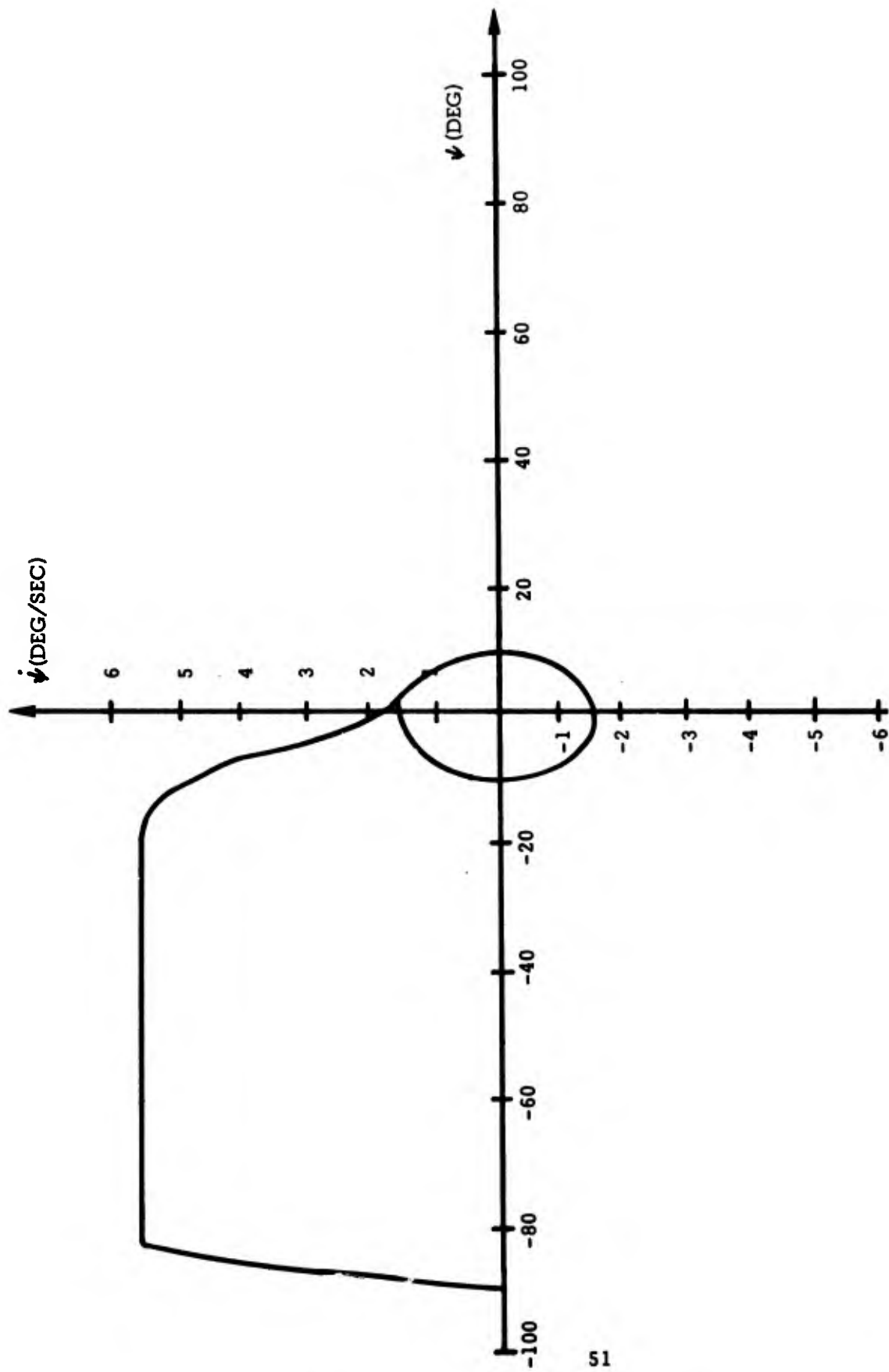
FIGURE 18.   PROBLEM STATE SPACE

FIGURE 19.   MODEL 1
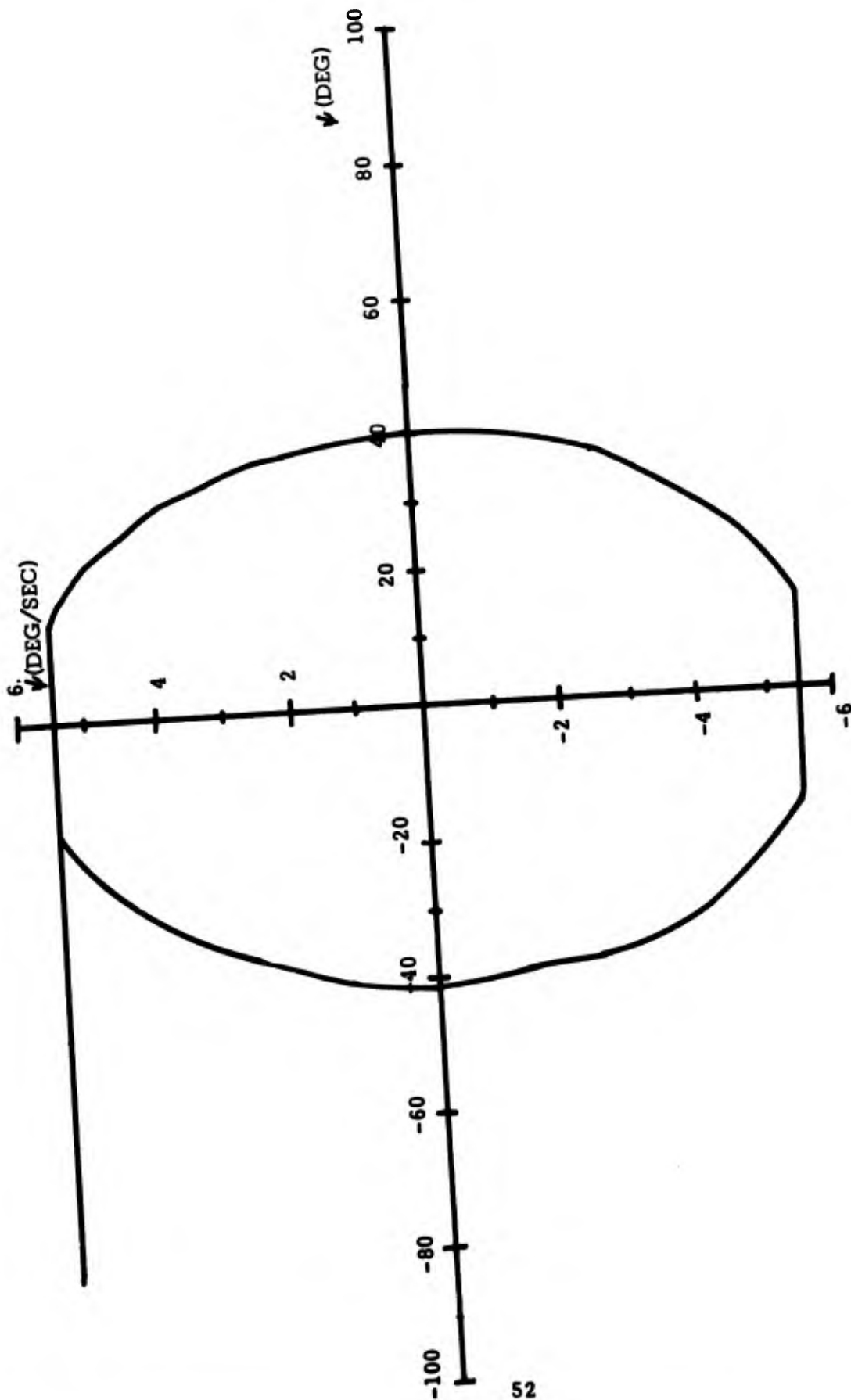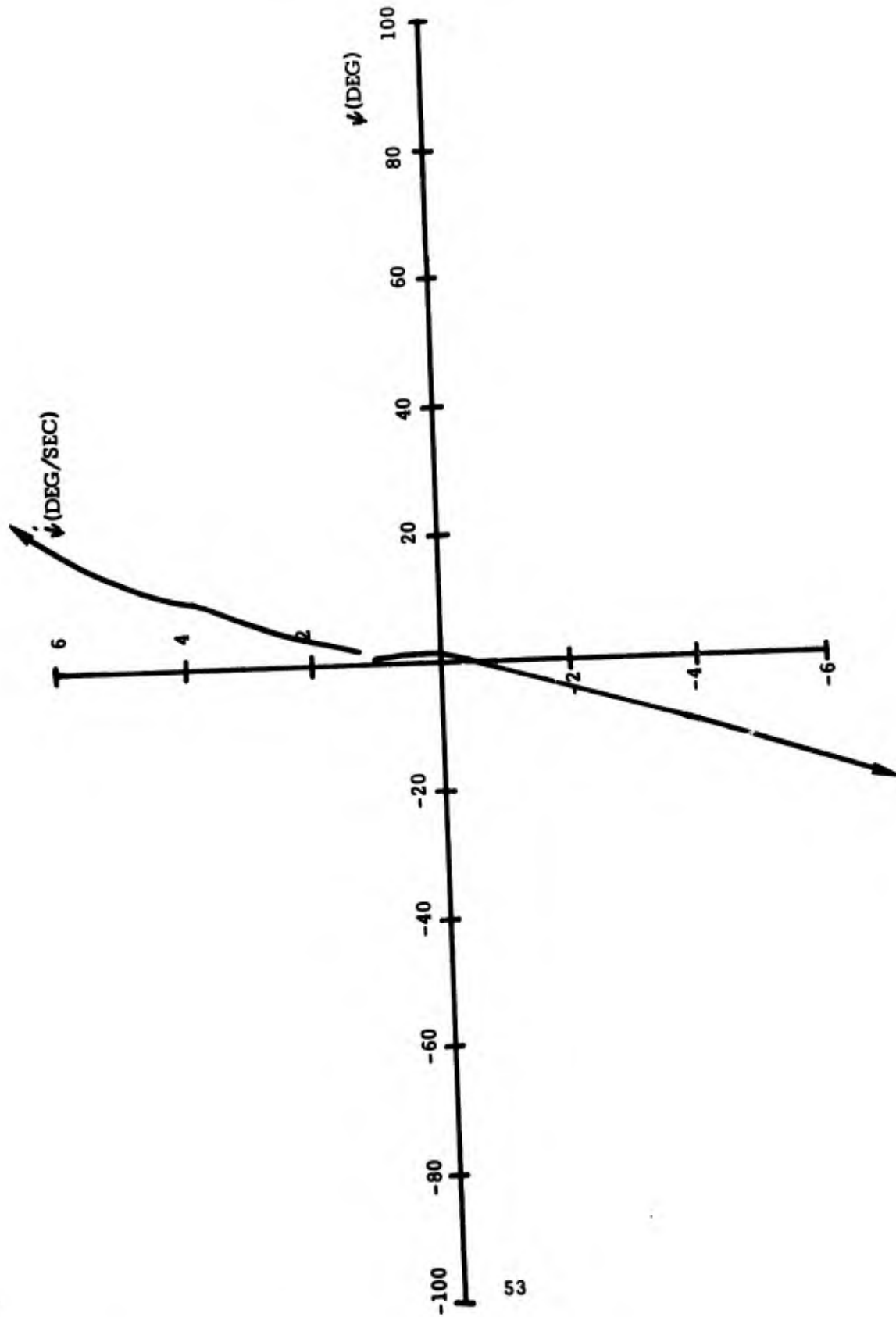
FIGURE 20. MODEL 2

FIGURE 21. MODEL 3

FIGURE 22.   MODEL 4

53

A characteristic response of Model 2 is shown in Figure 20. This model is similar to Model 1 in that a rapid climb to roll saturation is obtained. However, breakaway from roll saturation is achieved at approximately 20° steering error and a somewhat steeper error and error rate slope is maintained until the limit cycle is reached. The limit cycle in Model 2 is bounded by $\pm 10°$ error and $\pm 1.5°$ per second error rate.

Model 3 characterizes the actions of many operators who were unable to converge to a small limit cycle. Instead, their performance resulted in a large limit cycle in which the aircraft is rolled from one roll saturation level to another. Figure 21 shows a characterizing trajectory for Model 3. The initial rapid rise to roll saturation is similar to that found in Models 1 and 2 and was included because every operator in the simulation runs examined used that technique. The roll saturation trajectory runs directly to the limit cycle trajectory, which is bounded by $\pm 40°$ steering error and $\pm 5.5°$ per second steering error rate.

Model 4 was developed to provide an unstable or divergent characteristic which was frequently representative of operator steering performance while attempting radar lock-on. Figure 22 provides a characterizing trajectory for Model 4.

Construction of Models 1, 2 and 3 required different response trajectories in different portions of the state space. Therefore, the state space was divided into the three subspaces shown in Figure 23. In subspace 1, the absolute value of the steering error rate is less than 5.5° per second. This is the region in which the operators tend to roll the aircraft away from the neutral position to get a satisfactory turning rate. Subspace 2 exists where the absolute value of the steering error rate exceeds 5.5° per second. It is used for the roll angle saturation model. Finally, subspace 3 is the remaining area near the origin that contains the "limit cycle" and "converge to limit cycle" control laws.

Computer program J1 which implements the pilot models includes a coding for each model and a simulation of the F-106 aircraft. Thus, it is possible to test models by observing how the model control laws fly the aircraft from a specific

54
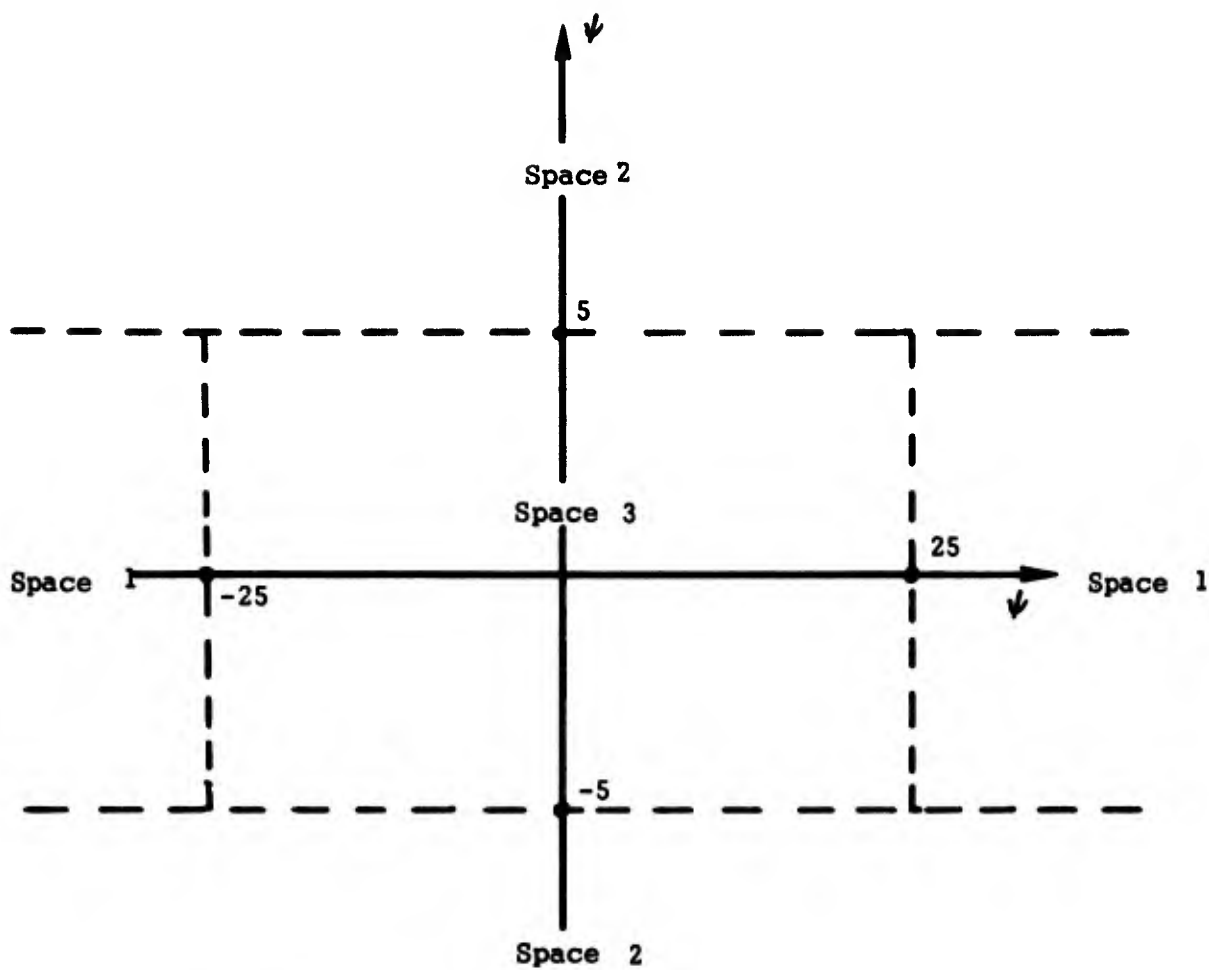
FIGURE 23. THREE MODEL SUBSPACES

initial state. As shown in the flow diagram given in Figure 24, the computation technique employed reads the initial conditions, determines the state space cell, identifies the model parameters associated with the cell, computes the control stick value of the model control law, and finally computes an increment of the aircraft trajectory for the specified number of iterations. The listing of program Jl appears in Reference 2.

Comparing Model and Simulator Trajectories

A diagram of the procedure used in model selection for each cell is shown in Figure 25. Each input data point contains (or is used to obtain) values for ψ, $\dot{\psi}$, MLT, LO and MT. These parameters are used to determine in which state space cell the data point lies. The stick position at the data point is computed for each of the four models (STK_i, $i = 1,4$). The program uses the position STK (ψ, $\dot{\psi}$) to compute the four resultant model trajectories, as shown in Figure 26. Model trajectories are computed for N iterations, where N is the number of simulator data samples falling in that cell. The error for each model is computed as follows:

$$ERROR_{ij} = (\psi - \hat{\psi}_i)^2 + (\dot{\psi} - \hat{\dot{\psi}}_i)^2$$

where: i = model number ($i = 1,4$)

j = cell number ($j = 1,360$)

$(\hat{\psi}, \hat{\dot{\psi}})_i$ = end point of trajectory as predicted by

Model i

Physically, the error is the square of the vector between the actual and predicted end points of the trajectory. Since many runs are analyzed before the cell model is selected, the four error values are stored as sums for each cell. If only one run is being analyzed, the model with the smallest ERROR value is selected as the model that is most representative of that cell. This procedure is repeated until all cells through which the flight
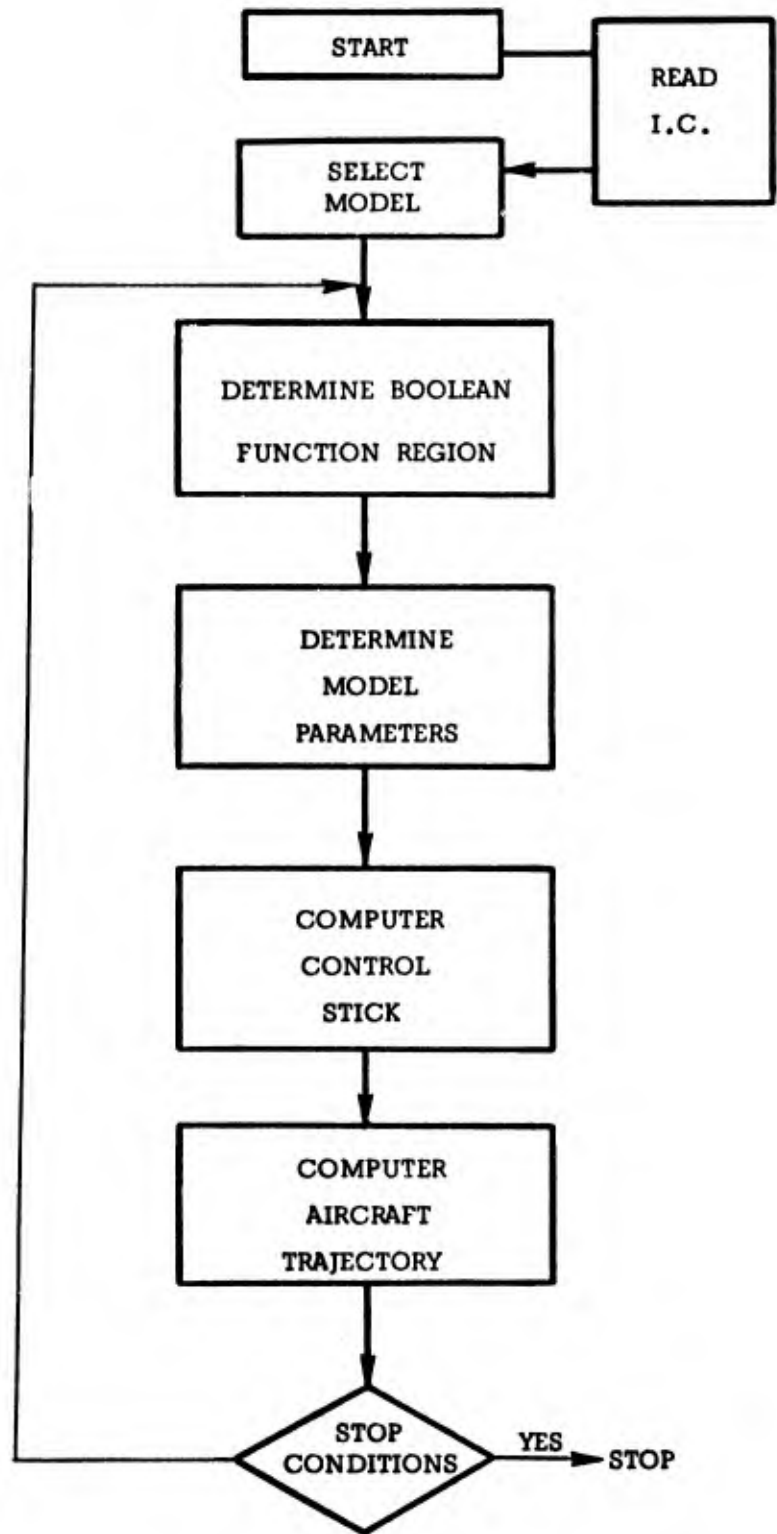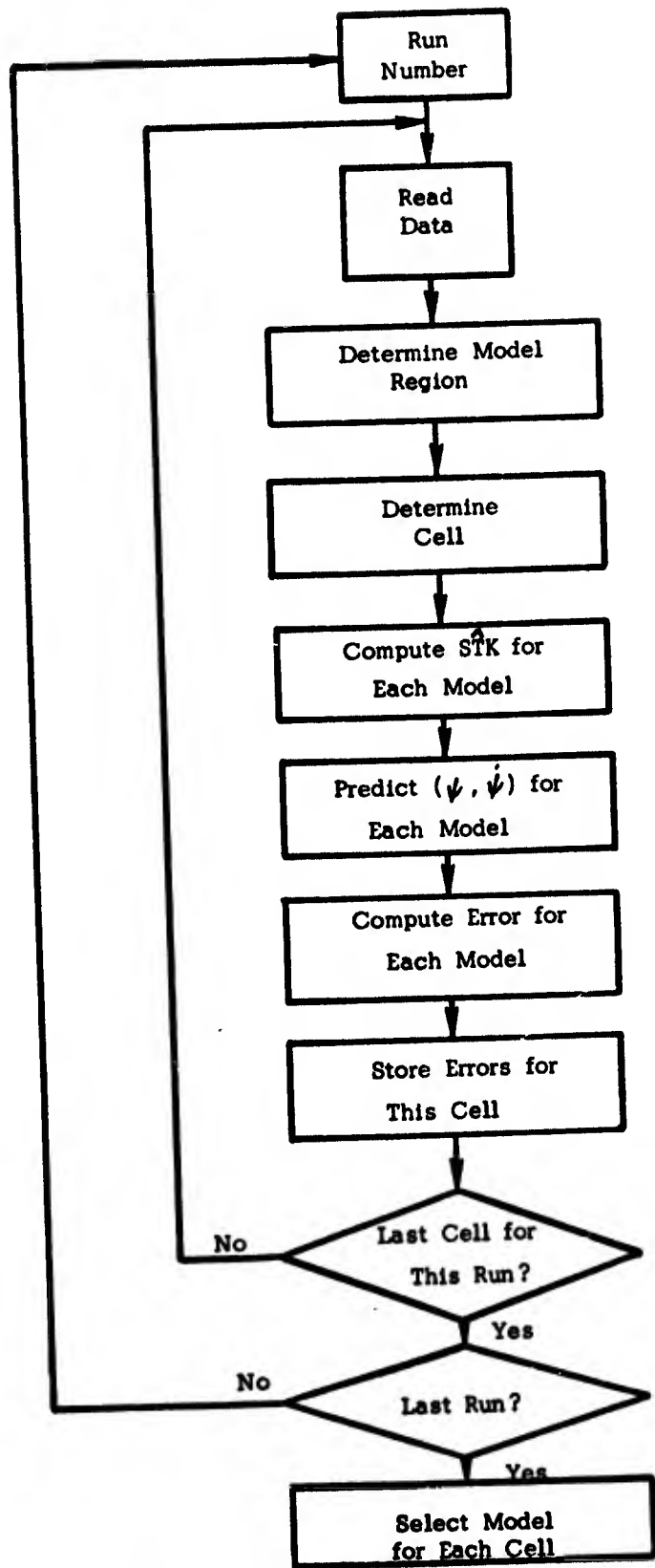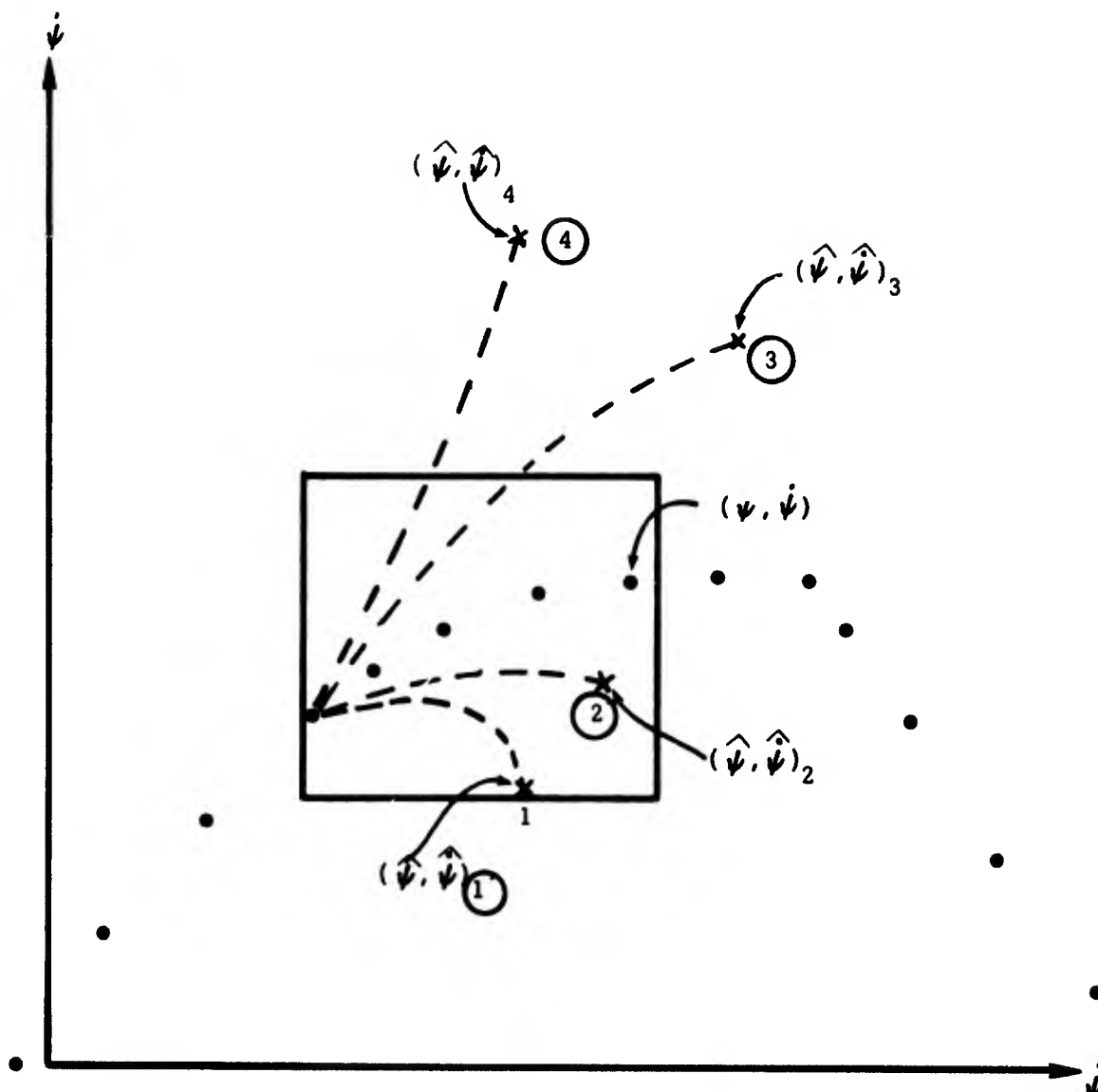
FIGURE 24. FLOW CHART OF PROGRAM J1

FIGURE 25. CELL MODEL SELECTION

- A/C Trajectory From F-106 Simulator Data
- - - Model Trajectories
- X Predicted (ψ, $\dot{\psi}$) From Each Model

FIGURE 26.   CELL MODEL COMPARISON

path passes have been analyzed. By superimposing the six planes, the flight path is reconstructed by using the cells containing non-zero values.

Experimental Results

The cells in the $\psi - \dot{\psi}$ space containing the limit cycles of Models 1, 2 and 3 are shown in Figure 27. This figure is helpful in evaluating the importance of the representative models assigned to each cell. The limit cycles of Models 1 and 2 exist only in the cells marked 1 and 2 surrounding the origin. Thus, if an operator maintains a small error, either Model 1 or Model 2 will represent his control policy in those four cells. Should his control policy be divergent in those cells, it will be represented by Model 3 or Model 4. Model 3 produces a limit cycle locus that includes the cells marked 3 in Figure 27. The trajectories diverging to the locus from inside and those converging to it from outside can be represented by Model 3. Thus, this model can represent converging trajectories for large errors and also diverging trajectories for small errors. Model 4 represents divergent trajectories everywhere. At the turning rate boundaries ($\pm 5.5^{\circ}$ per second), the F-106 simulator cannot diverge further so a hard saturation limit is obtained. In this case, Model 4 can represent trajectories moving along that boundary.

Figure 28 shows cells in the $\psi - \dot{\psi}$ space which are important in controlling convergence and divergence. These cells were selected from an examination of the flight data associated with Performance Level 1 (excellent). Cells marked R and S are used to roll-to-saturation and maintain roll saturation, respectively. Cells marked C are those in which critical error convergence is achieved and those marked L contain the small limit cycles of Model 1 and Model 2. The crosshatched regions represent the cells not usually used by the operators achieving Performance Level 1 (excellent) control.

Simulator trajectory data for each performance level (PL) were compared to trajectories generated by the four candidate models and a representative model selected according to the method shown in Figure 25. Data from each performance level were processed in two ways: all runs of each category were
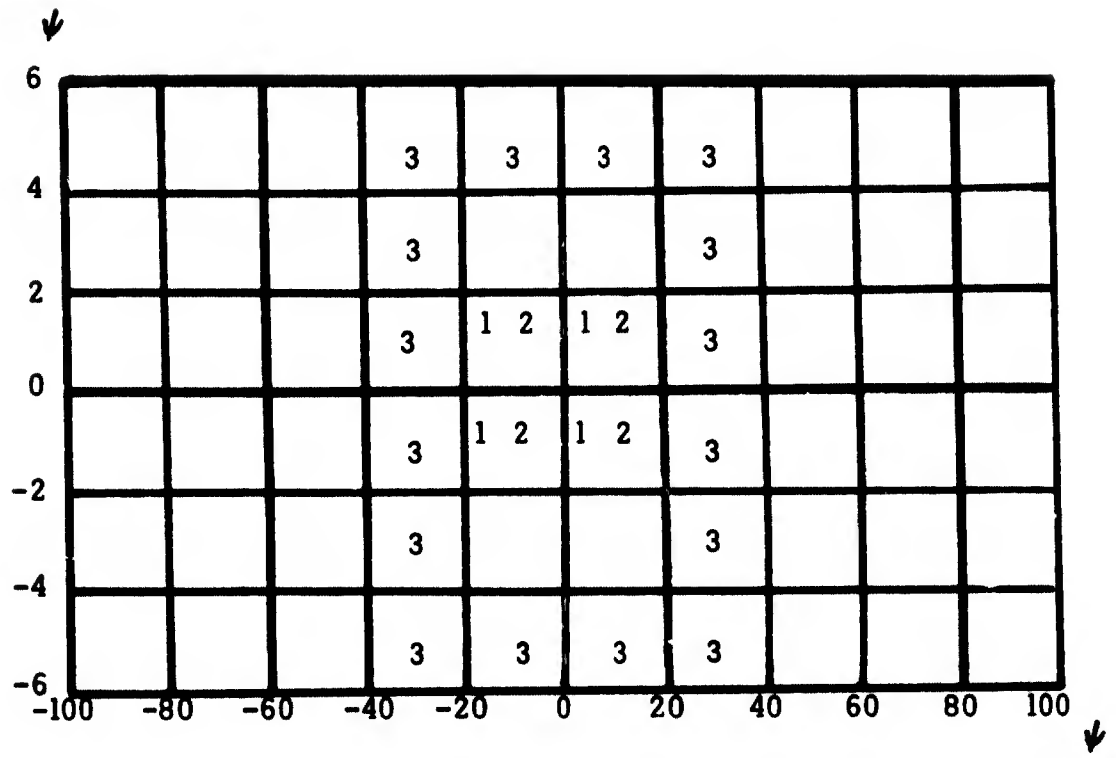
60

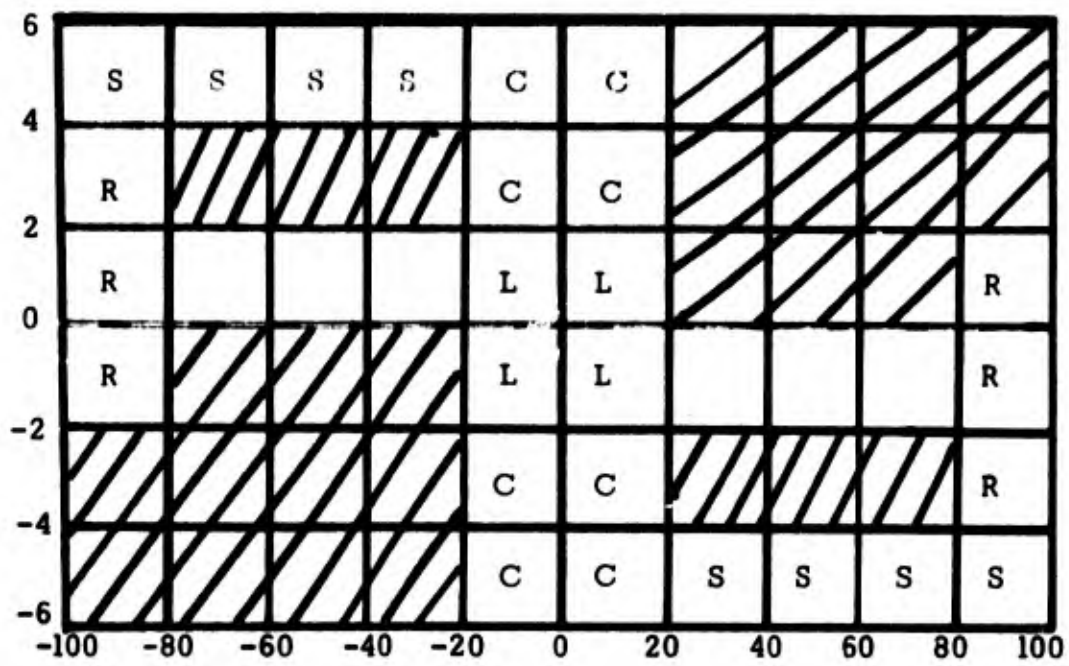FIGURE 27. CELLS CONTAINING LIMIT CYCLES OF MODELS 1, 2 AND 3

FIGURE 28.   CELL FOR CONVERGENCE AND DIVERGENCE

divided into two groups and each group run separately, and several individual runs were processed together. The results of this processing are illustrated via 2 examples, Tables 8 and 9. The number(s) written in the cell indicate the model(s) most appropriate in that cell.

Consider the control properties of the Performance Level 1 (PL 1) (excellent) operators. Table 8 shows representative models selected for 12 Level 1 runs, primarily from Problem Type A. The first problem situation (PS 0) is prelock-on with no attempt at lock-on and greater than 20 seconds to go. Observe that the L cells (refer to Figure 28) contain 1's, indicating that a small limit cycle was maintained once the region near the origin was reached. Also, the convergence cells (C) contain 2's and 3's indicating convergence to the L cells. In Problem Type A, the runs start at -90° error and near 0° error rate. The aircraft is rolled to saturation and subsequently rolled to wings level, achieving near zero error and zero error rate conditions. This shows that steering errors were reduced to a small value before lock-on was attempted, a characteristic of proficient runs on Problem A.

Runs starting at 90° error and near zero error rate (Problem Type B) require lock-on attempts before the steering error is reduced to near zero, as indicated by the truncated path in the fourth quadrant. Attempts to achieve radar lock-on cause a change in the control pattern, as shown in PS 2. The models of the limit cycle cells (L) change from all 1's to 1, 2 and 4 while the convergent cells (C), previously unused, contain a 3. Clearly, attempted lock-on results in an unstable control policy even for operators achieving high performance. This characteristic is consistent for all operators of all skill levels and demonstrates that attempting radar lock-on does interfere with aircraft flying.

Post lock-on, PS 4, control is represented by Model 1 in cells (L) and Models 2 and 3 in the convergence cells (C). The operator is therefore able to recover from the steering error introduced by the radar lock-on operation. The second page of Table 9 shows the representative models for the

$\dot{\psi}$ (DEG/SEC)

Problem State 0

LO 0
MLT 0
MT 0
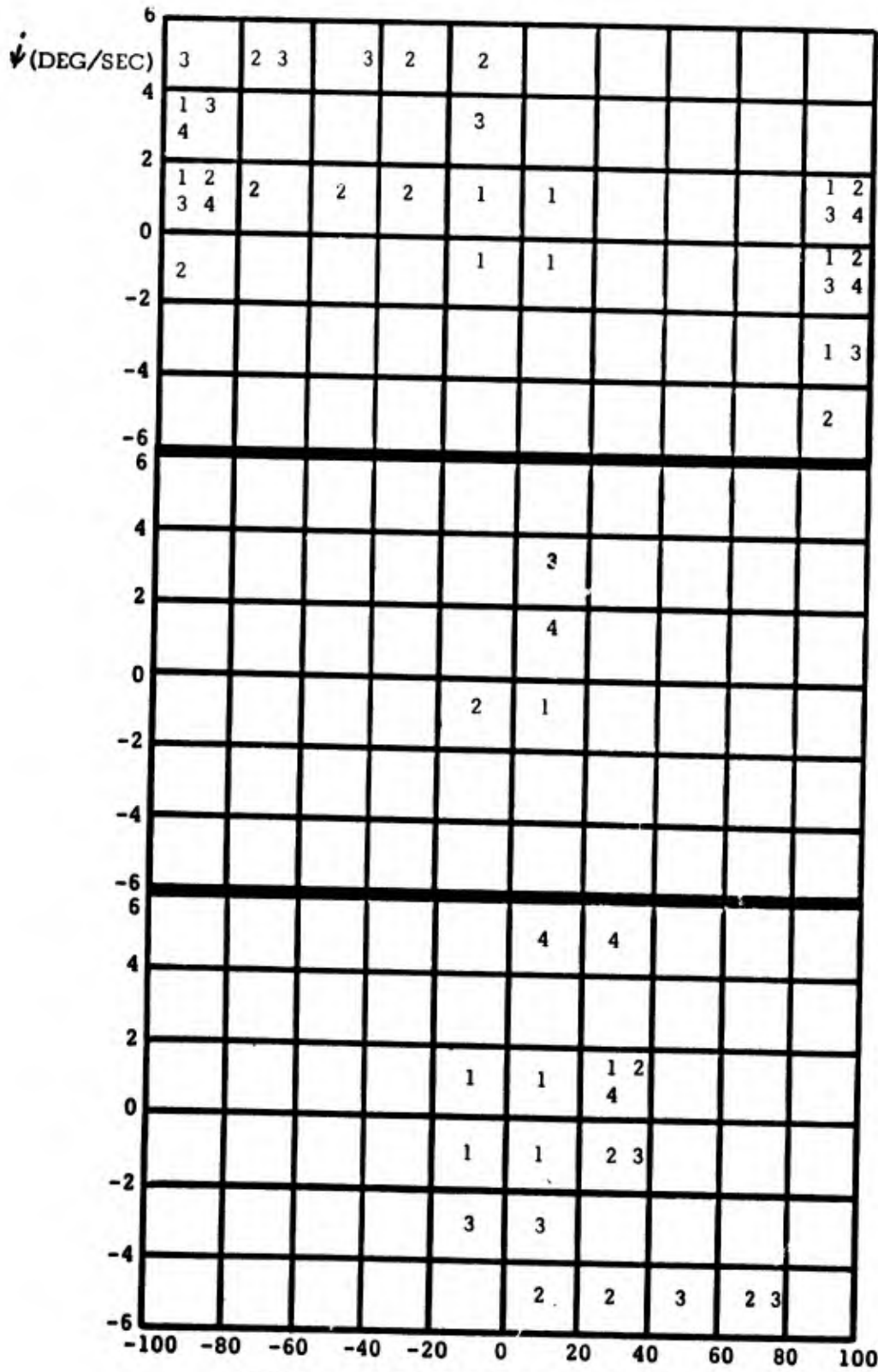
Problem State 2

LO 0
MLT 1
MT 0

Problem State 4

LO 1
MLT 0
MT 0

ψ (DEG)

-100 -80 -60 -40 -20 0 20 40 60 80 100

**TABLE 8.   MODEL SELECTION FOR PERFORMANCE LEVEL 1
RUN NUMBERS 1-12**
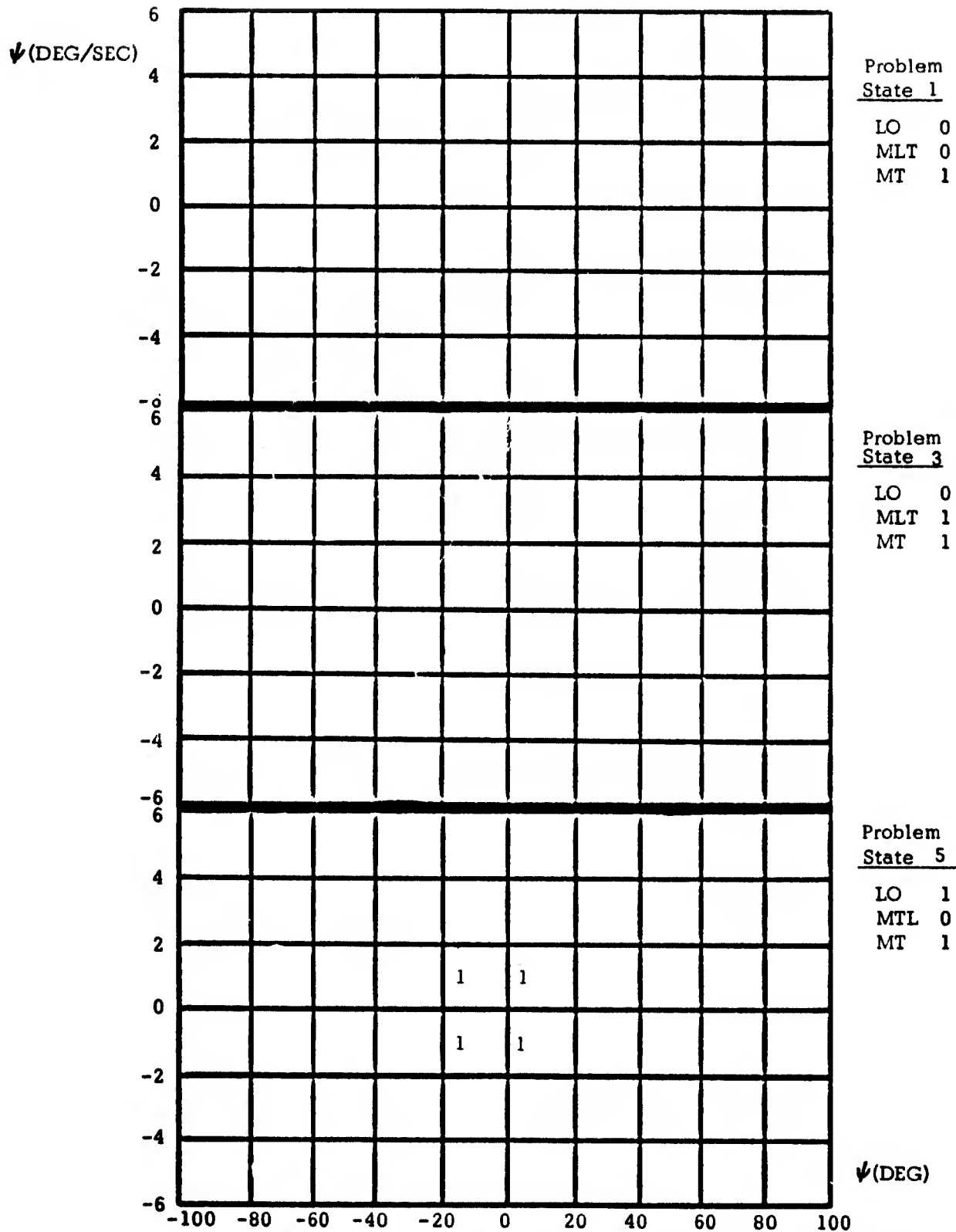
TABLE 8. MODEL SELECTION FOR PERFORMANCE LEVEL 1
RUN NUMBERS 1-12 (Concluded)

ψ(DEG/SEC)

Problem
State 0

LO   0
MLT   0
MT   0

Problem
State 2

LO   0
MLT   1
MT   0

Problem
State 3

LO   1
MLT   0
MT   0

ψ(DEG)

-100 -80 -60 -40 -20   0   20   40   60   80   100

**TABLE 9.   MODEL SELECTION FOR PERFORMANCE LEVEL 1
RUN NUMBERS 13, 14, 25, 27, 28, 30, 34, 35,
36, 38, 39, 54, 70**

66

ẏ(DEG/SEC)

6
4
2
0
-2
-4
-6

Problem
State 1

LO   0
MLT   0
MT   1

Problem
State 3

LO   0
MLT   1
MT   1

1

Problem
State 5

LO   1
MTL   0
MT   1

4   4   4

1   4   3

1 2   1 2   4   1   1 2
3 4   4

3   1   1   1 3
                    4

3   3   1   1 3

4   4   4   4   2 3   2 3

ẏ(DEG)

-100 -80 -60 -40 -20   0   20   40   60   80   100

TABLE 9.   MODEL SELECTION FOR PERFORMANCE LEVEL 1
RUN NUMBERS 13, 14, 25 (Concluded)
27, 28, 30, 34, 35, 36, 38, 39, 54, 70

67

PS 5 control policy, when time-to-go is less than 20 seconds. The only active situation for this group of Level 1 operators is post lock-on in which Model 1 represents the control policy on all runs.

Table 9 presents the representative models for a second group of PL 1 operators working on Problem Types A, B and C. Aircraft control during prelock-on, PS 0, is not represented in the L cells by all 1's, as it was in the previous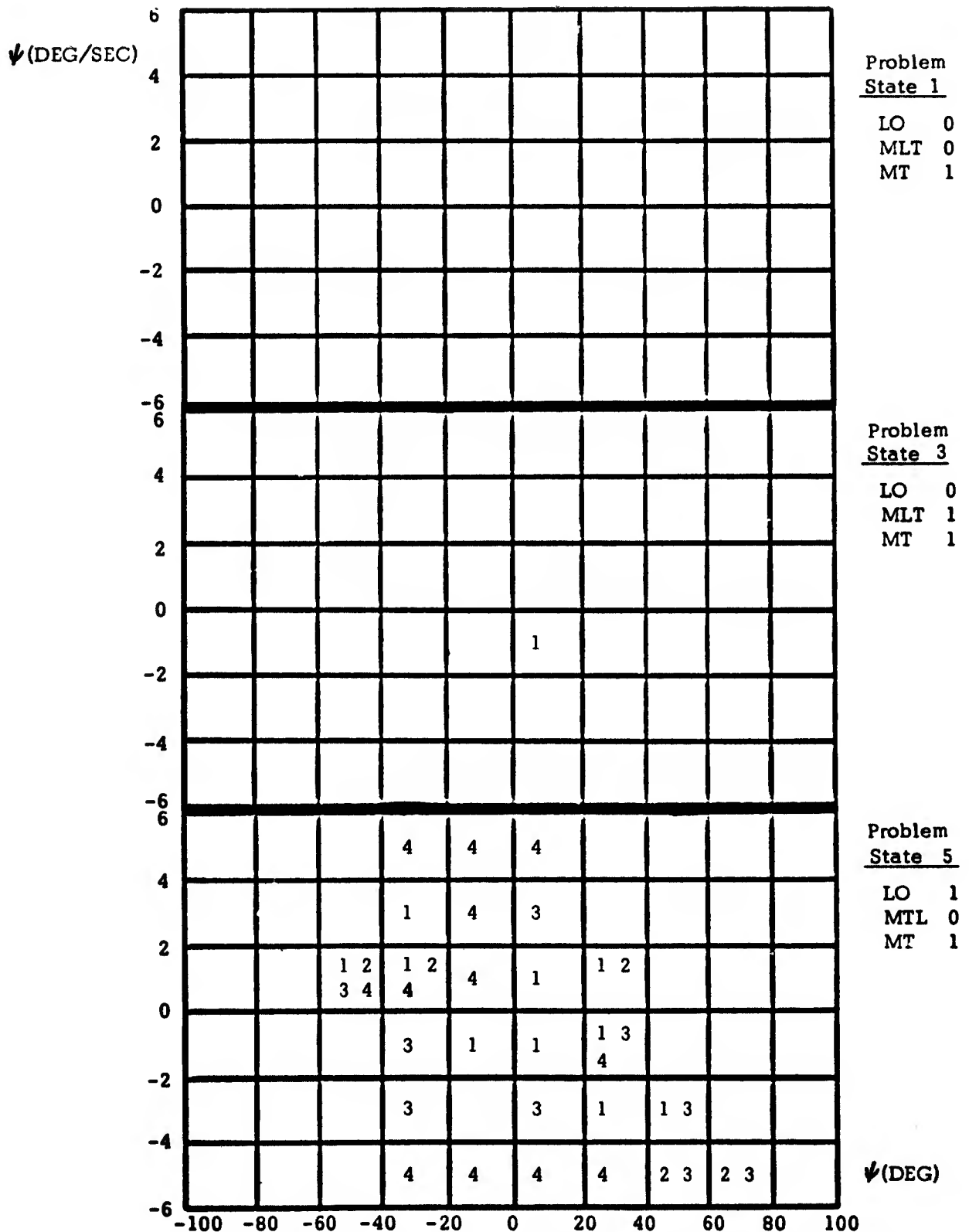 table. The sequence of 2's for a 0 to 2 degrees per second error rate represents convergent control in which the pilot has a tendency to undershoot, i.e., a premature reduction of the aircraft roll angle to near zero is made. At the right half of the diagram, the truncated roll to saturation is similar to that found in Table 8. Examination of all charts in Table 9 reveals that Model 3 appears frequently in the inner convergence cells (C), where the absolute value of the error rate is 2^O to 4° per second. Model 3 often appears in the inner convergence cells for all performance levels and indicates an overshoot control characteristic.

Table 8 and Table 9 entries indicate good control characteristics in the critical L and C cells for pre and post lock-on situations. However, in the attempt to lock-on (condition PS 2) Table 9 entries show that additional cells, many in the crosshatched area of Figure 28, were used. The crosshatched region includes the first and third quadrants, where the sign of the error and error rate are the same, which are usually associated with unstable control policies. The fact that an operator uses these cells indicates that he has difficulty controlling the aircraft while attempting radar lock-on with a large steering error and roll angle. This could be due to the large turning rates associated with the large aircraft roll angle and/or the stress of time, since Problem Types B and C are started with a short range to the target. Comparison of Tables 8 and 9 for post lock-on with less than 20 seconds to go also shows a remarkable difference. In the latter case, a stable limit cycle at the origin is not achieved and, as evidenced by the 4's in the L cells, control is divergent.

In summary, PL 1 (excellent) operators demonstrate the ability to control the aircraft to small heading errors and to maintain those errors, provided sufficient time is available. A tendency for unstable operations exists during lock-on causing an increase in the steering errors. Also, when lock-on is attempted at other than wings level, aircraft control is more difficult.

The results of the remainder of the processing have not been included because they are quite lengthy, but they are summarized here. In the case of a PL 1 operator attempting Problem C, a small error exists at prelock-on and he is able to maintain that small error and achieve lock-on rapidly. In post lock-on he is able to maintain a somewhat larger limit cycle; however, when time-to-go is less than 20 seconds, he tends toward the divergent control.

Analysis of Performance Levels 2, 3 and 4 shows that critical regions, such as the limit cycle cells (L), frequently use Models 1 and 2 and occasionally Model 3 to represent the control policy. Also, the convergence cells (C) are frequently filled with 2's and 3's, indicating a sharp convergence and convergence overshoot respectively. Thus, we can conclude that at least some operators in these performance levels can successfully reduce the steering error and maintain a small limit cycle; however, three factors occur that may prevent superior performance. These factors are:

1. The frequent use of cells in quadrants 1 and 3, indicating greater difficulty in maintaining aircraft control,

2. Extreme control difficulty during lock-on attempts, and

3. Frequent use of divergent control when time-to-go is less than 20 seconds.

Table 10 shows the number of divergent cells used by each performance level group for each problem situation. For example, the first group of Performance Level 1 runs, consisting of runs 1 through 12, used only two cells in the crosshatch

69

LEVEL	1	1	2	2	3	3	4	4
RUNS	1 – 12	13 – 21	22 – 29	31 – 72	20 – 65	66 – 84	15 – 51	52-85
SITUATION STATE								
000	0	2	7	4	16	10	22	20
010	0	10	17	8	19	13	19	26
100	2	7	2	4	7	6	19	9
001	0	0	0	0	0	2	0	5
011	0	0	9	0	1	20	10	17
101	0	7	4	0	8	10	14	14

TABLE 10. NUMBER OF DIVERGENT CELLS USED FOR EACH PERFORMANCE LEVEL AND PROBLEM SITUATION

region, while Performance Levels 2, 3 and 4 show an increasing usage of cells in this region. This suggests that a function of the frequency of cell usage might be a good performance metric for an F-106 pilot. The table also shows that radar lock-on is the most difficult phase of the attack problem.

V.   MODELING SYSTEM PERFORMANCE

Performance on the F-106 simulator is measured in terms of the heading error and heading error rate (refer to Table 4) at the time of fire.   This serves as the independent performance measure criterion for sorting data into performance levels. This is an empirical approach to measuring performance for the entire flight in which the experimental data are sorted into classes via the terminal performance measure.   The classes are then examined to determine the control techniques that result in excellent performance and those that result in less than excellent.   Once these techniques are extracted, a system performance model is formulated which quantifies the various control policies throughout the flight and relates them to total system performance.   Again, the problem space is quantized into 6 problem situations, but the error-error rate plane is broken into 15 cells instead of 90 (see Figure 29).

Transition Analysis Methodology

To derive control techniques that are representative of each of the four levels of operator performance, we apply a technique known as transition modeling, which is discussed in References 3 - 5.   This technique applies concepts of Markov theory to relate the sequence of pilot control actions in the problem state space to performance.   We want to be able to characterize each performance level differently in terms of the transition patterns.

The transition modeling technique requires the computation of several matrices. One matrix is the transition matrix (T) which is a 15 by 15 matrix whose elements are the probabilities of transfer from state i to state j on a given trial, i.e., from sample to sample. This matrix is constructed by counting the number of times the system is in each state and computing the proportion of times it moves to each possible neighboring state.   If the resulting transition matrix represents a regular Markov process (Reference 6), the state of the system after N transitions, starting from an initial state distribution represented by π_0, is given by:
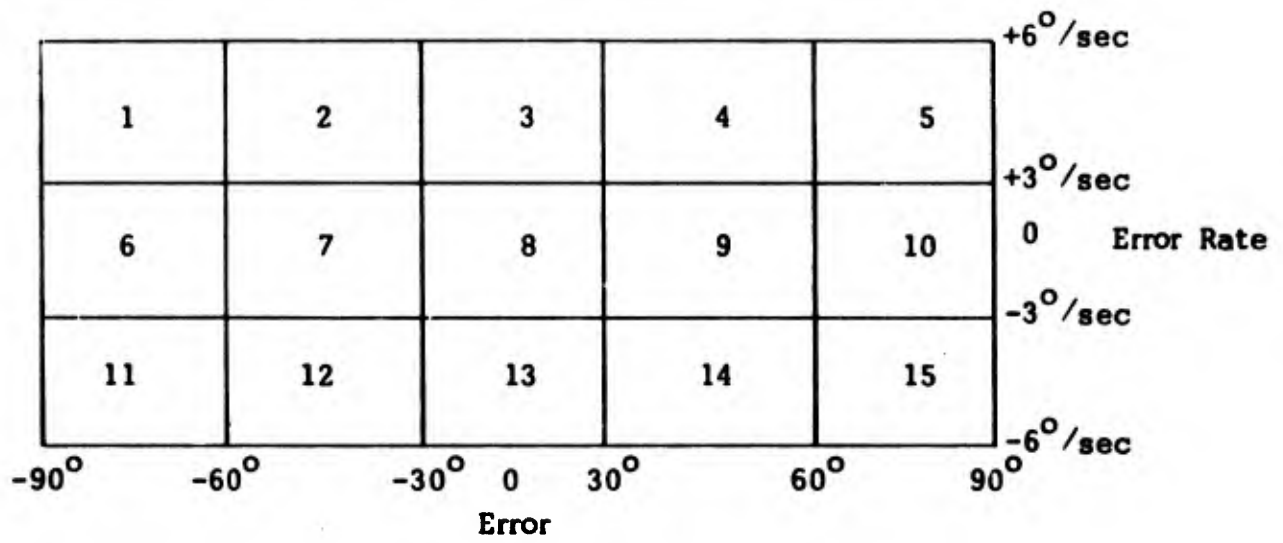
FIGURE 29.   15 CELLS (TRANSITION STATES) OF
ERROR-ERROR RATE PLANE

73

$$\pi_N = T^N \pi_o \tag{1}$$

As N approaches infinity, there is a limiting distribution α given by:

$$\text{limit } \pi_N = \alpha \tag{2}$$

$$N \to \infty$$

where α is the system state distribution after a large number of trials. The α vector gives the probability of finding the system in each of the 15 cells. The sum of the α_i equals 1.0. The limiting distribution can be regarded as a steady state distribution when:

$$\alpha T = \alpha \tag{3}$$

That is, if a system starts with a state distribution α, it will remain with that distribution forever. This distribution is used as a weighting function for the system.

A second matrix used in the transition analysis of operator control policies is a weighted transition matrix, D, where each element is given by:

$$D_{ij} = T_{ij} \alpha_i \tag{4}$$

The D matrix is obtained by multiplying each row of the transition matrix by the probability that the system will be in the corresponding state. The elements of the D matrix correspond to the probabilities that a particular transition (transtate) will be used in a given control policy. Elements of the D matrix are also used to generate a performance metric according to:

$$P = \sum_i \sum_j D_{ij} \, TSM_{ij} \tag{5}$$

where TSM is a transtate score matrix whose element values correspond to the relative importance to performance of each transtate. Equation 5 shows that the performance measure is the sum of the products of the probability of being in each transtate times the importance of that transtate to performance.

Transition analysis is applied here to model operator control policies to learn how the superior operators achieve superior results, and to derive system performance metrics. This technique will allow us to answer the following:

1. What techniques do operators use to produce excellent control?

2. Can we determine where performance differences occur in the state space?

3. Can we determine how the control policy changes with different problem situations within a performance level?

4. Can we determine policy changes or policy differences across performance levels?

5. Can the transition matrix be used to develop performance metrics?

Analysis of Operator Control Policies

Operator control policies can be characterized by the way the origin (cell #8) is reached and the probability of remaining in that state once it has been achieved. Table 11 contains state 8 transition probabilities taken from transition matrices for the four performance levels (PL 1-4) in the final problem situation, PS 5 (i.e., lock-on achieved with less than 20 seconds to go).* The probability of remaining in state 8 is

---

* In the performance code, the performance level is the left digit and the problem situation is the right digit.

75

	Performance Code			
	15	25	35	45

1.

Probability of Staying				
in State 8	.96	.67	.65	.83
99% Confidence	.97	.81	.76	.91
Limits	.87	.52	.55	.69

2.

Probability of Transferring				
to State 8 on One Trial	.69	.51	.42	.20

3.

Probability of Being in				
State 8	.71	.53	.44	.21

TABLE 11.   PERFORMANCE PROBABILITIES

0.96 for PL 1 and decreases to 0.67 and 0.65 respectively for the second and third performance levels. Surprisingly, the corresponding probability for PL 4 is 0.83. One explanation for this apparent anomaly is that once the heading error is zero and the wings are level, it is relatively easy to remain at a zero heading error. The performance level, however, is determined by the heading error at missile launch. This error is high for a PL 4 operator because, even though the probability of remaining in state 8 is high, the probability of rapidly returning to it is low.

The second data line in Table 11 is the probability of transferring from an adjacent state to state 8 on a single transition. These values range from 0.69 for PL 1 to 0.20 for PL 4. The numbers represent the transition matrix (T) weighted by the limiting distribution matrix, α. Thus, they reflect the probability of transferring to state 8 from state i times the probability of being in state i.

The third line in Table 11 is the probability of finding the system in state 8. Again, the probabilities are largest for PL 1 and smallest for PL 4. Thus, it appears that the probability of being in state 8 is a good indicator of the performance level.

The way state 8 is entered is an important descriptor of that portion of the operator's control policy. Table 12 shows the unweighted transition probabilities from adjacent states to the origin. In PL 1, transfer to state 8 is made from only states 3 and 9, showing an unsymmetrical control policy. These transfers from states 3 to 8 are indicative of a control policy producing a high convergence rate, while state 9 to 8 transitions represent a low convergence rate. No transitions are made from states 7 or 13 to state 8. The zero probability of transfering from states 7 and 13 is not the result of a data void because there is a non-zero probability of finding the system in either of those states. However, since less than 20 transitions occur from states 3, 7, 9 and 13, the confidence interval for the respective transition probabilities is broad and care must be taken in drawing conclusions from this data.

TABLE 12. SELECTED TRANSITION PROBABILITIES TO STATE 8

				Performance Code		
			15	25	35	45
Probability of Transferring From A to B						
A		B				
2	–	8				
3	–	8	.4	.35	.39	.21
13	–	8		.37	.40	.25
14	–	8				
7	–	8			.11	
9	–	8	.5	.50	.20	

TABLE 13. SELECTED TRANSITION PROBABILITIES FROM STATE 8

				Performance Code		
			15	25	35	45
Probability of Transferring From A to B						
A		B				
8	–	3	.01	.14	.11	.05
8	–	13	.03	.19	.19	.08
8	–	7	0		.05	.02
8	–	9	0			.02

Table 12 shows that the distribution of probabilities for PL 2, PL 3 and PL 4 transitions from states 3 and 13 to state 8 is more balanced than for the superior performance level. The lower three performance levels also have more transitions from each state than does PL 1 because the superior operators simply move along the sequence of states leading to the origin and tend to remain there. Although the results are not statistically significant, neither PL 1 nor PL 2 operators utilize the 7 to 8 transition. Third level operators use all four states, 3, 7, 9 and 13 to reach state 8, while the poorest operators tend to ignore the low convergence rate 7 and 9 states. One reason for the varied approaches is that the superior operators tend to use an overshoot control technique followed by a slow, low error rate correction to state 8 to avoid further overshoots, providing an ultrastable control. Review of the trajectories produced by PL 4 operators shows that they tend to approach the origin with a large roll angle so that considerable overshoot is achieved, producing a transition through state 8 via states 3 and 13.

Operator control can also be characterized by observing the pattern of transfers from state 8 to the neighboring states (Table 13). A slow drift with increasing error rate results in the transitions from state 8 to states 7 and 9. This is caused by failure to maintain the wings at or near a zero roll attitude, perhaps because the operator's attention is on another task. Transitions from state 8 to 3 and 13 require a considerable roll attitude, which can result from a sudden movement of the control stick or failure to bring the stick to the neutral position after the heading error and roll angle reach zero. All performance levels exhibit a tendency to leave state 8 via states 3 or 13 rather than states 7 and 9. One reason for this is that the probabilities were extracted from the PS 5 transition matrix where the operators may have been attempting rapid correction of small errors in an attempt to reduce their score before problem termination. As a result, the system transfers from state 8 with a large angular rate rather than with a small one. The proportionally large probabilities of PL 2 or PL 3 transferring to states 3 or 13 are statistically significant due to the size of the data samples and reflect the operator's inability to maintain stable control of the aircraft.

The characteristic probabilities described above were taken from transition matrices representing operator control policies in the terminal portion of the maneuver (PS 5). These characteristic probabilities can be determined for each of the problem situations and performance levels. Table 14 contains the probabilities of the system remaining in state 8, and Table 15 contains the probabilities of the system being in state 8 for each PS and PL. (PS 1 is eliminated from these tables because in no case was an operator still in spotlight when the time-to-go was less than 20 seconds.)

Referring to Table 14, a high probability (exceeding 0.90) exists for PL 1 subjects remaining in state 8 during problem situations 0, 4 and 5. The probability decreases to 0.83 in PS 2, where the operator attempts lock-on. No data are available in this performance level for PS 4 because the superior operators were always able to obtain lock-on prior to the terminal portion of the mission. The lower probability of staying in state 8 while attempting lock-on reflects the influence of the secondary tasks on the flying performance at every level. This suggests that the radar lock-on task interferes with the pilot's ability to fly the aircraft even where it was only necessary to maintain a wings level attitude.

A similar analysis can be applied to the probability of being in state 8 (as shown in Table 15). For PL 1, there is a 0.49 probability of being in state 8 prior to lock-on attempt, a 0.0 probability during lock-on, and 0.72 and 0.71 probabilities in the post lock-on states, 4 and 5 respectively. The 0.49 probability associated with prelock-on for the excellent operators indicates that the sequence of states used in achieving superior performance allows only a 0.5 probability of being in the desired state. This serves as a norm against which other performances can be judged. The near consistency of being in state 8 for PS 4 and 5 shows that good operators do not allow time stress to significantly degrade their performance.

The probabilities of remaining in state 8 (Table 14) for performance levels 2, 3 and 4 tend to be in the 0.5-0.6 range until lock-on is achieved. During post lock-on prior to time stress (PS 4), a relatively high (0.80) probability of remaining in

TABLE 14.   PROBABILITY OF STAYING IN STATE 8

	PL	1	2	3	4
PS 0		.91	.58	.54	.51
2		.83	.67	.56	.53
3		ND	.50	.43	ND
4		.94	.80	.80	.87
5		.96	.67	.65	.83

TABLE 15.   PROBABILITY OF BEING IN STATE 8

	PL	1	2	3	4
PS 0		.49	.13	.12	.06
2		0	.07	.13	.06
3		ND	0	.02	0
4		.72	.63	.80	.55
5		.71	.53	.44	.21

state 8 is achieved. In PS 5, however, probabilities for PL 2 and PL 3 drop to 0.67 and 0.65 respectively due to time stress. As mentioned previously, these probabilities are significant and indicate the effect of time stress on the operator's ability to maintain stable control of the aircraft and reduce small steering errors. The corresponding probabilities for PL 4 are high and, as indicated previously, possibly reflect that some operators were able to achieve state 8 and maintain it. The PS 3 entry for PL 4 contains no data because these operators never achieved state 8 in PS 3. This should be distinguished from the corresponding lack of data for PL 1 where no lock-on attempts are made during the terminal portion of the problem. Thus, the poor operators were attempting lock-on during the terminal portion of the problem but were not able to achieve state 8, whereas the superior operators, except for one sample, had always achieved lock-on prior to that time.

The effect of attempting lock-on is clearly shown by the data shown in Table 15 where, for PS 3, near zero probabilities of being in state 8 exist for performance levels 2, 3 and 4. This indicates an almost complete lack of aircraft control while attempting radar lock-on. Also, post lock-on without time stress (PS 4) shows a marked increase in the probability of being in state 8. However, it is seen that there is a significant reduction in that probability under time strees (PS 5).

The ordering of the probabilities of being in state 8 are in complete agreement with the terminal performance metric (i.e., the steering error and error rate at missile launch). Table 14 shows that, although several factors affect performance of manned systems, the ability to maintain stable aircraft control and properly correct for small errors (i.e., remaining in state 8) is of critical importance. It is also indicated that PL 4 operators are unable to efficiently (rapidly) correct for errors under time stress and tend to move through a number of states before returning to state 8, resulting in a large error and/or error rate at missile launch.

Performance Measures

We can now examine the matrices discussed in the previous section for performance-related features. The transition analysis process, as described in References 2 and 3, searches the transition matrices to find the importance of each transition, (transtate) to performance. The resulting transtate score matrix (TSM) indicates which transitions are consistently employed by operators demonstrating excellent performance, and which are consistently used by operators with other levels of performance. Each element of the TSM is iteratively adjusted, or "trained", based on the independent performance variable. Transtate score matrices are constructed for each of the problem situations. Comparison of the TSM developed for each different problem situation reveals the differences in operator flight control for different problem situations and performance levels.

Transtate score matrices were developed for two problem situations, PS 0 and PS 5. In PS 0 the operators are simply attempting to reduce the heading error and bring the wings to a level position with no time stress. In PS 5 the subjects have the same task, but they are working against a time stress factor (less than 20 seconds to go). The measurement criteria developed from PS 5 conditions should reflect an increased emphasis on rapid reduction of heading errors and aircraft roll angle.

The transition score matrix produced by training on the transition matrices representing PS 0 is shown in Table 16. Most of the elements in the matrix have a value of 50, the initial value of each element in an untrained score matrix. Values greater than 50 indicate elements that are associated with the high performance level transitions. Other coefficients, valued lower than 50, indicate transitions representative of less than superior performance. The elements remaining with a value of 50 correspond to transitions which were not used. The transition score matrix for PS 5 is shown in Table 17. Its elements identify which transitions are consistently related to high performance and which are related to low performance.

TABLE 16. TRANSTATE WEIGHTINGS BASED ON PS 0

13.96	4.89	50.00	50.00	62.01	59.63	50.00	50.00	50.00	50.00	50.00
50.00	13.82	37.30	50.00	50.00	8.11	100.00	50.00	50.00	50.00	50.00
50.00	50.00	100.00	100.00	50.00	50.00	100.00	72.68	50.00	50.00	50.00
50.00	53.00	50.00	100.00	50.00	50.00	50.00	100.00	100.00	50.00	50.00
50.00	50.00	50.00	0.00	50.00	50.00	50.00	50.00	29.75	50.00	50.00
7.55	14.36	50.00	50.00	11.32	100.00	50.00	50.00	50.00	24.07	50.00
50.00	100.00	100.00	50.00	0.65	12.42	100.00	50.00	50.00	50.00	0.00
50.00	100.00	100.00	50.00	50.00	93.58	100.00	100.00	50.00	50.00	50.00
50.00	50.00	50.00	50.00	50.00	50.00	20.56	100.00	20.56	50.00	50.00
50.00	50.00	50.00	96.22	50.00	50.00	50.00	40.70	89.88	50.00	50.00
50.00	50.00	50.00	50.00	6.64	50.00	50.00	50.00	50.00	14.74	11.06
50.00	50.00	50.00	50.00	50.00	100.00	50.00	50.00	50.00	4.54	100.00
50.00	50.00	50.00	50.00	50.00	100.00	100.00	50.00	50.00	50.00	50.00
50.00	50.00	50.00	50.00	50.00	50.00	100.00	50.00	50.00	50.00	50.00
50.00	50.00	50.00	50.00	50.00	50.00	50.00	50.00	50.00	50.00	50.00
50.00	50.00	50.00	50.00	50.00	50.00	50.00	50.00	50.00	50.00	50.00
50.00	50.00	50.00	50.00	50.00	100.00	100.00	50.00	50.00	50.00	50.00

TABLE 17. TRANSTATE WEIGHTINGS BASED ON PS 5

51.64	50.00	50.00	50.00	50.00	53.52	50.00	50.00	50.00	50.00	50.00	50.00	50.00	50.00	50.00	50.00	50.00
53.29	0.58	50.00	50.00	50.00	50.00	0.98	50.00	83.91	50.00	50.00	50.00	50.00	50.00	50.00	50.00	50.00
50.00	1.06	2.33	50.00	50.00	50.00	50.00	50.00	50.00	52.41	50.00	50.00	50.00	50.00	50.00	50.00	50.00
50.00	50.00	0.45	0.00	50.00	50.00	50.00	50.00	50.00	50.00	50.00	50.00	50.00	50.00	50.00	50.00	50.00
50.00	50.00	50.00	50.00	50.00	50.00	50.00	50.00	50.00	50.00	50.00	53.82	50.00	50.00	50.00	50.00	50.00
50.00	50.00	50.00	50.00	50.00	51.76	50.00	50.00	50.00	50.00	50.00	50.00	50.00	50.00	50.00	50.00	50.00
50.00	50.00	50.00	50.00	50.00	50.00	1.48	54.81	50.00	50.00	50.00	0.83	50.00	50.00	50.00	50.00	50.00
50.00	50.00	50.00	50.00	50.00	50.00	50.00	50.00	41.76	100.00	29.37	50.00	100.00	50.00	50.00	50.00	50.00
50.00	50.00	50.00	50.00	50.00	50.00	50.00	50.00	50.00	60.58	0.13	50.00	0.95	50.00	50.00	50.00	50.00
50.00	50.00	50.00	50.00	50.00	50.00	50.00	50.00	50.00	50.00	50.00	50.00	50.00	51.35	50.00	50.00	50.00
50.00	50.00	50.00	50.00	50.00	50.00	50.00	50.00	61.13	2.08	0.02	50.00	77.27	50.00	50.00	50.00	50.00
50.00	50.00	50.00	50.00	50.00	50.00	50.00	50.00	50.00	50.00	50.00	50.00	50.00	50.00	50.00	50.00	50.00
50.00	50.00	50.00	50.00	50.00	50.00	50.00	50.00	50.00	50.00	50.00	50.00	50.00	50.00	50.00	50.00	50.00
50.00	50.00	50.00	50.00	50.00	50.00	50.00	50.00	50.00	50.00	50.00	50.00	50.00	50.00	50.00	50.00	50.00
50.00	50.00	50.00	50.00	50.00	50.00	50.00	50.00	50.00	50.00	50.00	50.00	50.00	50.00	50.00	50.00	50.00
50.00	50.00	50.00	50.00	50.00	50.00	50.00	50.00	50.00	50.00	50.00	50.00	50.00	50.00	50.00	50.00	50.00
50.00	50.00	50.00	50.00	50.00	50.00	50.00	50.00	50.00	50.00	50.00	50.00	50.00	50.00	50.00	50.00	50.00

Three types of performance measures have been examined using transition modeling:

1. A performance score,
2. Specific transitions, and
3. The limiting state distribution

Performance scores are generated by multiplying each element of the TSM by the corresponding probability in a weighted transition matrix (see equation 5). Table 18 shows the scores developed for each performance level of each problem situation by multiplying the appropriate weighted transition matrix by the TSM in Table 16. Since the TSM is based on PS 0, the scores for PS 0 are ordered based on the terminal performance metric (ψ, $\dot{\psi}$ at time of fire). However, the scores for the other problem situations are not ordered. The TSM for PS 0 indicates the transition policies required for aircraft flight control without time stress or secondary tasks; obviously these policies are different than those required for other flight control situations. Likewise, in Table 19, the scores formed by using the TSM for PS 5 (Table 17) are ordered for PS 5, but not for the other situations. Thus, this measurement technique shows that there are differences in flight control policies for each problem situation.

Referring to the TSMs in Tables 16 and 17, we see those transitions indicative of high and low performance in each problem situation studied. Figure 30 graphically portrays the PS 0 transitions. In the top portion of the figure, the solid dots and solid lines indicate the transitions associated with score values of 75 to 100. The open circles and dotted lines indicate transitions associated with incremental score values of 51 through 74. The lower half of the figure uses a similar coding; however, the solid line and solid dot indicate low scores rather than high scores. The transitions associated with high performance tend to favor a slow rate of change of error. A surprising factor is that transitions from state 8 to states 7, 3 and 9 are used to identify high performance policies. However, the solid dot in the center of state 8, which represents the "transition" value for remaining in state 8, is associated with a high performance level as expected. Transitions associated with low performance

TABLE 18.   PERFORMANCE MEASUREMENT BASED ON PS 0 MATRIX

	PL	1	2	3	4
PS	0	63.1	56.6	41.7	29.8
	2	15.2	46.9	50.8	35.2
	3	(ND)	2.8	26.7	10.6
	4	91.3	86.5	32.2	77.1
	5	83.4	49.7	70.8	63.5

TABLE 19.   PERFORMANCE MEASUREMENT BASED ON PS 5 MATRIX

	PL	1	2	3	4
PS	0	56.9	20.4	30.8	31.6
	2	70.1	28.5	26.4	33.2
	3	(ND)	45.1	26.7	21.8
	4	73.0	62.5	72.2	57.0
	5	69.8	62.3	44.0	24.0

● ———→ 75 - 100

o - - - 51 - 74

● ———→ 0 - 25
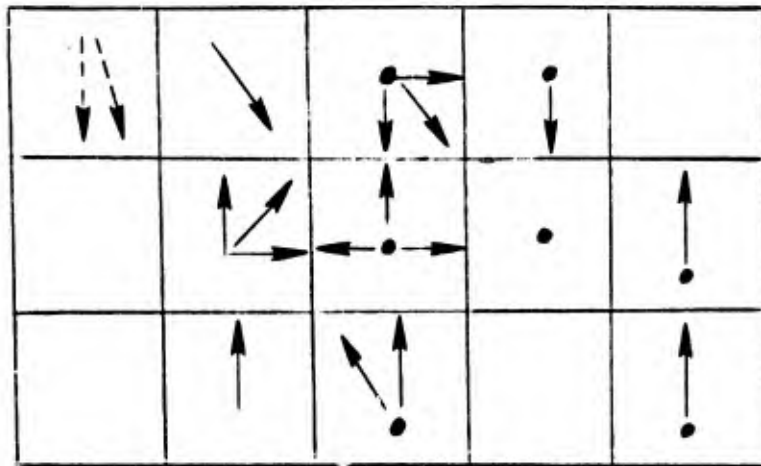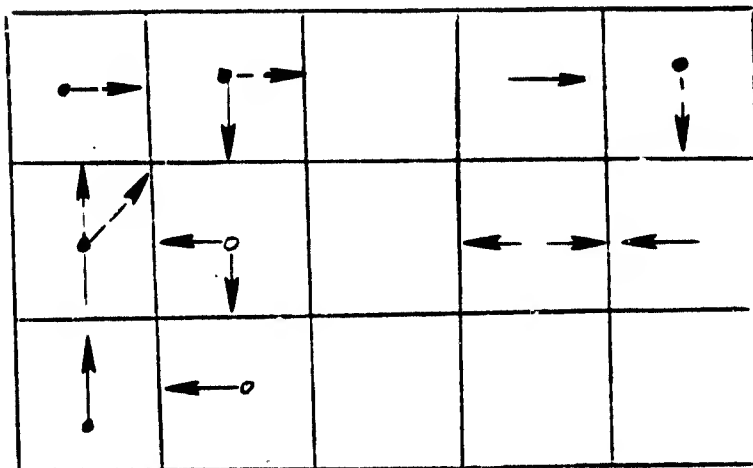
o - - - 26 - 49

FIGURE 30.   TRANSITIONS FOR PERFORMANCE DISCRIMINATION
BASED ON PS 0 MATRIX

tend to move the system towards high rates of change, that is, to states 1, 2, 5, 11 and 12. A companion transition diagram based on the PS 5 matrix is given in Figure 31. In this case, transitions from state 8 to its neighbors have been eliminated as a criterion for identifying high performance. In addition, there is a tendency for higher rates to be favored by the high performance system. Similarly low performances are revealed by transitions from state 8.

A direct comparison of these two transition performance diagrams is given in Figure 32 which shows a composite of the transitions shown in Figures 30 and 31. The entries in Figure 32 reflect transitions held by both the PS 0 and PS 5 matrices. The upper diagram is associated with high performance, and the lower with low performance. As shown, the extent of agreement is small. A high performance level in both cases is obtained by moving to and remaining in state 8. The tendency to remain in state 7 (maintain wings level with a substantial steering error) is always associated with poor performance. Surprisingly, there is agreement that transitions from 2 to 3 and 2 to 7 are consistently associated with poor performance.

An alternate way of analyzing the transition performance diagrams is to examine their differences and observe what transitions are required for a high performance under time stress but not required when time stress is removed. This information is shown in Figure 33. Trajectories required to produce only high scores in the time stress situations (with 20 seconds to go) are shown in the top half of the diagram. A tendency to move towards the high convergence rate cells 1, 6, 11 and 12, and to transfer from cell 9 to cell 8 is shown. This information indicates graphically that high performance control policies are not necessarily symmetrical. It also illustrates the superior operator's tendency to reduce large negative steering errors at a high rate, producing an overshoot, and to reduce the resulting error at a slower, more stable rate.

Firm conclusions regarding the PL 1 tendency discussed above cannot be drawn because the data lack statistical significance. In addition, operators in the lower performance levels did not show this tendency because their great difficulty in controlling
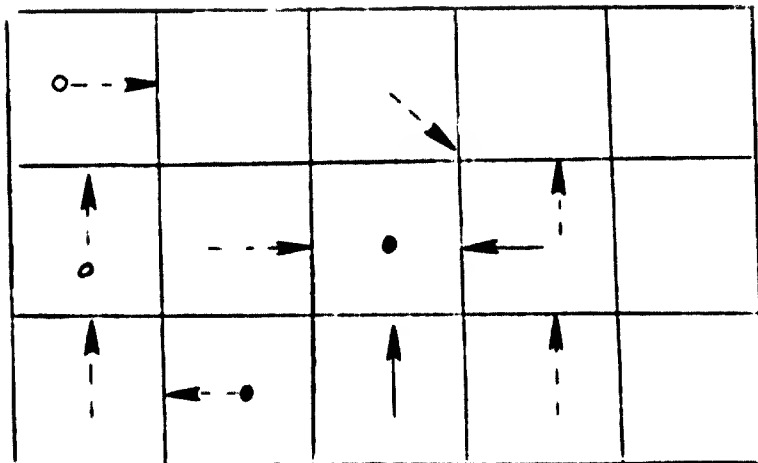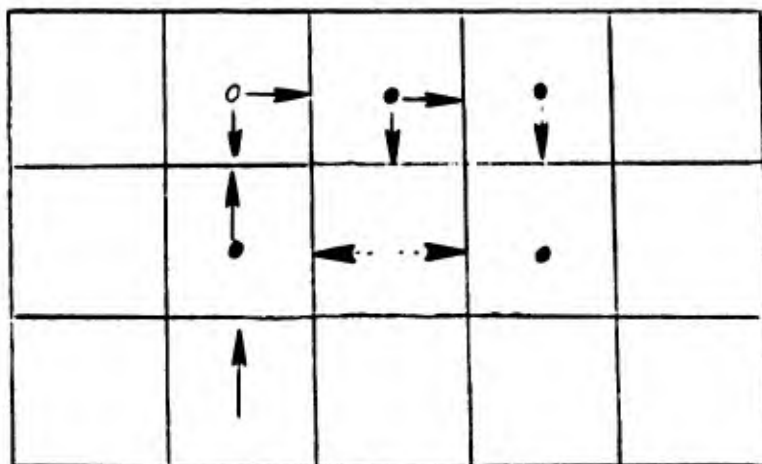
FIGURE 31.   TRANSITIONS FOR PERFORMANCE DISCRIMINATION
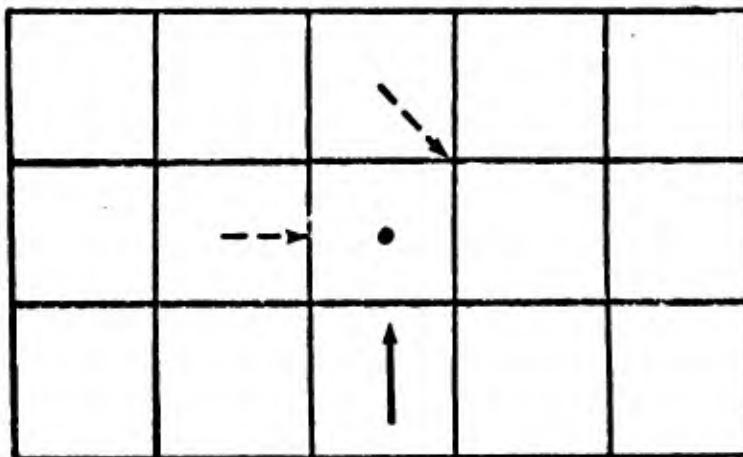BASED ON PS 5 MATRIX

HIGH PERFORMANCE TRANSITIONS

LOW PERFORMANCE TRANSITIONS

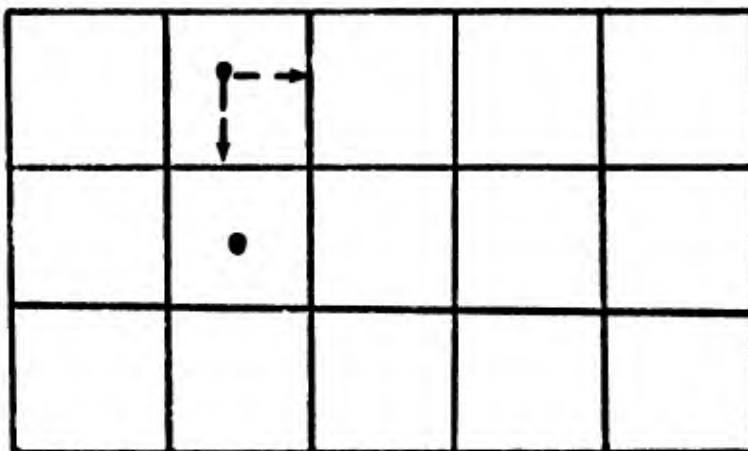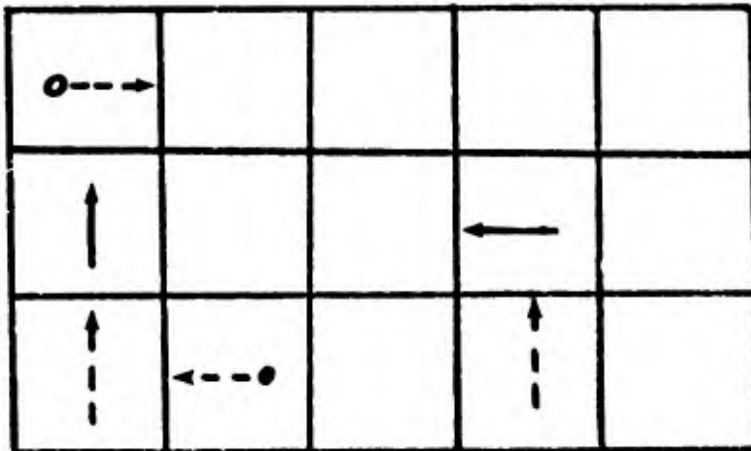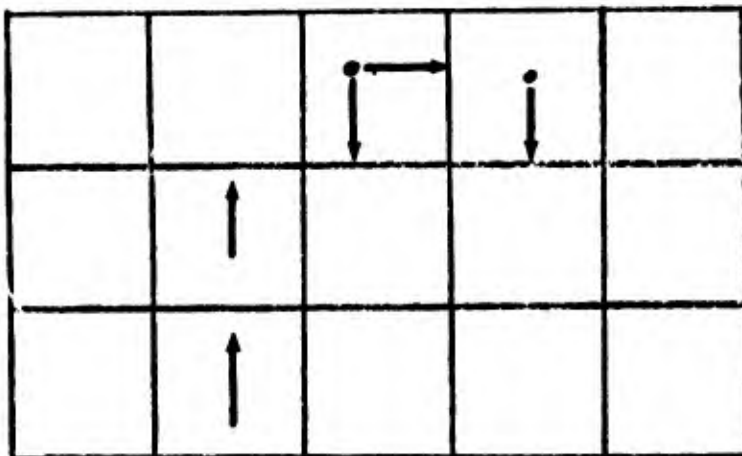FIGURE 32. TRANSITIONS COMMON TO
PS 0 AND PS 5 PERFORMANCE

FIGURE 33. TRANSITIONS REQUIRED FOR PERFORMANCE
DISCRIMINATION IN PS 5 AND NOT
REQUIRED IN PS 0

92

the aircraft resulted in many large overshoots, giving them numerous opportunities for attempts to correct both positive and negative errors. In spite of these cautions, the tendency for a nonsymmetrical policy is observed, which should be sufficient motivation to further investigate the property. Should the tendency to reduce flight control errors according to certain asymmetrical patterns be determined an important factor in air combat, as well as in other man-machine problems, operator models should reflect this property.

Operator performance can also be analyzed with respect to the distribution of states that remain invariant under a single transition. The distribution of states gives the limiting distribution for the transition matrix representing a regular process. Figures 34 through 37 show the invariant distributions for performance levels 1 through 4, respectively, in the five problem situations. As shown in Figure 34, the PL 1 operator in PS 0 has a probability of approximately 50 percent of being in state 8 and a probability of 10 percent or less of being in the remaining states. These probabilities indicate that skilled operators are able to move through the sequence of states leading to state 8 and remain there, or quickly return there. As shown in Figure 34, the transition characteristic for PS 2 yields two chains. One chain (A) includes states 1 through 10; while the other chain (B) includes states 12 through 15. These are absorbing chains such that once state 12 is reached, the system remains there. This reflects a case where the operator moved to state 12 while attempting lock-on and remained there during lock-on, which occurred very rapidly. The other chain transition probabilities yield a high probability of being in states 9 and 10 during lock-on and reflect a relatively low error drift rate. Only one sample value was found in PS 3. That is, in only one instance did a superior operator attempt radar lock-on with 20 seconds to go in the problem period. This probably occurred because the operator was attempting lock-on and the time decreased to 20 seconds to go just as he achieved it. Thus, this particular bar chart has no significance. The post lock-on condition, 4 and 5, indicate a high probability of being in the desired state (8) with a slight degradation in performance under time stress, as indicated by the diagram for situation 5.
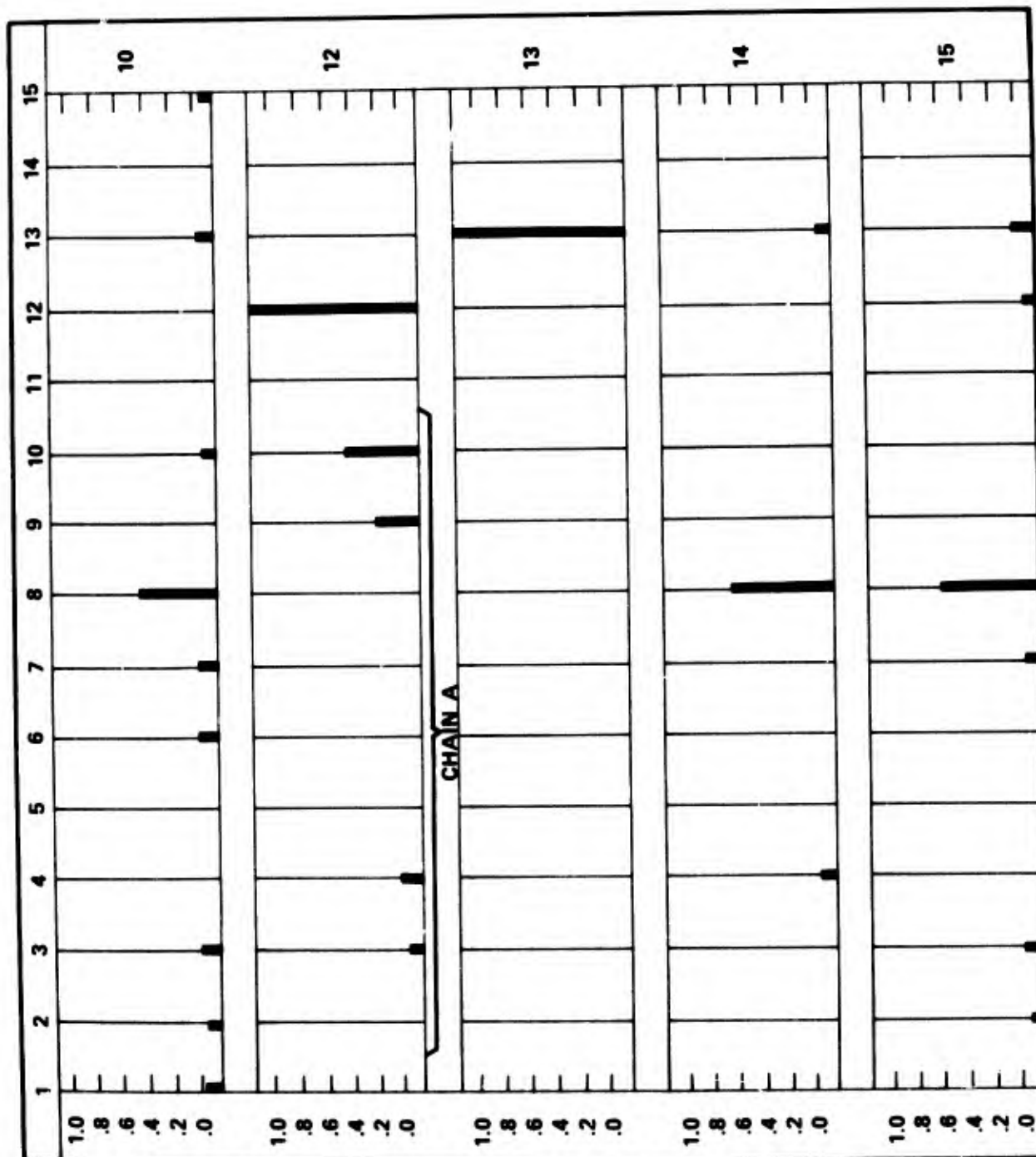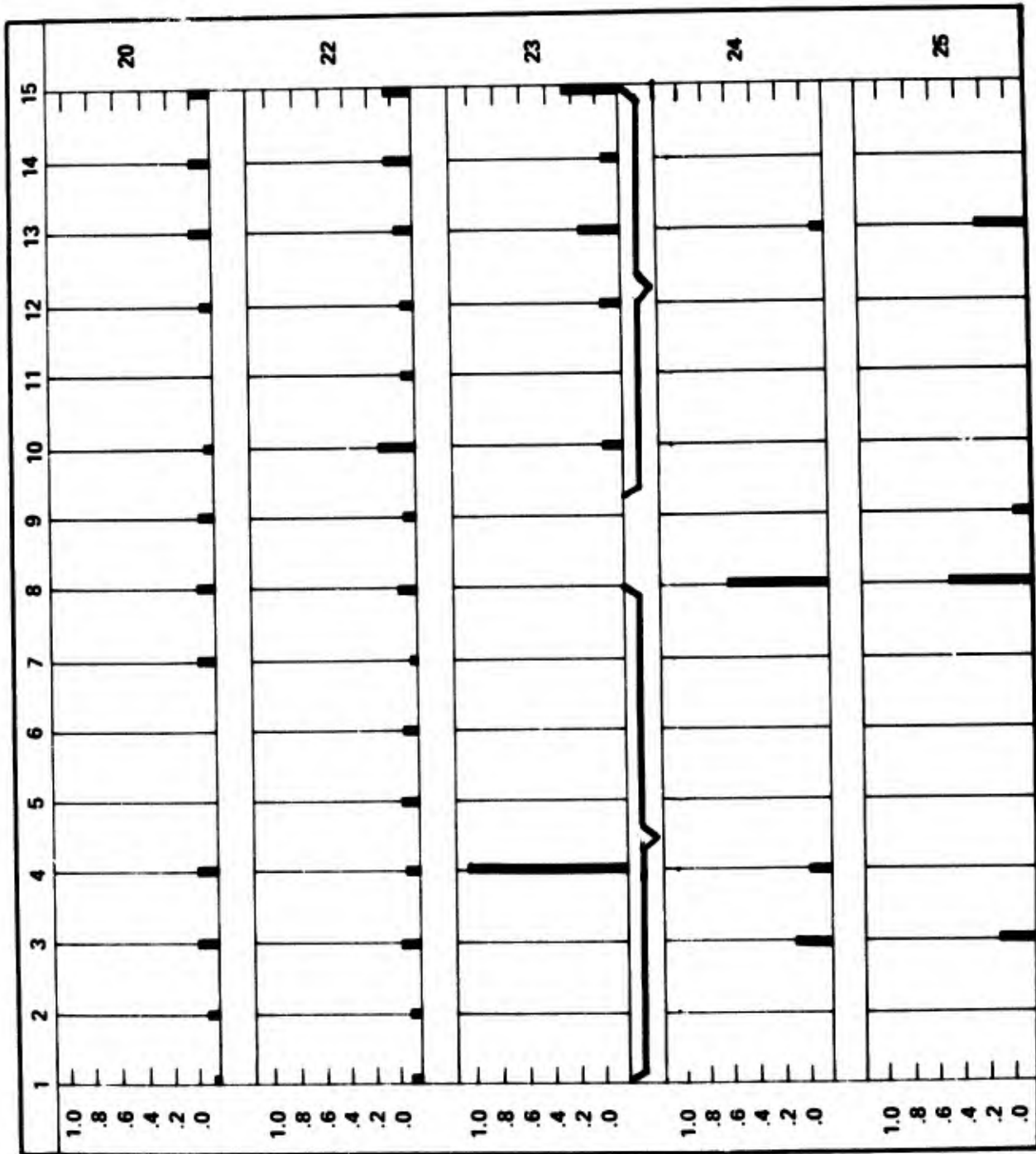
FIGURE 34. PL1 STATE DISTRIBUTIONS

94

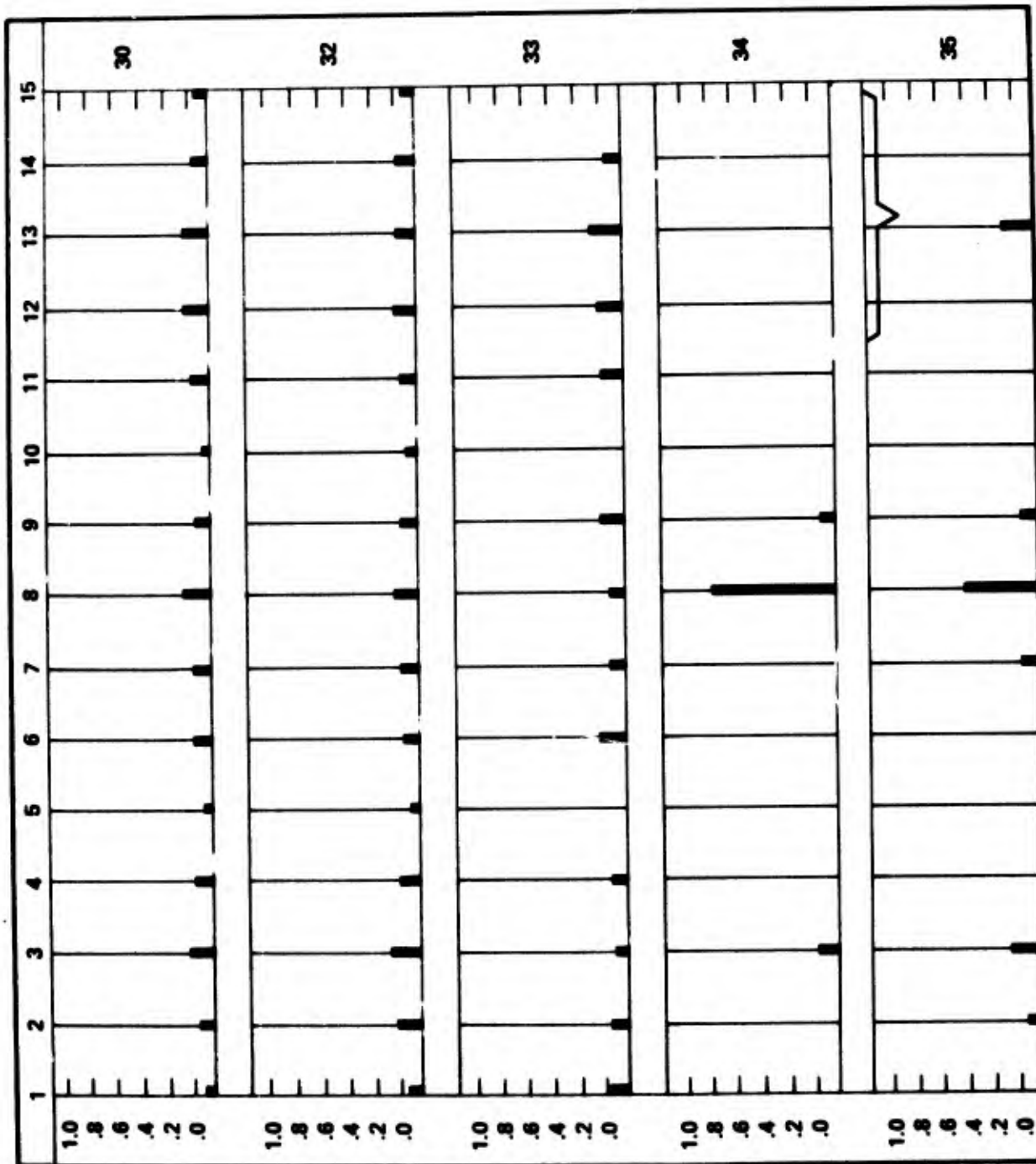FIGURE 35. PL2 STATE DISTRIBUTIONS

95

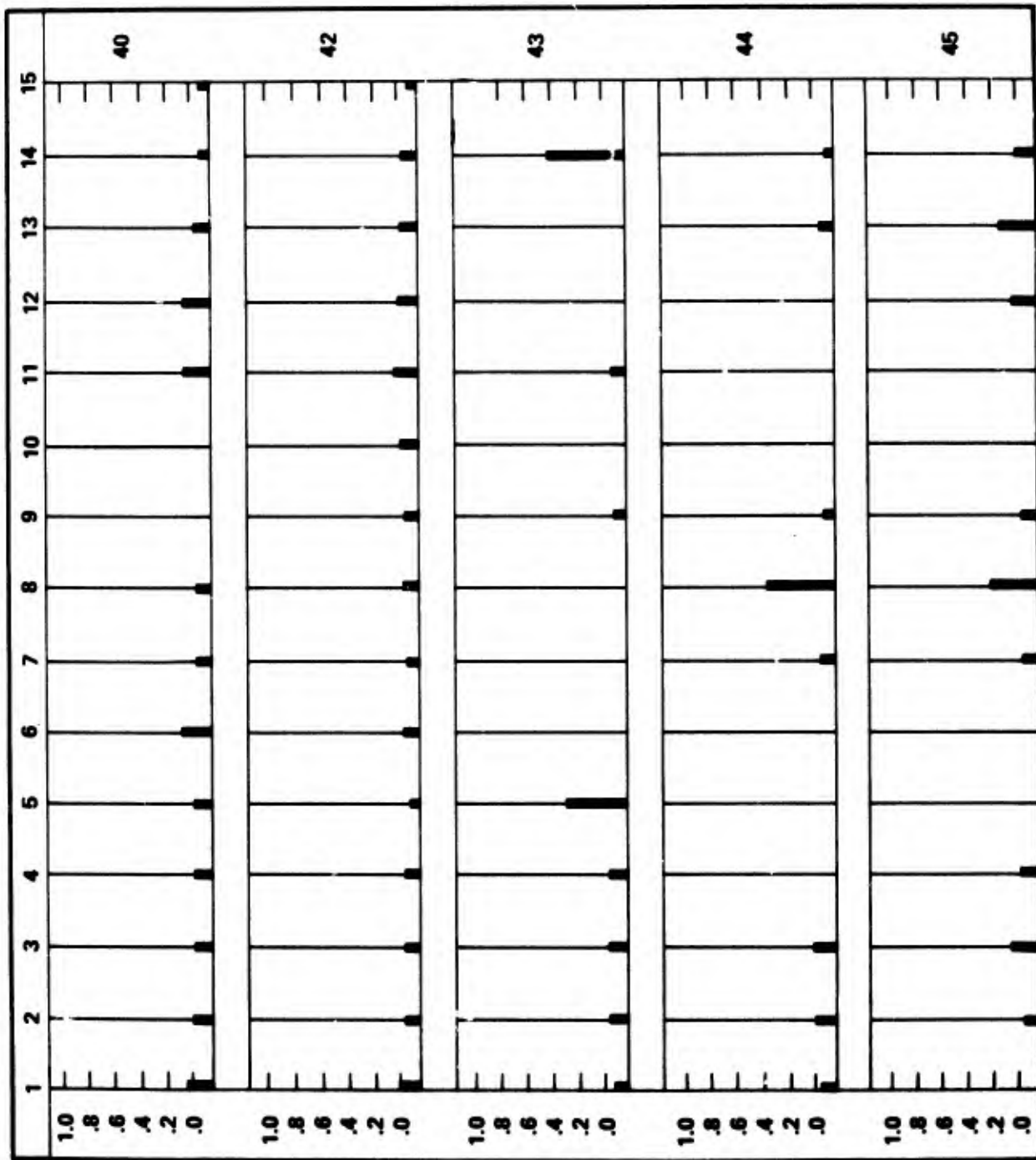FIGURE 36.   PL3 STATE DISTRIBUTIONS

96

FIGURE 37. PL4 STATE DISTRIBUTIONS

Performance level 2 control policies are illustrated in Figure 35. In contrast to the performance demonstrated by the PL 1 operators, PL 2 operators show no definite tendency to maintain a high probability of being in state 8 in PS 0. Instead, there is a uniform probability of being in each state with voids or near voids in states 5, 6, 10 and 11. A similar situation exists as the operator attempts lock-on without time stress. Performance in PS 0 and PS 2 does not seem significantly different, perhaps because the low level of performance in PS 0 left little room for degradation in PS 2. In problem situation 3 (attempted lock-on with time stress), the process is broken into two chains, one consisting of state 4 and the other comprising states 10 through 15. However, limited data in this problem situation prohibits meaningful analysis. Distributions for PS 4 and 5 show that the operators can do a reasonably good job in maintaining control of the aircraft prior to time stress but tend to deviate significantly from state 8 in PS 5. Note that deviations include states 3 and 13, which indicate that the operators are trying to correct for small errors with large roll angles, causing them to exit state 8 with large error rates. This is a common problem in terminal control tasks where the operators are aware of time limitations.

Figure 36 shows the distribution of states for PL 3 operators and indicates control difficulty in problem situations 0, 2 and 3. In these cases, a substantial amount of data is available for radar lock-on attempts (situations 2 and 3) since the operators had great difficulty in achieving radar lock-on. Their troubles are due to either failure to maintain the aircraft in a suitable attitude or lack of operator skill in adjusting antenna azimuth and range gate control to obtain radar lock-on. As a result, a substantial amount of time was devoted to attempting lock-on, and these operators were often still attempting lock-on in the terminal problem phase. This control policy results in a relatively flat distribution in PS 3, as shown in the figure. Post lock-on operation shows that the operators can maintain a high probability of being in state 8 when there is no time stress and after radar lock-on is achieved. However, there is a severe degradation in performance with time stress since the probability of being in state 8 decreases from 0.8 to approximately 0.5 as the problem moves to the terminal phase.

A similar situation exists with the PL 4 operator's performance, as shown in Figure 37. In PS 4, the probability of being in state 8 is 0.60 but the control policy yields a wide distribution of other states, including 1, 2, 3, 4, 7, 9, 13 and 14. This indicates that when the system leaves state 8, the operator has difficulty returning in an efficient and timely manner and requires great excursions throughout the state space to bring the system back to the origin. A significant degradation occurs under time stress for PL 4 operators. The favorable distribution in PS 4 is completely modified and the system concentrates in states 2, 3, 4, 7, 8, 9, 12, 13 and 14, which represents degeneration of control into a large limit cycle.

These three types of performance measures, i.e., a score, a characteristic transition, and a limiting state distribution, all appear valuable in assessing pilot performance. They are necessary because they can be used on data which doesn't contain the terminal portion of the flight, or in which the terminal portion may include an erratic error which is not representative of the entire flight. They are useful for training purposes because they show desirable control techniques.

VI.   CONCLUSIONS

The following conclusions are drawn from this study:

1. The nonlinear modeling technique described in Section IV can be used to generate pilot models that are representative of the F-106 operator's flight control policies and, in general, any nonlinear control policies.

2. Performance can be measured by the amount of deviation between the actual flight trajectory and the model trajectory.

3. The transition modeling technique described in Section V provides three types of performance measures: performance scores, transitions characteristic of a specific performance level, and state distributions. This technique is applicable to any performance measurement problem in which an error-error rate state space can be formulated.

4. Operator flight control policies tend to become unstable when radar lock-on is attempted and when time-to-go is less than 20 seconds. Instability while attempting lock-on is understandable because the operator is concentrating on a task other than flying. However, the simulator has antenna azimuth and range gate controls mounted on the flight control stick so any motion and/or force used for antenna control may affect flight control. Time-to-go of less than 20 seconds is indicated by a shrinking circle on the display. The control instability at this time may possibly be caused by this display, making its function questionable.

The following suggestions are made:

1. The nonlinear modeling techniques require further refinement and validation. The existence of saturation controls and limit cycles needs to be mathematically verified.

2. The performance measures that resulted from the transition analysis should be tested using more data.

3. Performance measures for problem situations 2, 3, and 4 should be formulated.

4. The hardware drift problems in the simulator should be corrected before any further data is collected.

5. Some of the instability in control might be alleviated by removing the antenna azimuth and range gate controls from the flight control stick, and by removing the Time-to-Go-to-Fire circle.

6. The $\psi - \dot{\psi}$ phase plane must be analyzed by an experienced person, say a fighter pilot, to generate a metric which weighs the relative importance of ψ and $\dot{\psi}$ to performance.

REFERENCES

1. "Program Documentation for the Manned Interceptor Simulation", HES Report #71-2, Systems Effectiveness Branch, AMRL, WPAFB, January 1971.

2. Connelly, E.M., Loental, D.G., "Nonlinear Pilot Response Model", Quest Research Corporation, McLean, Virginia, March 1974.

3. Connelly, E.M., Schuler, A.R., Bourne, F.J., Knoop, P.A., "Application of Adaptive Mathematical Models to a T-37 Pilot Performance Measurement Problem", 1971, AFHRL-TR-70-95, Air Force Human Resources Laboratory, WPAFB, Ohio.

4. Connelly, E.M., Schuler, A.R., Knoop, P.A., "Study of Adaptive Mathematical Models for Deriving Automated Pilot Performance Measurement Techniques", 1969, AFHRL-69-7, Volumes I & II, Air Force Human Resources Laboratory, WPAFB, Ohio.

5. Connelly, E.M., Schuler, A.R., "A Theory of Adaptive Man-Machine Systems Applied to Automated Training", presented at IEE - GMMS ERS, International Symposium on Man-Machine Systems, St. John's College, Cambridge, England, 1969.

6. Kemeny and Snell, Finite Markov Chains, Van Nostrand Co., New York, 1960.